MEASUREMENT OF TEMPERATURES IN UNSTEADY GAS FLOWS

by

ROBERT MATTHEW WALLER JOHNSON

B.Sc., University of British Columbia, 1963

A THESIS SUBMITTED IN PARTIAL FULFILLMENT
OF THE REQUIREMENTS FOR THE DEGREE OF

MASTER OF SCIENCE

in the department
of
Physics

We accept this thesis as conforming
to the required standard

[redacted]

Accepted by the Faculty of Graduate Studies

on April 2/1970 by [redacted] Dean of Faculty

University of Victoria

November 1969

Supervisor: John M. Dewey

ABSTRACT

The experimental research described in this thesis is devoted to providing instrumentation for the direct measurement of the temperature of unsteady gas flows in a shock tube. The range of mach numbers for which the present system is designed is 1.1 to 1.4. This corresponds to a temperature directly behind the shock front in the range of about 318^{o} K. to 373^{o} K.

The existing techniques of temperature determination are reviewed. It is evident that there is a lack of experimental temperature data for low mach number unsteady flows in which the temperature is only a few hundreds of degrees from ambient.

A thin platinum film resistance thermometer was developed, such that the temperature of the backing material could be varied independently of the temperature monitoring apparatus. From a knowledge of the temperature-time history of the platinum film, it was possible to calculate the heat transfer rate at the surface of the backing material at any time.

The temperature of the gas at any given time was measured by determining the gauge temperature for which the surface heat transfer

rate was zero. Comparisons are made between the measured temperature and that calculated from pressure and shock velocity measurements for several initial conditions of the test gas. To the best of the author's knowledge, this is the first use of such a technique to determine the temperature of an unsteady gas flow over an extended period of time.

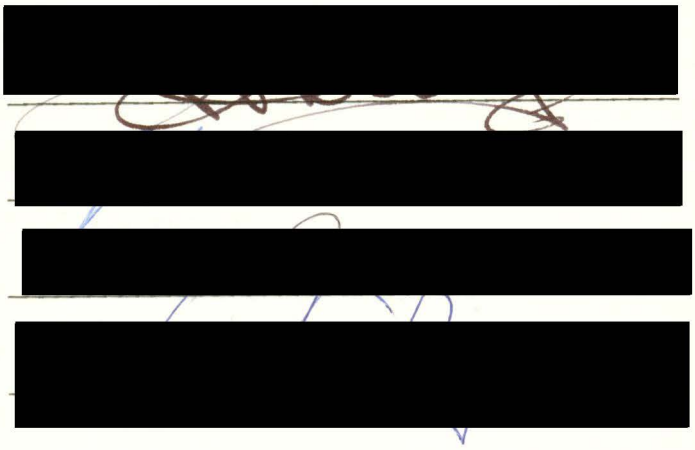

TABLE OF CONTENTS

LIST OF TABLES

LIST OF FIGURES

Page

Page

ACKNOWLEDGEMENTS

My first acknowledgement is to my supervisor, Dr. J.M. Dewey, to whom I owe my first interest in shock tube phenomena, and who, as a teacher, has been a source of inspiration and encouragement in carrying this research to a successful conclusion.

I am also indebted to Mr. B.C. Manning for his helpful suggestions concerning electronic apparatus and to Mr. E.A. Eisenberg who was most co-operative in the use of the University of Victoria glass blowing facilities.

Finally, I must express my appreciation to my wife for the production of the drawings and who has had the patience to bear with me in the quest for truth.

CHAPTER 1

INTRODUCTION

Temperature measurements, to date, have been confined to steady and quasi-steady state high temperature gas flows. The temperatures have been well in excess of 1000^{o} K. Thus a need exists for an experimental method to measure steady and unsteady gas flows in the range of 300 - 1000^{o} K, which correspond to gas flows with a shock wave mach number of less than about 3.5.

The shock tube has been exploited as a practical research facility to produce unsteady gas flows. In its simplest form it consists of a constant cross-section tube in which a diaphragm initially separates two bodies of gas at different pressures. After initial removal of the diaphragm, a shock wave travels into the low pressure gas, while an expansion or rarefaction wave travels into the high pressure gas. The shocked gas and expanded gas are separated by a contact surface across which the pressure and velocity are equal, but the density and temperature are different. The shock heating of the low pressure gas and expansion cooling of the high pressure gas permit a very wide range of flow temperatures to be achieved.

Since the strength of the shock wave is not constant, the entropy of the gas behind the shock also varies. This means that at a fixed position in the tube there is no single valued relationship between any two parameters such as temperature and pressure. A method

of determining the temperature of such a flow by direct measurement is therefore desirable, for the calibration of shock tubes, aerospace studies, and high temperature chemistry.

In 1962, Thureau and de Casteljau suggested the use of a thin film resistance thermometer heated to such a temperature that it attained thermal equilibrium with the gas flow directly behind a shock front. The method presented in this paper is based on the same principle but avoids the use of elaborate null point determinations.

The temperature transducer was mounted flush to the inside surface of the shock tube wall. A theoretical study indicated that the temperature variations of the wall surface were very small. Thus a transducer suitable for sensing small temperature changes over time intervals of 1 - 4 msec. was required. To satisfy these conditions, a thin platinum film resistance thermometer, mounted on a glass substrate, was developed. The temperature gauge was designed in such a manner that the film temperature could be controlled independently of the film resistance-measuring circuit. This circuit consisted of a simple bridge and integrated circuit amplifier designed to detect the voltage change across the resistance thermometer.

The initial measurements were made in a section of the shock tube where a portion of the flow was well defined in the sense that parameters such as pressure and temperature could be calculated from the knowledge of the shock velocity or pressure-time variation.

In addition to the quasi-steady state flow regions, there were also regions of the gas in a state of decreasing temperature; and it was these regions which were of major interest.

In determining the operational capability of the temperature transducer, tests were conducted using one gauge and several duplicated shock tube firings. Each firing was made with the thin film at a known starting temperature so that the sequence bracketed the expected temperature range within the gas flow under study. A film which was cooler than the gas would show an increase in temperature when exposed to the flow while a film which was hotter would show a decrease in temperature.

With knowledge of both the temperature and the rate of change of temperature of the film for each trial, it was hoped that an interpolation to determine the temperature at which the film was in thermal equilibrium with the gas could be found. This method proved impractical after approximately 3 msec. of flow time, at which time there was a second shock wave or a decaying flow situation.

A second method of determining the temperature of the gas flow was therefore adopted. The surface temperature of the glass substrate was measured with the resistance thermometer from which it was possible to calculate the heat transfer rate at the glass-gas interface. The film temperature for which the latter parameter was zero was assumed to be the temperature of the experimental gas.

In two of the three shock flows considered, there was excellent agreement between the measured temperature and that calculated from pressure measurements. In the third case, the deviation was less than 10%. A subsidiary study showed that the number of duplicated shock tube firings could be reduced to four without significantly affecting the accuracy of the results.

CHAPTER 2

SURVEY OF TEMPERATURE MEASURING TECHNIQUES

Several methods have been used to measure the temperature of shock tube flows. These methods include the spectrum line reversal, hot-wire anemometer, thermocouple, ultrasonic and thin-film resistance thermometer techniques.

The spectral line reversal technique developed by A.G. Graydon and I.R. Hurle (1963) is the most successful method for measuring high temperatures. The theory is based on Kirchoff's radiation law for a medium which is in thermal equilibrium. The compressed gas is usually seeded with a sodium compound. The bead of a tungsten arc Pointolite lamp, the image of which is brought to focus in the centre of the tube, is used as a continuous background source. The spectrum lines of the sodium appear bright or dark against the continuous background, depending on whether the brightness temperature of the background source is higher or lower than the gas temperature. When the continuum is the same brightness as the metal, the spectrum lines become indistinguishable from the background spectrum. Since the technique requires the determination of a null point, many reproducible experiments are required to establish the gas temperature. Figure 2.1 shows the optical arrangement for single-beam determination of the reversal temperature.

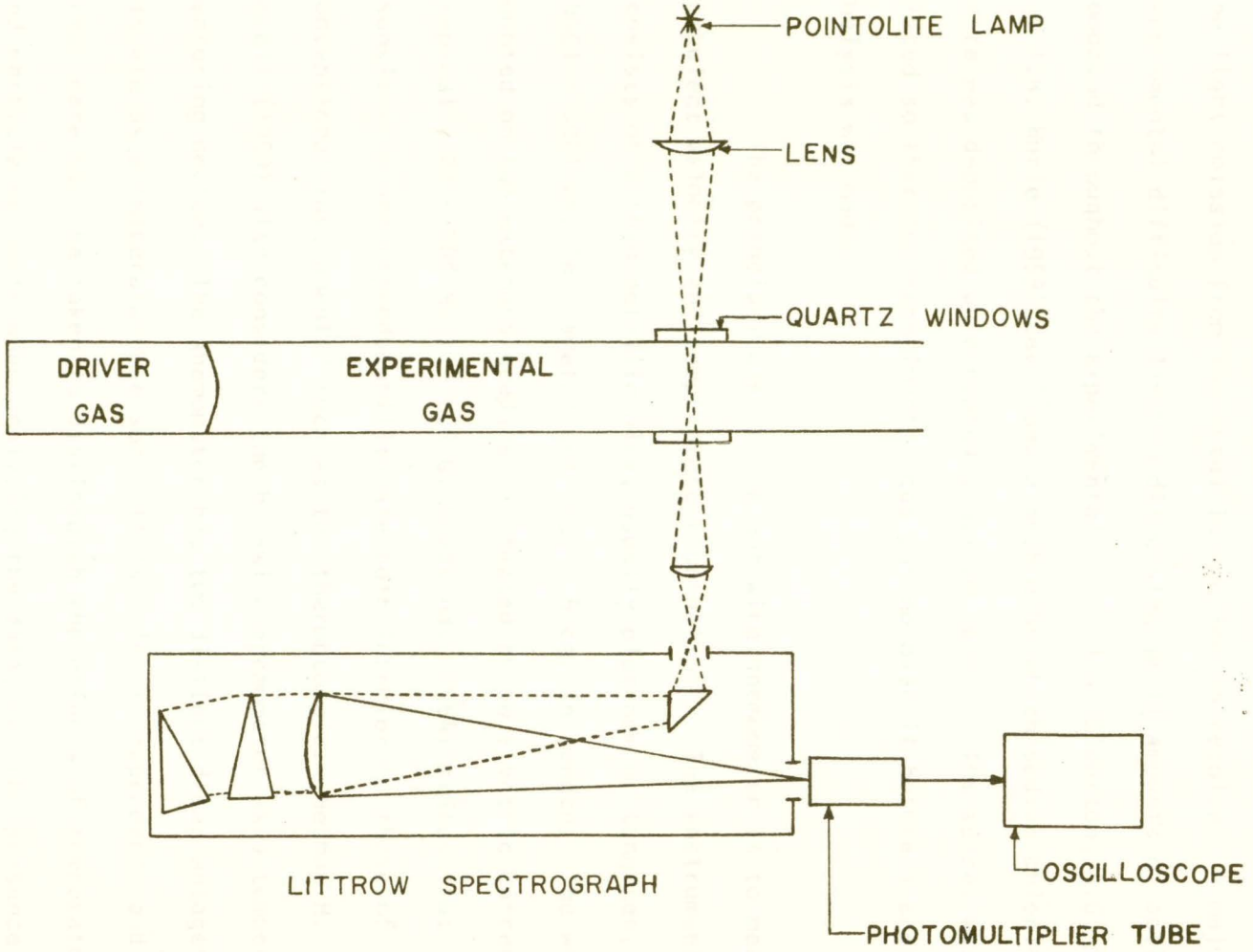

Fig. 2.1 Optical arrangement for single-beam determination of reversal temperature

This method works well for shock mach numbers of 5.7 to 7.3 or equivalent temperatures of 2000° K to 3000° K. At lower temperatures the light emission from the metal is too low to resolve. A major experimental difficulty lies in dispersing small amounts of sodium compound throughout the experimental gas. J.G. Clouston, A.G. Gaydon and I.R. Hurle (1959) developed a method by which sodium chloride paste was deposited on a heated platinum spiral. The spiral was placed so that the experimental gas passed over it before a spectrum analysis was made.

The principal use of the hot-wire anemometer is to measure turbulent velocity and temperature fluctuations. The instrument consists of a thin metallic wire, usually platinum or tungsten, .0001 - .001 cm. in diameter and .05 - .5 cm. in length. The wire, mounted on two extended needles, is heated by an electric current (typically 20 - 200 MA.). L.S.G. Kovásznay (1964) states that "sensitivity and reproducability are both inferior to those of conventional instruments" such as the thermocouple. Herman H. Lowell (1950) also considers the hot-wire anemometer as a temperature measuring device. The anemometer has two distinct disadvantages in its use as a temperature sensor. It is velocity dependent, and great care must be taken to distinguish the effects of temperature and particle velocity when analysing the data, and the presence of the hot wire in the flow creates turbulence, thus obscuring the true flow temperature.

Thermocouples have also been investigated by several authors as a possible method of measuring transient temperatures in a gas. Bendersky (1953) succeeded in making a nickel-iron thermocouple with a response time of .25 msec. The sensitivity (Volts/^{o}F) for such an instrument has been shown by Vidal (1956) to be seventy-five times lower than for a thin-film resistance thermometer. The thermocouple technique has the advantage, however, that the signal is self generating and thus no external energizing source is required.

The ultrasonic method of measuring the temperature directly behind the shock front is described by D.G. Marlow (1949) and R.I. Soloukhin (1966). A beam of ultrasonic sound waves produced by a quartz crystal is emitted normal to the direction of the gas flow. If the wavelengths ahead of and behind the shock front are measured for waves which are parallel to the crystal, one can use the equation

$$\left(\frac{T_2}{T_1}\right)^{\frac{1}{2}} = \frac{C_2}{C_1} = \frac{\lambda_2}{\lambda_1} \quad . \tag{2.1}$$

As reported by Marlow (1949), the ratio T_2/T_1 agrees with the Rankine Hugoniot equations to within 3%. There is no mention of boundary layer effects, although an average value is taken over ten wavelengths.

The thin-film resistance gauge has been used by Vidal (1956), J. Rabinowicz (1957) and B.W. Taylor (1959) as a method of logging heat transfer data in shock tube flows. A secondary function of the heat sensor has been the determination of the surface temperatures. The gauges have been flush mounted to the walls of shock tubes or experimental models. Because of the finite lag time of the gauge response to thermal inertia, the temperature observed is not necessarily that of the gas flow. The thin-film transducers fabricated by R.J. Vidal (1956) are reported to have response times in the order of 10^{-9} seconds and sensitivities in the order of 10^{-3} Volts/^{o}F. The mach numbers of the flows investigated by the above authors were respectively 4.0 - 10.0, 1.8 - 2.0 and 4.29.

CHAPTER 3

THERMOMETER THEORY

The theoretical discussion to follow will introduce the basic heat conduction parameters, and Fourier's heat conduction equation for a solid. The theory will be specifically applied to a temperature transducer constructed by the deposition of a thin platinum film onto a borosilicate glass base, and mounted so that the metallic surface is flush with the surface of a flat metal plate.

3.1 Heat conduction parameters

When different parts of a solid body are at different temperatures, heat flows from the hotter to the colder portions by a process of transfer known as conduction. The rate at which heat will be transferred depends on a number of conditions which will now be considered.

Consider a body composed of two parallel planes of area A and distance X apart, over each of which the temperature is constant, being T_1 in one plane and T_2 in the other. Heat will flow from the hotter of these isothermal surfaces to the cooler, and the quantity, Q, which will be conducted in time, t, will be given by

$$Q = K \frac{(T_1 - T_2)}{X} At \qquad (3.1.1)$$

where K is defined as the thermal conductivity of the solid.

The limiting value of $(T_1 - T_2) / X$, or $\partial T/\partial X$ is known as the temperature gradient at any point X. If $\partial T/\partial X$ is taken in the direction of the flow of heat, it is intrinsically negative. Hence the rate at which heat is transferred across an isothermal surface, per unit area, is

$$W = -K \frac{\partial T}{\partial X} \qquad (3.1.2)$$

and W is known as the heat flux across a surface at a point. It should be noted that, since only the differences of temperature are involved, the actual temperature of the system is immaterial, assuming that K is a constant for the temperature range considered. Of course W will be zero when the temperature difference is zero.

While the rate at which heat is transferred in a body is dependent only on the conductivity, and the temperature gradient, the change in temperature which the heat will produce will vary with the specific heat, C, and density, ρ, of the material. Thus a new constant, k, defined by

$$k = \frac{K}{\rho C} \qquad (3.1.3)$$

must be considered in heat conduction theory. This parameter is known as the thermal diffusivity of the material under consideration.

3.2 Fourier's heat conduction equation

The equation governing the linear flow of heat in a body is known as Fourier's equation. In its one dimensional form it is written as

$$\frac{\partial T}{\partial t} = k \frac{\partial^2 T}{\partial X^2} \qquad (3.2.1)$$

A complete derivation of the equation is given by Ingersoll and Zobell (1913). It may be seen from equation 3.2.1 that the temperature is a function of a space coordinate X, and time t. Thus the equation holds for steady and unsteady heat flows, depending on whether $\partial T/\partial t$ is zero, or non zero, respectively.

From Fourier's equation for heat conduction in a solid, Ingersoll and Zobel have derived the expression

$$t = \frac{X^2}{2k} \qquad (3.2.2)$$

to calculate the time required for heat to diffuse through a material of thickness X after a sudden heat pulse is applied. The use of this equation provides a measure of the time required for heat to diffuse from the outer surface of a platinum film to

the interface between the film and a glass backing. The thermal diffusivity of platinum, obtained from tables provided by E.B. Shand (1958), is 0.240339 (C.G.S. units). Assuming a film thickness of 1 micron, a diffusion time of approximately 1×10^{-12} seconds is obtained. Thus, under all transient conditions, the film temperature can be assumed to be uniform across its thickness, and equal to the instantaneous surface temperature of the glass substrate on which it is mounted.

It is important to distinguish between the temperature of the main body of a gas flow over a wall, and the temperature attained at the wall surface. Because of the high gas velocity, 200 - 300 m/sec., a wall initially at ambient temperature will not acquire the free-gas temperature in a characteristic time interval of 1 - 4 msec.

An indication of the instantaneous rise in temperature at the surface of a borosilicate glass surface, mounted flush to the wall surface, when a mass of hot gas, characterized by a step-like temperature profile, traverses it, can be obtained by assuming the effect is equivalent to suddenly immersing a body, initially at temperature T_w, in a gas at temperature T_g, where T_w and T_g are the free-wall and free-gas temperatures.

If the specific heat, density, and thermal conductivity of the glass and gas are C_w, ρ_w, K_w and C_g, ρ_g and K_g respectively,

the Fourier equations for the heat conduction in the two media are, respectively,

$$\frac{\partial T_w}{\partial t} = \frac{K_w}{\rho_w C_w} \frac{\partial^2 T_w}{\partial X^2} \tag{3.2.3}$$

and

$$\frac{\partial T_g}{\partial t} = \frac{K_g}{\rho_g C_g} \frac{\partial^2 T_g}{\partial X^2} \tag{3.2.4}$$

From equation 3.2.2 it is seen that the heat will penetrate a distance of the order of $(t\ K_w / \rho_w C_w)^{\frac{1}{2}}$ in the glass, and $(t\ K_g / \rho_g C_g)^{\frac{1}{2}}$ in the gas. If the surface temperature of the glass becomes T_s, upon equating the amount of heat lost by the gas in time, t, to that gained by the solid glass surface, it follows that

$$(T_g - T_s)\rho_g C_g (tK_g/\rho_g C_g)^{\frac{1}{2}} = (T_s - T_w)\rho_w C_w (tK_w/\rho_w C_w)^{\frac{1}{2}} \tag{3.2.5}$$

or

$$T_s = \frac{T_g + nT_w}{1 + n} \tag{3.2.6}$$

where

$$n = \frac{\rho_w C_w K_w}{\rho_g C_g K_g}^{\frac{1}{2}} \tag{3.2.7}$$

For borosilicate glass and air the values of ρ, C and K are respectively

$\rho_w = 2.23$	$\rho_g = 1.19 \times 10^{-3}$	gm. cm.$^{-3}$	
$C_w = .20$	$C_g = .17$	cal. gm.$^{-1}$ ^{o} c.$^{-1}$	
$K_w = .0023$	$K_g = 62.2 \times 10^{-6}$	cal. cm.$^{-1}$ sec.$^{-1}$ ^{o} c.$^{-1}$	

Thus air at 88^{o}C passing over a borosilicate glass surface at 25.4^{o}C will raise the surface temperature of the glass 0.28^{o}C.

If the flow of hot gas continues for several milliseconds, it can be anticipated that the temperature of the glass will continue to rise above 25.68°C.

Two important results of the preceding example are: one, the instantaneous change in the surface temperature of the glass is small, and two, this change decreases linearly as the difference between the wall and gas temperature decrease. The change is positive for initial wall temperatures less than the free-gas temperature, and negative for initial wall temperatures greater than the free-gas temperature. Figure 3.2.1 illustrates the above characteristics for a gas flow of 88°C.

Since the above example is independent of time, it is only valid for instantaneous temperature measurements. For longer periods of time heat flow between the glass surface and gas, plus heat flow between the surface of the glass and its interior, must be considered.

3.3 The heat transfer equation

In 1956 R.J. Vidal did a detailed study on the rate of heat transfer between air and a thin platinum film on a glass substrate. The thin-film resistance thermometer measures the surface temperature of the glass, and does not function directly as a gauge to measure heat transfer to the glass surface. However, the theory for heat conduction in an inhomogeneous body can be used to relate the surface temperature history to the heat transfer rate. Thus, if it is possible

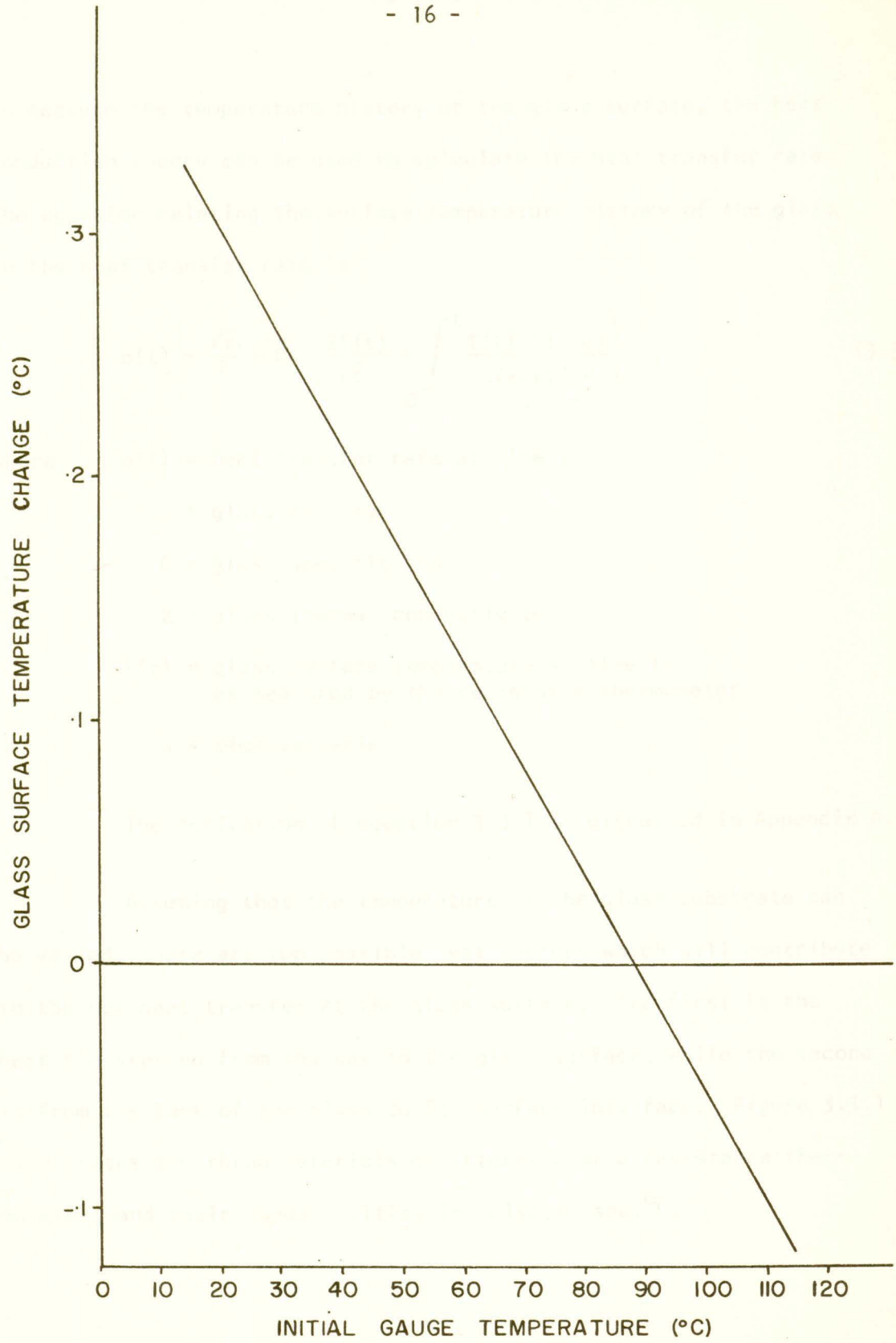

Fig. 3.2.1 The surface temperature change of borosilicate glass suddenly exposed to a gas at $88^{o}C$.

to measure the temperature history of the glass surface, the heat conduction theory can be used to calculate the heat transfer rate. The equation relating the surface temperature history of the glass to the heat transfer rate is

$$q(t) = \frac{\sqrt{\pi}}{2}\sqrt{\rho CK}\left(\frac{2T(t)}{\sqrt{t}} + \int_0^t \frac{T(t)-T(\lambda)d\lambda}{(t-\lambda)^{3/2}}\right) \qquad (3.3.1)$$

where $q(t)$ = heat transfer rate at time t

ρ = glass density

C = glass specific heat

K = glass thermal conductivity

$T(t)$ = glass surface temperature at time t, as measured by the resistance thermometer

λ = time variable.

The derivation of equation 3.3.1 is discussed in Appendix A.

Assuming that the temperature of the glass substrate can be varied, there are two possible heat sources which will contribute to the net heat transfer at the glass surface. The first is the heat transferred from the gas to the glass surface, while the second is from the back of the glass to its surface interface. Figure 3.3.1 illustrates the three materials of interest for a resistance thermometer, and their conductivities in cals/cm. sec.^{o}C.

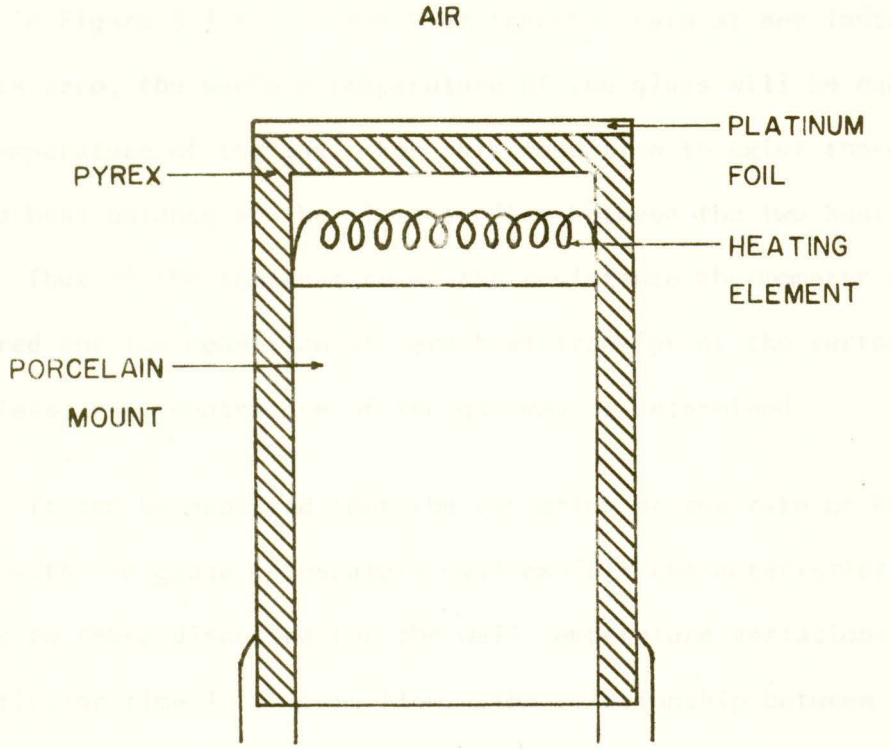

K_{air} = ·000055 Cal./cm. sec. °C

K_{Pt} = ·166 Cal./cm. sec. °C

K_{glass} = ·0023 Cal./cm. sec. °C

Fig. 3.3.1 The resistance thermometer cross-section

In equation 3.3.1, the heat transfer rate is given as a function of the surface temperature of a resistance thermometer as depicted in Figure 3.3.1. If the heat transfer rate at any instant in time is zero, the surface temperature of the glass will be equal to the temperature of the gas. For this condition to exist there will be a heat balance at the glass surface between the two heat sources. Thus if the temperature of the resistance thermometer can be measured for the condition of zero heat transfer at the surface of the glass, the temperature of the gas may be determined.

It can be expected that the variation of the rate of heat transfer with the gauge temperature will exhibit characteristics analogous to those discussed for the wall temperature variations at a particular time in the gas flow. The relationship between the heat transfer rate and the gauge temperature for a particular time will not necessarily be linear. This is because the heat transfer rate through the glass depends on the time history of the temperature gradient $\frac{\partial T}{\partial X}$, which will be different for each gauge temperature at that time.

CHAPTER 4

EXPERIMENTAL APPARATUS

4.1 The shock tube

A shock tube consists of a tube, usually of circular or rectangular cross-section, which is separated into two parts by a diaphragm. One part, the low pressure chamber, is filled with the test gas. The compressed driver gas is fed into the second part, the high pressure chamber. The tubes used for the experiment described here have a rectangular cross-section. The test gas was air at atmospheric pressure and the driver gas was compressed air. Figures 4.1.1 and 4.1.2 show the details of the 4" x 4" and 3" x 10" shock tubes at the University of Victoria.

The main difference between the two shock tubes is the method used for producing the shock wave. In the 4" x 4" tube, the floating piston functions as the shock wave valve rather than the diaphragm material. The bursting of the diaphragm in this case allowed the piston to move rapidly away from the upstream end of the tube with the resultant sudden release of gas into the tube, producing the shock. In the 3" x 10" tube, the diaphragm took the place of the piston. Upon rupture, the diaphragm material was carried several meters by the sudden gas flow. Rupture of the diaphragm in both tubes was initiated by a spring loaded, pointed plunger.

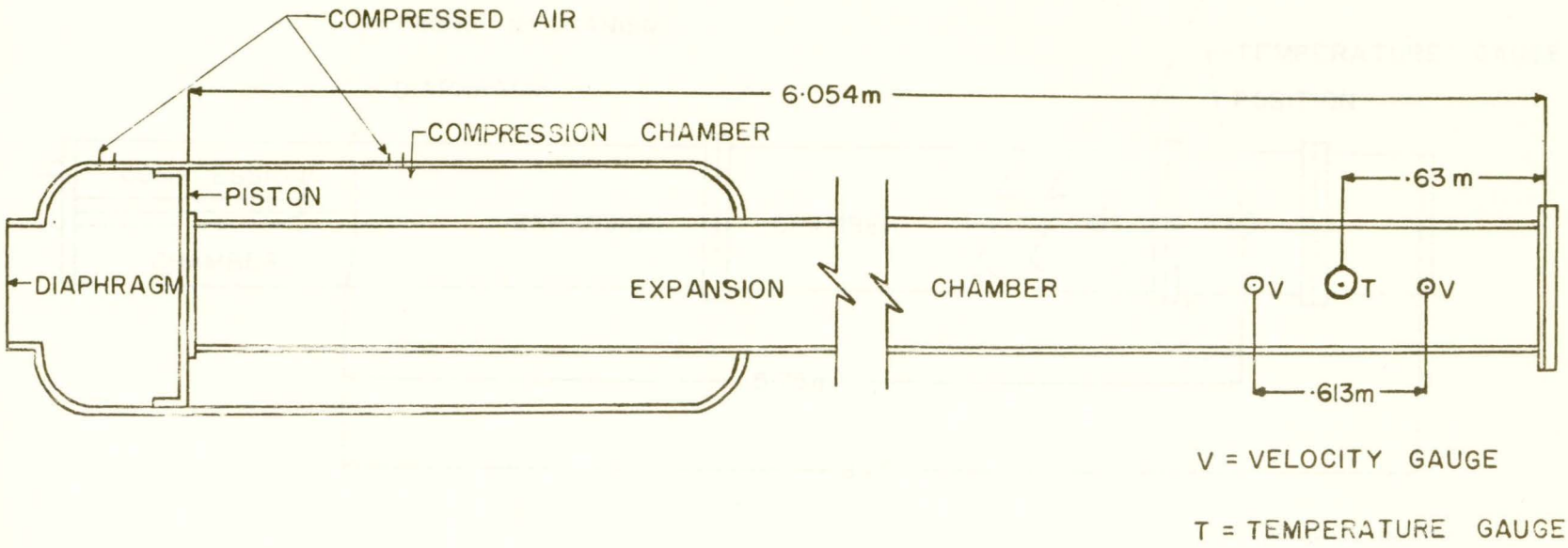

Fig. 4.1.1 The 4" x 4" constant cross-section shock tube

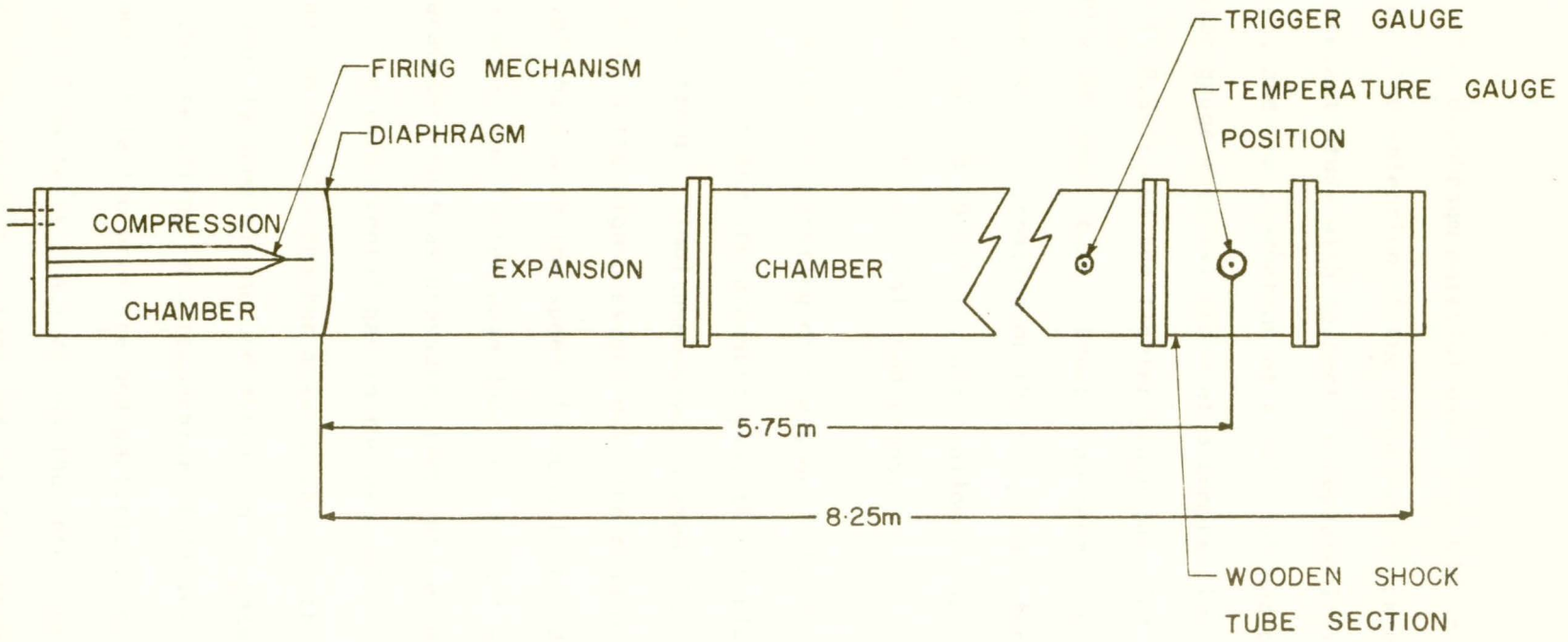

Fig. 4.1.2 The 3" x 10" constant cross-section shock tube

The diaphragm material used was .005 or .01 inch thick celluloid. The selection of the diaphragm thickness was important for the present study with respect to repeatability of the flow parameters, and the production of a well-defined planar shock front. The heavier gauge material broke at a compression chamber pressure of about 55 P.S.I. and the lighter gauge material at about 25 P.S.I. in the 3" x 10" shock tube. These diaphragms produced a minimum of attenuation to the formation of the shock wave for respective over-pressures of 50 and 20 P.S.I., while allowing sufficient control for establishing the initial conditions.

After the bursting of the shock tube diaphragm, a compression wave is formed in the low-pressure gas, this rapidly steepening to form a shock front. Simultaneously, an expansion or rarefaction wave moves back into the high-pressure gas; the head of this rarefaction wave travels back with the speed of sound in the driver gas. Unlike the shock wave, the latter wave does not exhibit abrupt discontinuities of gas parameters such as pressure, temperature, density and particle velocity. The experimental gas in the expansion chamber and the driver gas in the compression chamber make contact at the "contact surface". There is usually some mixing and diffusion of gases at the contact surface, thus resulting in a temperature fall less sudden than at the shock front, while the pressure and particle velocity remain equal since no gas flow takes place across the interface. The movements of the shock front, contact surface and rarefaction wave are shown in the "x-t" diagram in Figure 4.1.3.

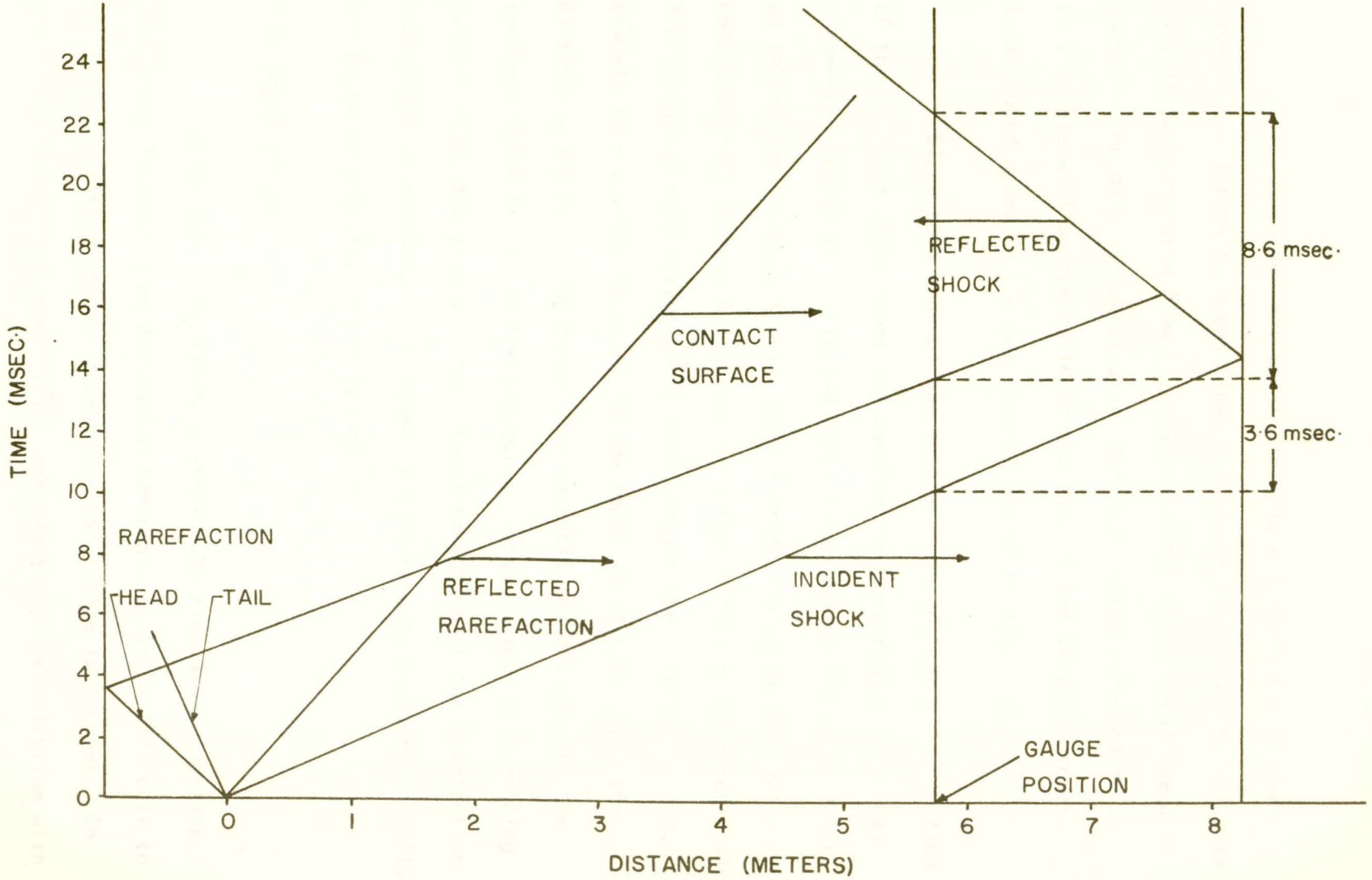

Fig. 4.1.3 An x-t diagram of the flows in the 3" x 10" shock tube with respect to a gauge located 5.75 meters from the diaphragm

It is convenient now to introduce the concept of mach number in relation to a gas flow; this is the ratio of the velocity of a disturbance or a flow in a gas relative to the local speed of sound in the gas. In particular, the mach number referred to in this thesis will be the ratio of the shock front velocity to the local sound speed in the gas directly ahead of the shock wave.

Since both ends of the tube are closed, normal reflection of the incident shock front and rarefaction wave result. The gas parameters behind the reflected shock front follow the same pattern as behind the incident front; the one exception being the particle velocity which is zero with respect to the shock tube upon reflection. The reflected rarefaction wave, once through the rarefaction fan, travels with a velocity equal to the local sound speed plus the particle velocity of the flow. Consequently the gas between the incident shock front and the contact surface, instead of remaining quasi-steady, decays with time. The interaction of the rarefaction wave produces a monotonic decrease in temperature, pressure, density and particle velocity of shocked gas.

4.2 Gauge design

Since many portions of a shock tube flow are in a state of rapidly increasing or decreasing temperature, it is difficult to construct an instantaneous temperature monitoring instrument. On the other hand, a device which can achieve thermal equilibrium with

the flow temperature at some instant in time can be used to furnish the gas temperature at that particular time. The technique involves the use of a metallic film, in the order of 1 micron thick, used as a resistance thermometer. The prime requirements for such a transducer are rapid response time and a high sensitivity to heat transfer. Rapid response time is required to provide suitable resolution of temperature as a function of time, while a high sensitivity to heat transfer rates is required in order to produce a usable signal.

In 1956 R.J. Vidal made a survey of materials suitable for the fabrication of thin films, considering their durability, operational reliability and ease of construction. The material which best satisfied the above qualities was Hanovia Liquid Bright Platinum #05-x* deposited on a pyrex base.

4.3 Gauge construction

A six-inch length of one-centimeter diameter pyrex tubing was sealed at one end. The closed end was ground flat by using, successively, 500 A soft-black waterproof silicon carbide paper, Crystal Bay Crocus cloth #105, and gold rouge. The glass was thoroughly cleaned with alcohol. A strip of platinum about 1/8" wide was applied with a brush across the polished end and about 1/2" down the sides. The tube was immediately placed in a cool

---

* Hanovia Liquid Gold Division, 1 West Central Avenue, East Neward, New Jersey.

oven (200°F) and heated to 1250°F. The average time for the curing process was about 1¼ hours. At termination of heating, the tube was immediately extracted from the furnace and air quenched.

The first paint application produced a film resistance of about 700 ohms. A second brushing followed by the above curing procedure provided a film with a resistance of 30 - 100 ohms. A resistance in this range produced negligible joule heating with a current of 1 milliampere.

Size 26 copper lead wires were attached with #60 Kister solder to the side extensions of the thin film. The wires were placed as close to the polished face as possible. This procedure insured that only the face of the probe contributed to its total resistance. During application of the film surface, several short deposits of paint were made down either side of the pyrex tube. These patches provided additional attachment points for the lead wires and added strength to the copper-platinum joint. The final step consisted of coating the wires with epoxy resin to increase their durability against excessive loading strains. The tube was then glued into a plexiglass sleeve as shown in Figure 4.3.1.

The heating element, Figure 4.3.2, was constructed with size 29 chromel-A wire. Thirteen turns were wound on a 1/16" diameter copper rod. The coil was removed from the rod and .020"

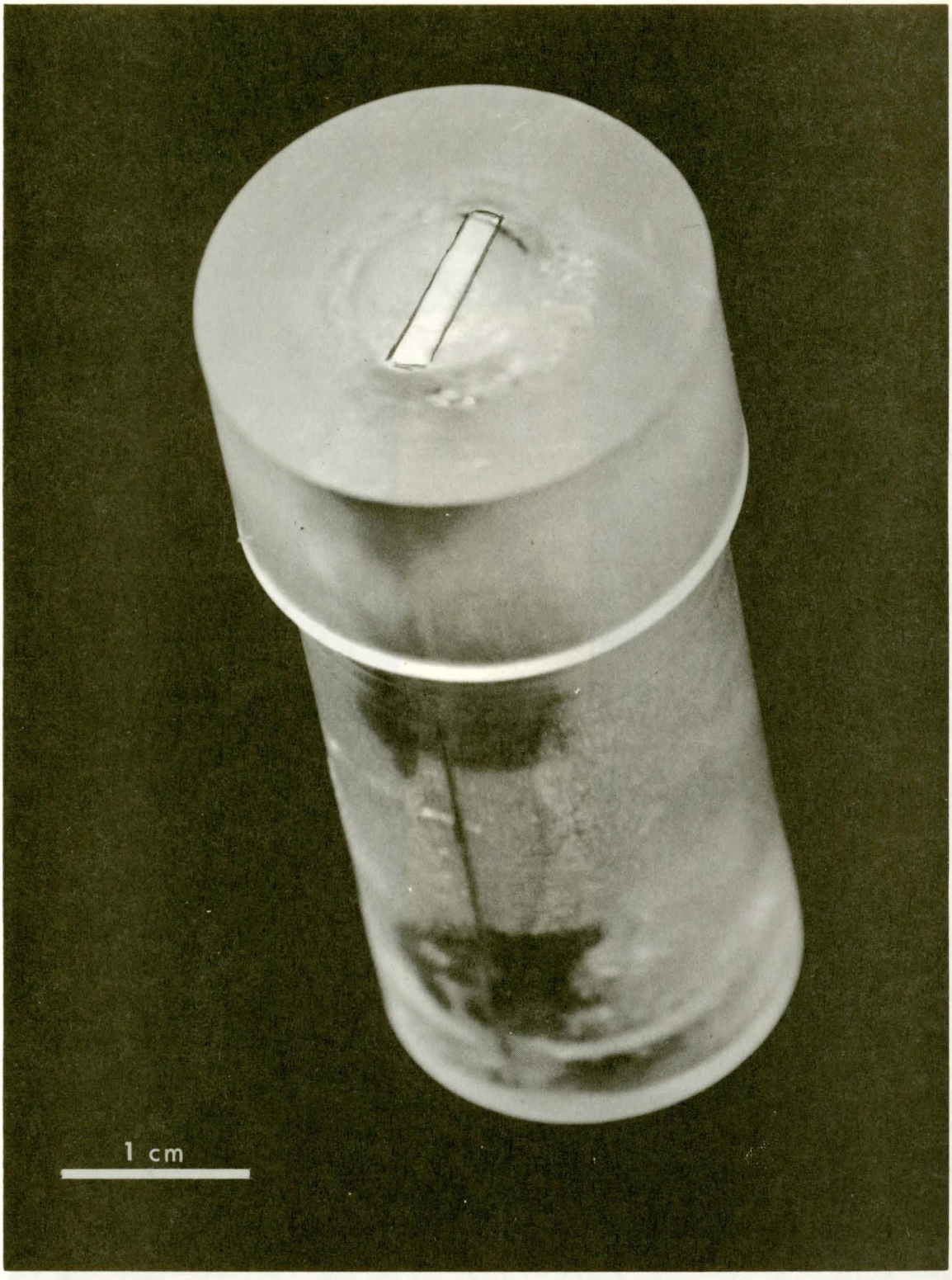

Fig. 4.3.1 The pyrex tube supporting the platinum film imbedded in a plexiglass sleeve

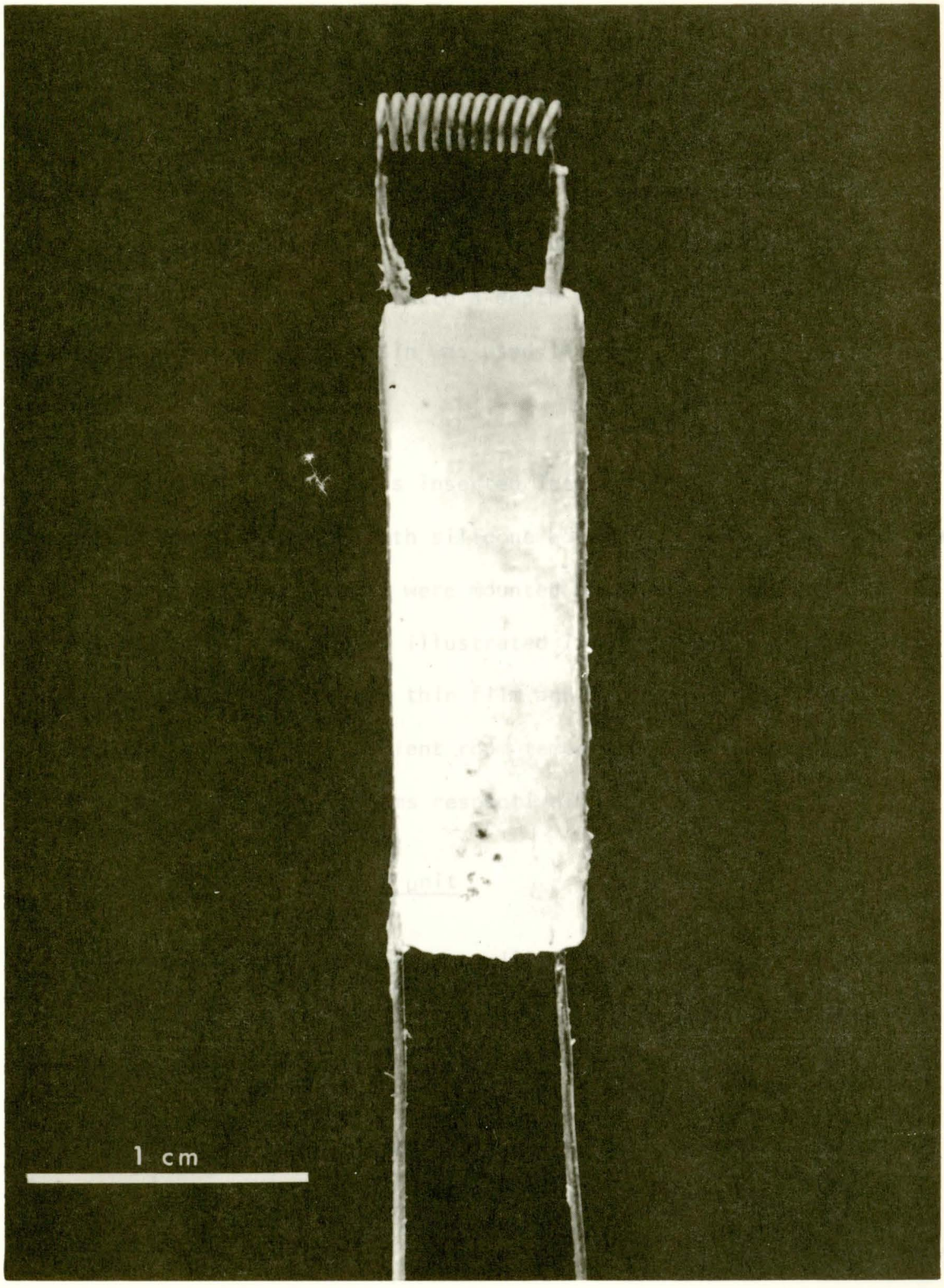

Fig. 4.3.2 The temperature transducer heating element

copper lead wires were silver-soldered to the element. The average resistance of such elements was about 1.2 ohms. The element was mounted on a circular ceramic insulator which was ground to the inside diameter of the pyrex tube. Slots were cut with a diamond tooth saw down the sides of the insulator to a depth sufficient to insert the copper lead wires. Epoxy resin was used to bond the lead wires to the base.

The heating unit was inserted into the pyrex tube 1/4" from the closed end, and sealed with silicone adhesive. The sleeve containing the gauge and heating element were mounted as shown in Figure 4.3.3. A plexiglass collar was made as illustrated in Figure 4.3.4 to facilitate electrical connections to the thin film and heater element. The approximate resistance at ambient room temperature of the two gauges constructed were 45 and 75 ohms respectively.

4.4 Oscilloscope and plug-in unit

A Tektronix 549 storage oscilloscope with a type 1A2 plug-in unit was used to monitor and display pressure-time and temperature-time records.

The type 1A2 Dual-Trace Plug-In Unit contained two identical fastrise calibrated preamplifier channels with maximum sensitivities of 50 mv./cm. Either channel could be used independently, or electronically switched through the chop mode, to produce dual-trace displays. Each channel had its own input, gain, polarity, and position controls which allowed each display to be adjusted independently for optimum viewing.

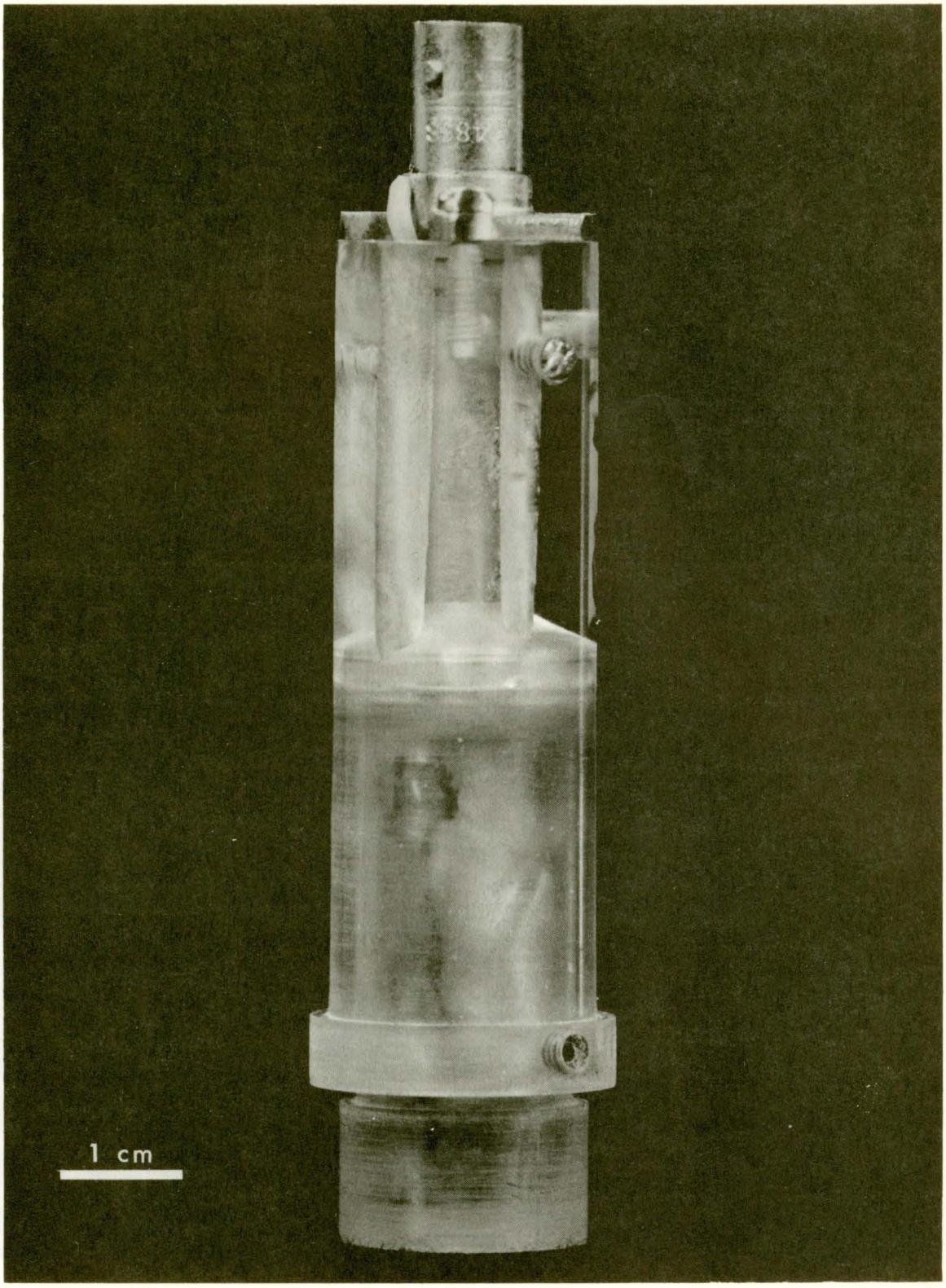

Fig. 4.3.3 Sleeve containing platinum film and heating element

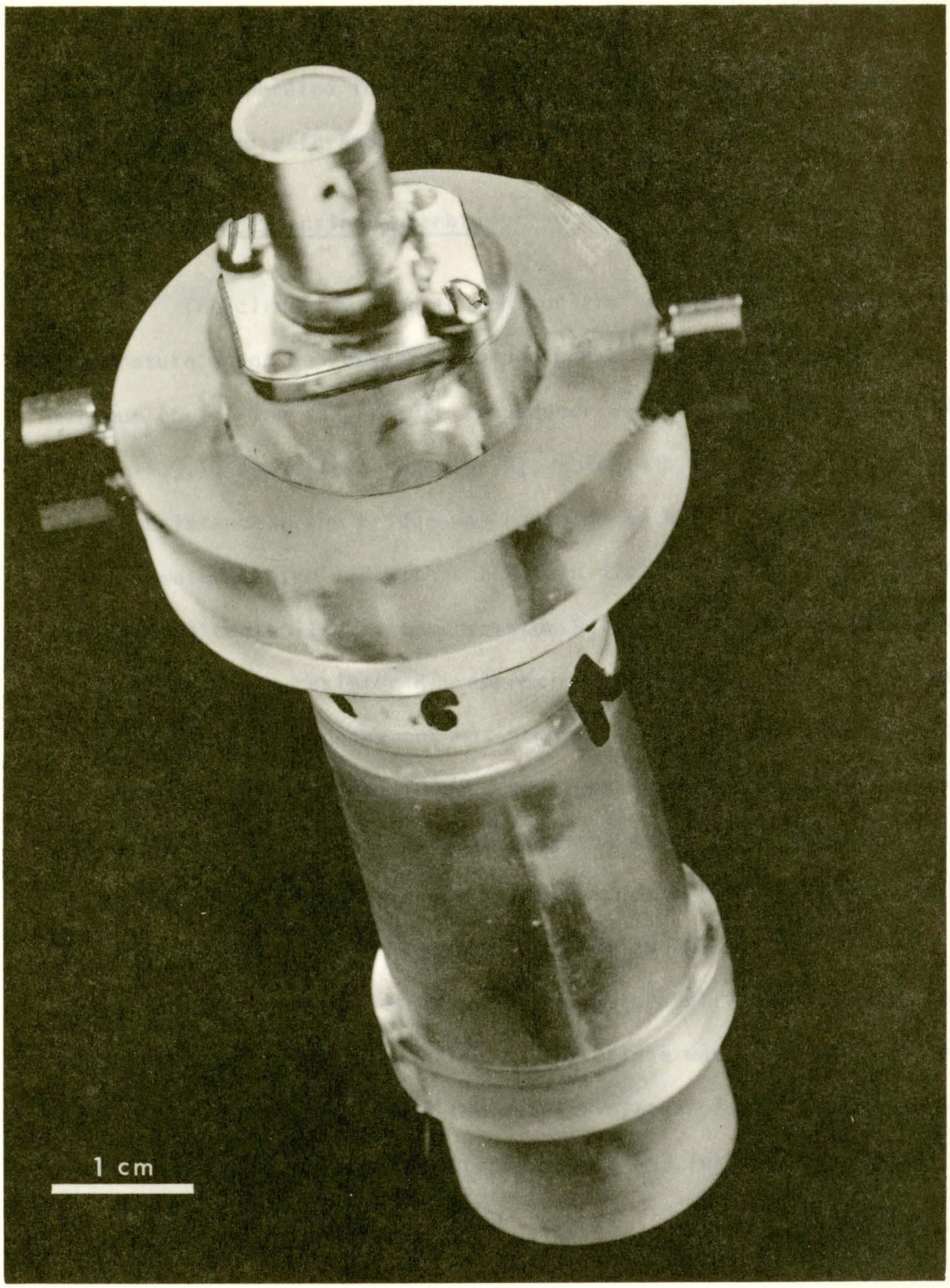

Fig. 4.3.4 Transducer with plexiglass collar to facilitate connections to the heating element

Both channels operated in the DC coupling mode. The ground mode was used as a ground reference.

4.5 Temperature sensing apparatus

The circuitry used to monitor the voltage change across the temperature gauge was designed to produce a large voltage output at a minimum cost. The temperature transducer was incorporated in a bridge, Figure 4.5.1, opposite a resistor R_1, which was the mean value of the gauge-resistance. The bridge was balanced by R_2, a 1000 ohm precision potentiometer controlled with a ten turn dial. The 1 milliampere bridge current was controlled by the resistor R_3. The ammeter was placed in parallel with the resistor R_a, approximately equivalent to its internal resistance. This arrangement was necessary since small vibrations of the ammeter coil produced induced voltages which appeared as noise on the oscilloscope. Thus, before firing the shock tube, the switch S was set to include R_a in the bridge circuit and a slight adjustment of R_2 was made to rebalance the bridge. A Phillips TAA243* operational amplifier was connected across the bridge to amplify the voltage change with respect to a balanced bridge. The bridge was in balance for a given gauge temperature when the output voltage of the amplifier was zero. This condition was monitored by the 549 Tektronix storage oscilloscope.

---

* Philips Electron Devices, 116 Vanderhoof Avenue, Toronto 17, Ontario

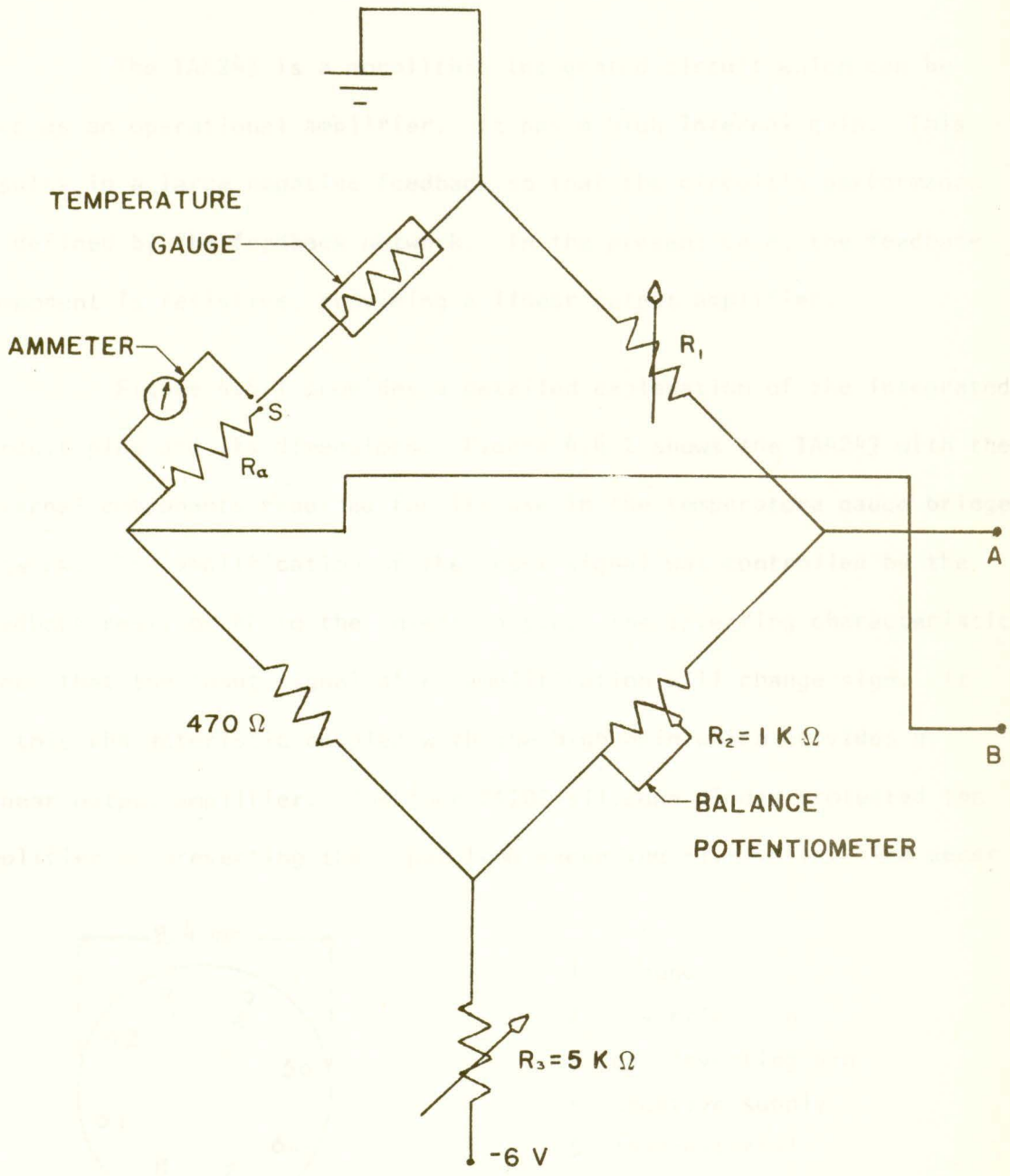

Fig. 4.5.1 The temperature bridge

4.6 Phillips TAA243 operational amplifier

The TAA243 is a monolithic integrated circuit which can be used as an operational amplifier. It has a high internal gain. This results in a large negative feedback so that the circuit's performance is defined by the feedback network. In the present case, the feedback component is resistive, providing a linear output amplifier.

Figure 4.6.1 provides a detailed explanation of the integrated circuit pins and its dimensions. Figure 4.6.2 shows the TAA243 with the external components required for its use in the temperature gauge bridge network. The amplification of the input signal was controlled by the feedback resistor RF to the inverting pin. The inverting characteristic means that the input signal after amplification will change sign. It is this characteristic coupled with the high gain which provides a linear output amplifier. The four 0A205 silicone diodes protected the amplifier by preventing the input from exceeding -1.4 volts. The zener

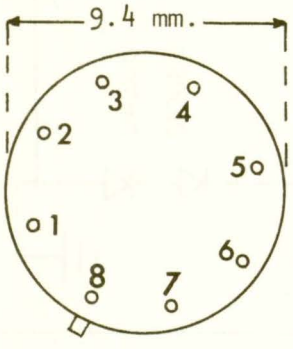

Fig. 4.6.1 Pin locations of the TAA243 op. amp.

1 ground
2 inverting pin
3 non-inverting pin
4 negative supply
5 lead-external
6 lag-frequency compensation
7 output
8 positive supply

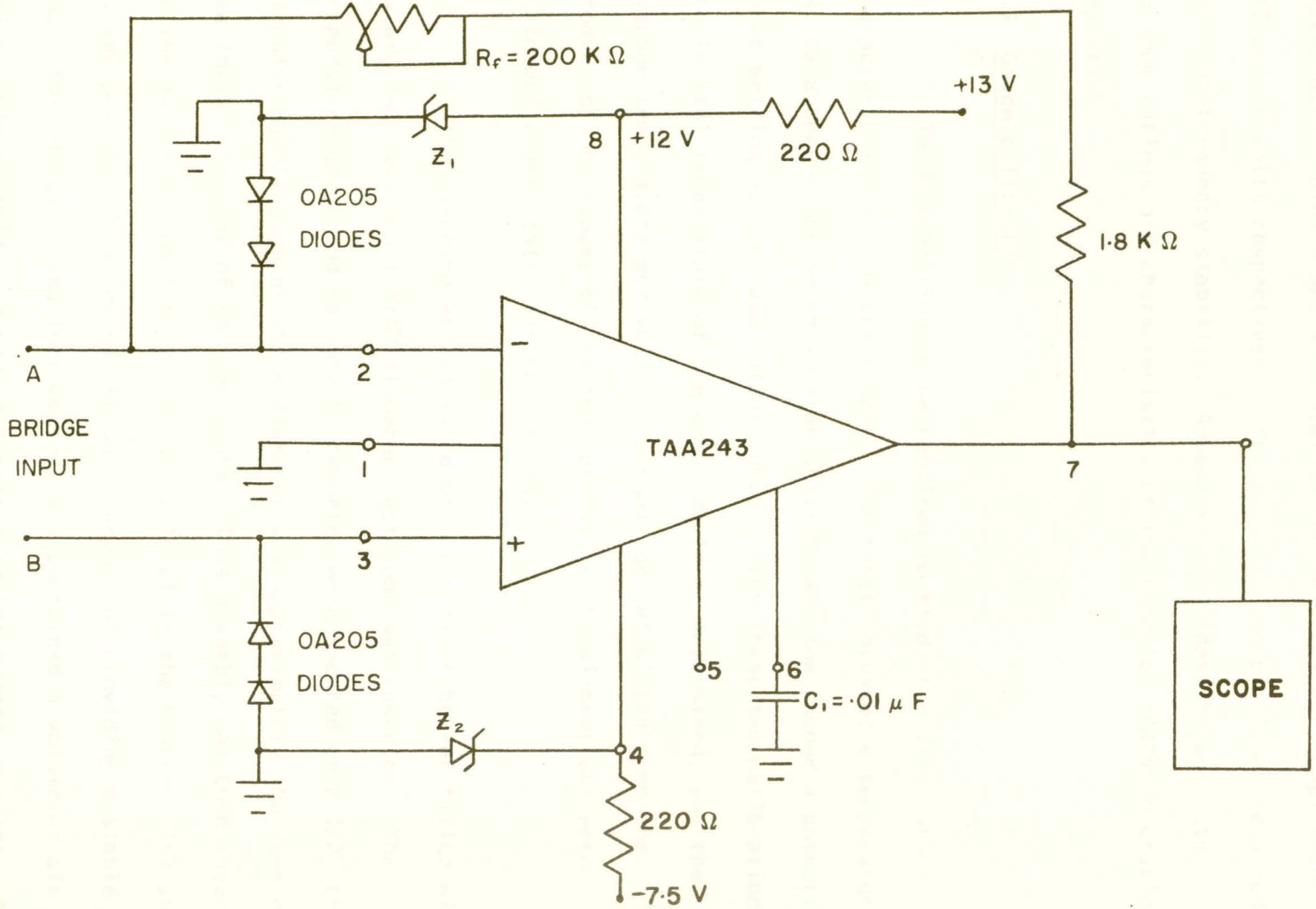

Fig. 4.6.2 The TAA243 amplifier with external components

diodes across pins 8 and 4 maintained constant voltage supplies of +12 and -6 volts respectively. The capacitor to pin 6 was required for high frequency stability. Appendix B provides the absolute maximum ratings and characteristics of the Phillips TAA243 operational amplifier.

4.7 Gauge calibration

Two calibrations were required to study the temperature characteristics of the transducer. The first involved a temperature vs. balanced bridge potentiometer setting, and the second a potentiometer setting vs. voltage output curve. From these two calibrations the initial temperature of the gauge could be determined, and the average temperature per volt ratio could be calculated from the product of the slopes of the two curves. Both calibrations were performed under static air conditions.

The calorimeter consisted of a two liter beaker filled with water, into which a 1-3/4" diameter test tube was inserted. The temperature gauge and mercury thermometer were secured on a 1/2" thick circular paxoline mount whose diameter was approximately the same as the inside diameter of the test tube. This assembly was then inserted in the test tube, well below the water level in the beaker. The snugly fitted paxoline disc served the dual purpose of providing a stable mount for the gauge and thermometer, and contained a volume of air which could be held at a stable temperature for several minutes. A thermostatically controlled heater was used to vary the temperature

of the water bath. Figure 4.7.1 shows the assembled apparatus for the gauge calibration.

The bridge potentiometer dial reading vs. the gauge temperature calibration was performed as follows. The calorimeter heater was preset to provide a specific air temperature in the test tube. Once a stable temperature had been attained, the bridge circuit was balanced with the precision potentiometer ten turn dial. With the storage oscilloscope amplifier sensitivity set at 0.5 volts/cm., the balanced condition was obtained by comparing the bridge voltage output to the ground level mode of the oscilloscope. It was found that at lower oscilloscope sensitivities, the change in the trace position compared to a small incremental turn of the potentiometer dial was too large to be of any value in determining the null point. The ten turn dial was read to .005 parts of a turn. Figure 4.7.2 is a potentiometer reading vs. temperature calibration for gauge #2.

The second calibration entailed the measurement of the output voltage from an initially balanced bridge with respect to the potentiometer dial reading. Since the maximum output voltage of the operational amplifier was ±5 volts, several curves were plotted which covered the full range of potentiometer settings corresponding to temperatures from ambient to 100° C. This was accomplished by heating the gauge to successively higher constant temperatures for which the bridge was balanced, and varying the potentiometer to produce output voltages in increments of .4 volts up to a maximum of 2.8 volts. The voltage

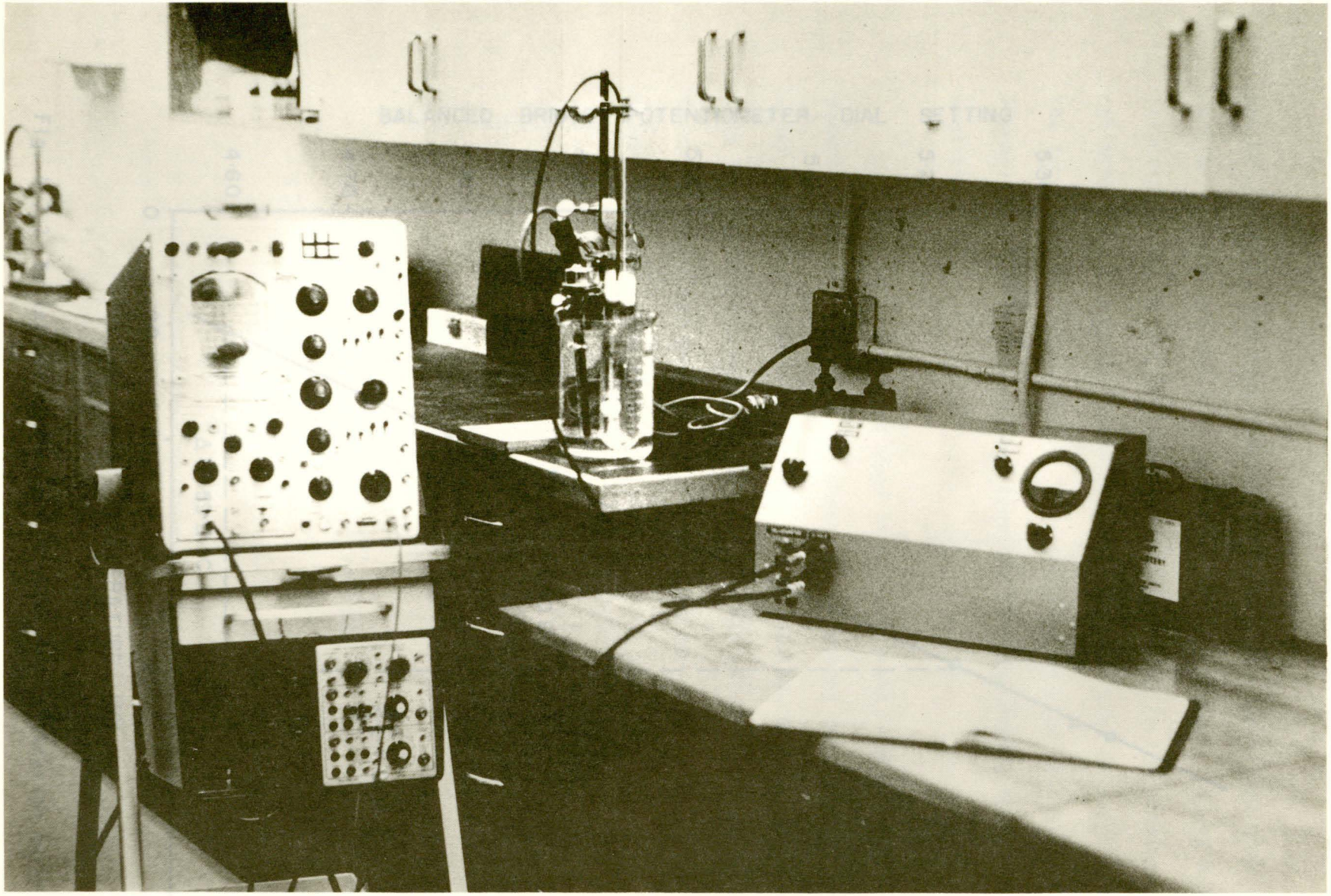

Fig. 4.7.1 View of electronic apparatus for gauge calibration

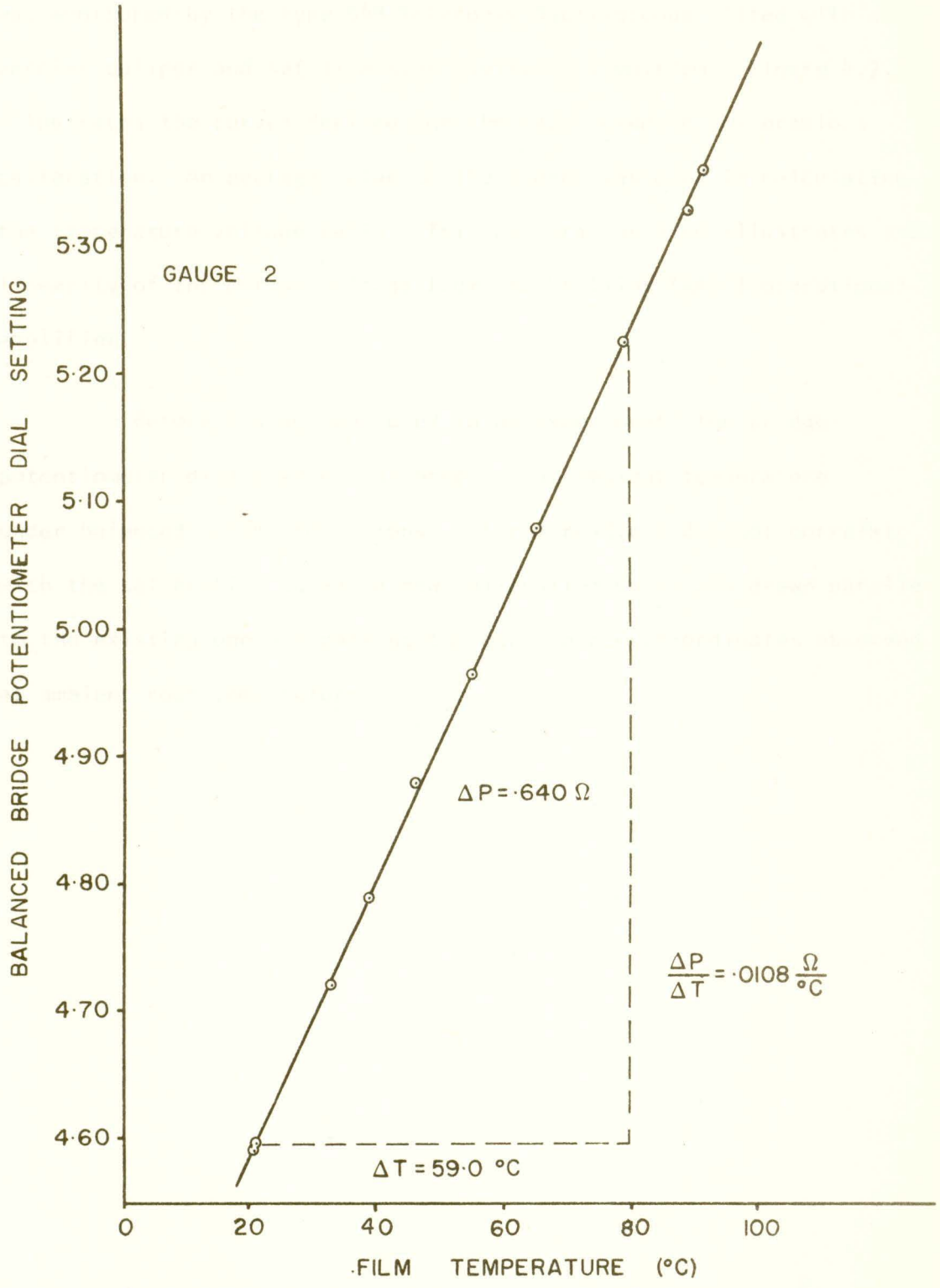

Fig. 4.7.2 Resistance thermometer temperature calibration curve

was monitored by the type 549 Tektronix Oscilloscope fitted with a vernier caliper and set at a sensitivity of 1 volt/cm. Figure 4.7.3 illustrates the curves derived for the gauge used in the previous calibration. An average value of the slopes was used in calculating the temperature voltage ratio. This calibration also illustrates the linearity of the output voltage from the Phillips TAA243 operational amplifier.

Before a gauge was used in an experiment, the bridge potentiometer dial reading was observed at ambient temperature under balanced bridge conditions. If the readings did not correlate with the calibration curve, a new calibration curve was drawn parallel to the existing one and passing through the new co-ordinates observed at ambient room temperature.

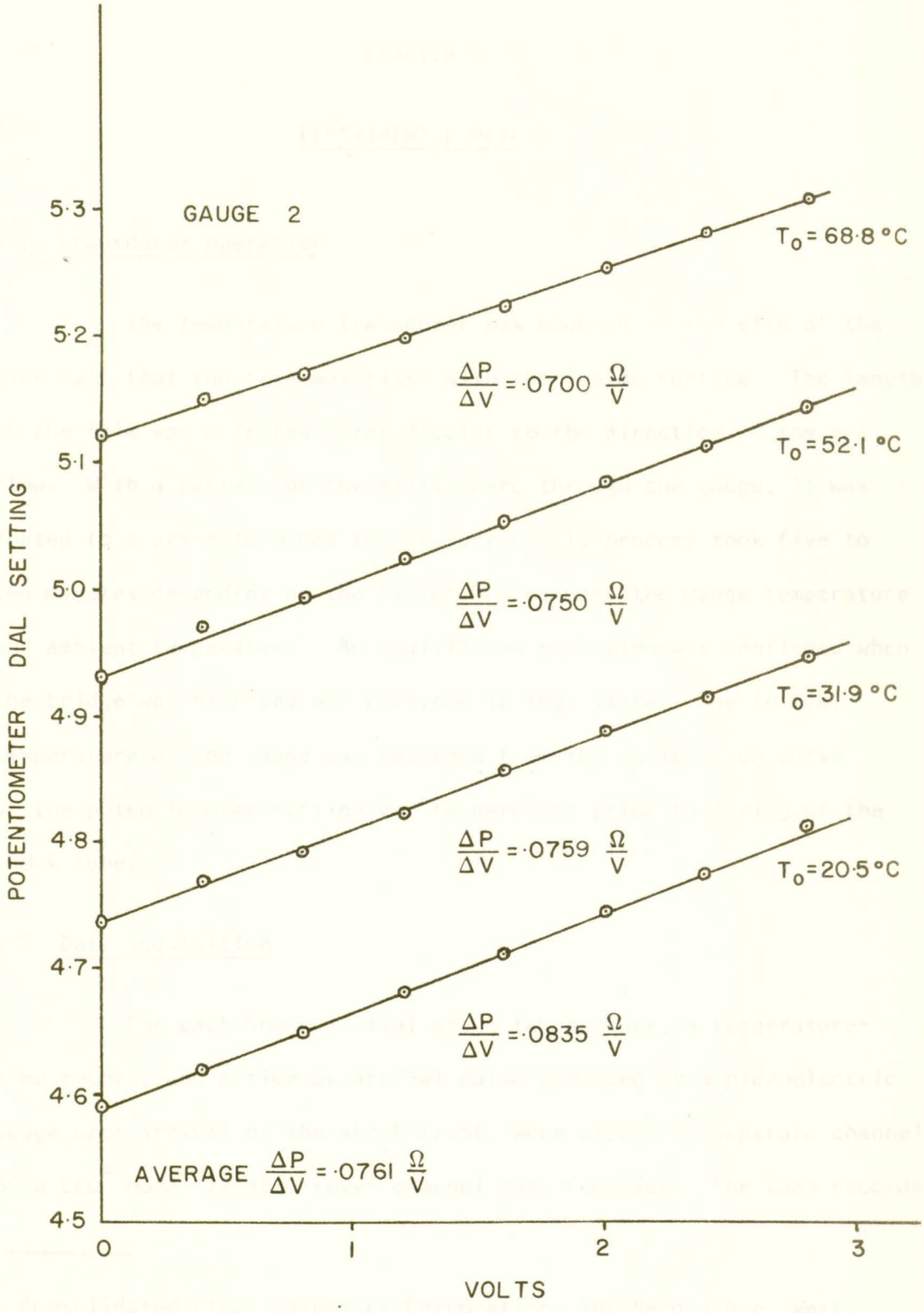

Fig. 4.7.3 Resistance thermometer voltage calibration curves for a balanced bridge

CHAPTER 5

EXPERIMENTAL METHOD

5.1 Transducer operation

The temperature transducer was mounted in the side of the tube such that the face was flush with the inside surface. The length of the film was oriented perpendicular to the direction of the gas flow. With a current of one milliampere through the gauge, it was heated to a pre-determined temperature. This process took five to ten minutes depending on the difference between the gauge temperature and ambient temperature. An equilibrium condition was confirmed when the bridge was balanced and remained in that state. The initial temperature of the gauge was recorded from the calibration curve of the potentiometer setting vs. temperature prior to firing of the shock tube.

5.2 Data acquisition

For each known initial gauge temperature, a temperature-time record, and a time of arrival pulse produced by a piezoelectric gauge upon arrival of the shock front, were stored on separate channels of a CEC* Model V2-3600 seven channel tape recorder. The tape recorder

---

* Consolidated Electrodynamics Corporation, 302 Second Ave. West, Seattle, Washington.

made it possible to set up the oscilloscope time base and sensitivity for optimum viewing by replaying the stored results. The temperature vs. time signal from the tape recorder, and its differential wave form, were simultaneously displayed on the 549 storage oscilloscope. The time of arrival pulse from the tape recorder was used to trigger the oscilloscope. A 35 mm. picture (Johnson, 1968) of the stored oscilloscope traces was taken for a permanent record. Measurement of the traces was made from large photographic prints. Figure 5.2.1 shows the electronic components used for gathering and processing the data.

To determine the rate-of-change of voltage of the temperature transducer, the output signal was input into a Tektronix Type-O operation amplifier arranged in the differentiating mode.

Electronically, an operation amplifier is simply a high-gain amplifier designed to remain stable with large amounts of negative feedback from output to input. Since an operational amplifier with a resistor as a feedback element responds with an output voltage equal to the product of the input current and feedback resistance, a differential output may be obtained using a capacitor as an input impedance. The current through a capacitor is proportional to the rate-of-change of voltage across the capacitor. For a steady DC voltage, then, there is no passage of current and the output of the operational amplifier is zero. If the voltage output across the capacitor is changed,

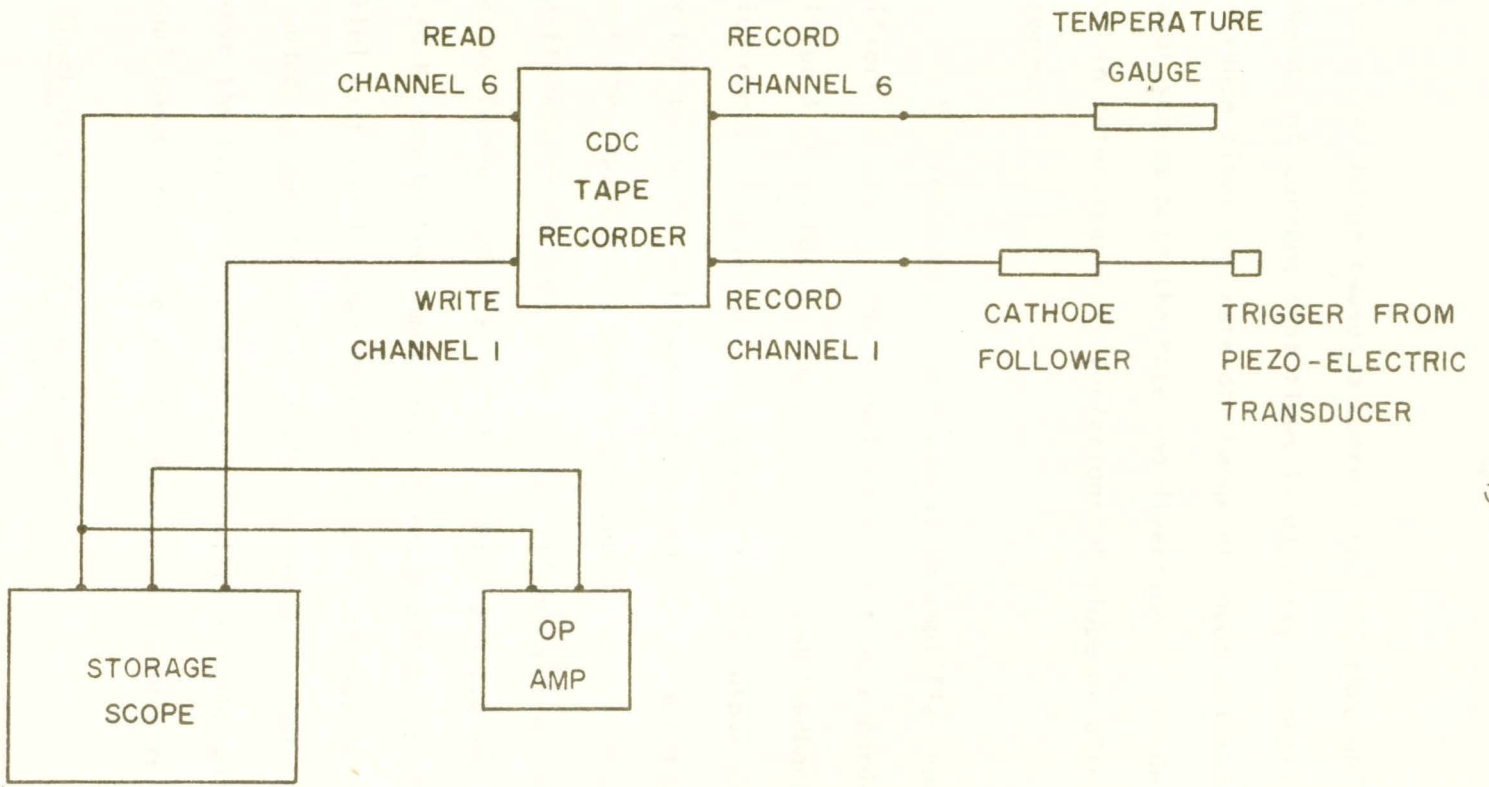

Fig. 5.2.1 Instrumentation block diagram for data acquisition

however, the change causes a current to flow through the capacitor. The amount of current that flows is directly proportional to the capacitance times the rate-of-change of input voltage. The differentiator senses both the rate and direction of change and is very useful in detecting small variations of slope or discontinuities in waveforms.

The Tektronix Type-0 operation amplifier had two identical amplifiers, A and B. The signal from the tape recorder was input into amplifier A which had an input resistance and feedback resistance of 1×10^6 ohms. The gain of the signal at the output of A was thus unity but the high resistance of the amplifier acted as a buffer between the tape recorder and amplifier B. The latter was used in the differentiating mode with a capacitive input of .01 μf and a resistive feedback of 1×10^6 ohms. Figure 5.2.2 indicates a resistance of 5.36 K ohms between amplifiers A and B and a 476 pf capacitor in parallel with the impedance feedback of B. These latter two components were added to amplifier B to diminish the noise and at the same time conserve the rapid response of the amplifier. The values of the external components were determined by trial and error.

5.3 Shock tube initial conditions

Three experiments, A, B and C were performed; A in the 4" x 4" shock tube, and B and C in the 3" x 10" tube. The former

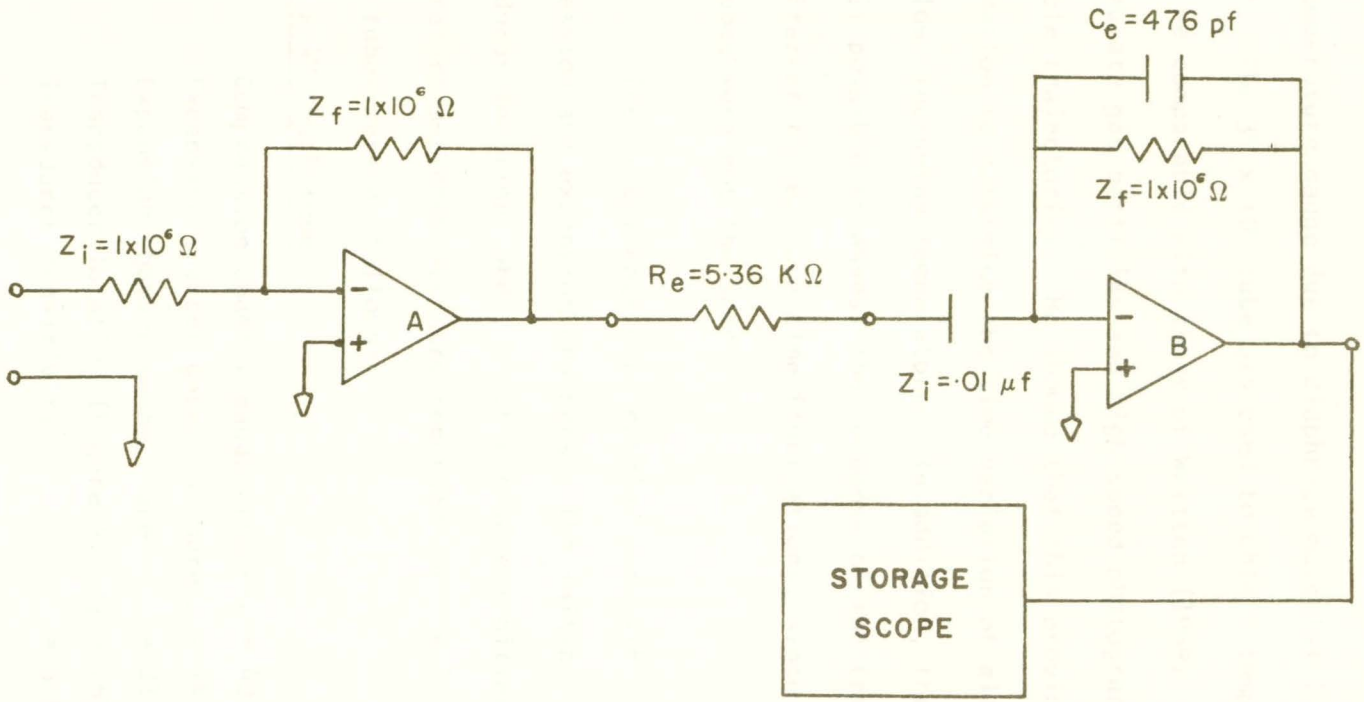

Fig. 5.2.2 Tektronix Type-0 operation amplifier arranged in the differentiating mode

tube was chosen for the initial tests to alleviate possible damage to the temperature gauge due to diaphragm material in the gas flow (Figure 4.1.1). The 3" x 10" tube was used to obtain temperature results which would be comparable with those of Whitten (1969), who used smoke tracers to simulate gas particles and high speed photography to follow the particle trajectories. He showed that this provided sufficient information to determine the time variation of all the parameters of the flow, including temperature. In addition, the use of two tubes made it possible to assess the response of the temperature transducer to different temperature-time fluctuations, since the flows in the two tubes were not the same.

The experiments were carried out with air in both the compression and expansion chambers. The initial conditions and transducer locations under which pressure (Whitten (1969)) and temperature measurements were recorded for the 4" x 4" and 3" x 10" shock tubes were as follows:

A. 4" x 4" shock tube

Compression chamber gauge pressure = 40 P.S.I.
Expansion chamber gauge pressure = 14.6 P.S.I.
Expansion chamber temperature = 23.5° C
Transducer location (Figure 4.1.1) = .63 m.
Transducer sensitivity = 5.5° C/volt

B. 3" x 10" shock tube

Compression chamber gauge pressure = 50.0 P.S.I.
Expansion chamber gauge pressure = 14.8 P.S.I.
Expansion chamber temperature = 25.4° C
Transducer location (Figure 4.1.2) = 5.75 m.
Transducer sensitivity = 7.04° C/volt

C. 3" x 10" shock tube

Compression chamber gauge pressure = 20.0 P.S.I.
Expansion chamber gauge pressure = 14.8 P.S.I.
Expansion chamber temperature = 23.5° C
Transducer location (Figure 4.1.2) = 5.75 m.
Transducer sensitivity = 7.04° C/volt

5.4 The 3" x 10" wooden shock tube section

The temperature gauge was mounted in a wooden section of the 3" x 10" tube. The section was 0.5 meters long and constructed of two layers of 3/4" plywood reinforced with angle iron. The inner surfaces were lined with 1/8" thick arborite. A brass recepticle was built onto one side, into which the temperature transducer was fitted. Figure 5.4.1 shows the wooden section and electronic apparatus.

5.5 "Theoretical" temperature determinations

Gas temperature profiles were derived from pressure-time measurements to provide a comparison with temperatures obtained using the thin film resistance thermometer. The pressure transducer was calibrated by measuring the shock velocity at the gauge position and

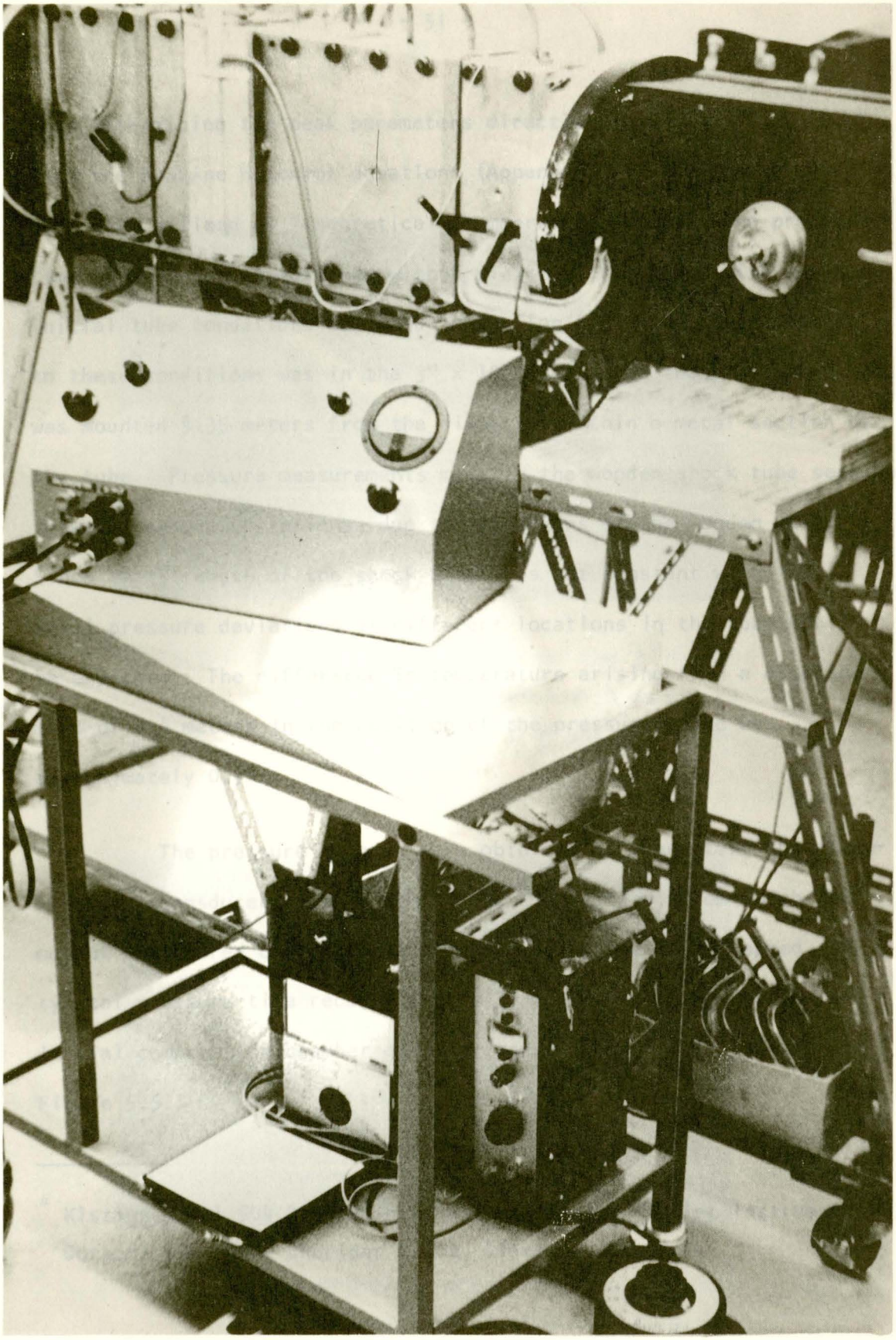

Fig. 5.4.1 View of the 3" x 10" wooden shock tube section with the temperature gauge mounted

thus determining the peak parameters directly behind the shock front from the Rankine Hugoniot equations (Appendix C). The former profiles have been defined as "theoretical" temperature curves. The pressure-time measurements were taken with a piezoelectric gauge with the same initial tube conditions outlined in section 5.3. The one exception to these conditions was in the 3" x 10" tube where the pressure gauge was mounted 5.35 meters from the diaphragm within a metal section of the tube. Pressure measurements made in the wooden shock tube section showed pressure variations, due to vibrations of the wooden walls. Since the strength of the shock front was not constant with time, small pressure deviations at different locations in the tube could be expected. The difference in temperature arising from a displacement of 0.4 meters in the position of the pressure gauge was approximately 0.3%.

The pressure records were obtained by connecting the piezoelectric transducer to a linear Kistler* amplifier, from which the output was stored on the oscilloscope display and photographed. A typical pressure-time record for the 3" x 10" shock tube having an initial compression chamber gauge pressure of 50 P.S.I. is shown in Figure 5.5.1.

---

* Kistler Model 504 Dial-Gain Charge Amplifier, Kistler Instrument Corporation, 8989 Sheridan Drive, Clarence, New York

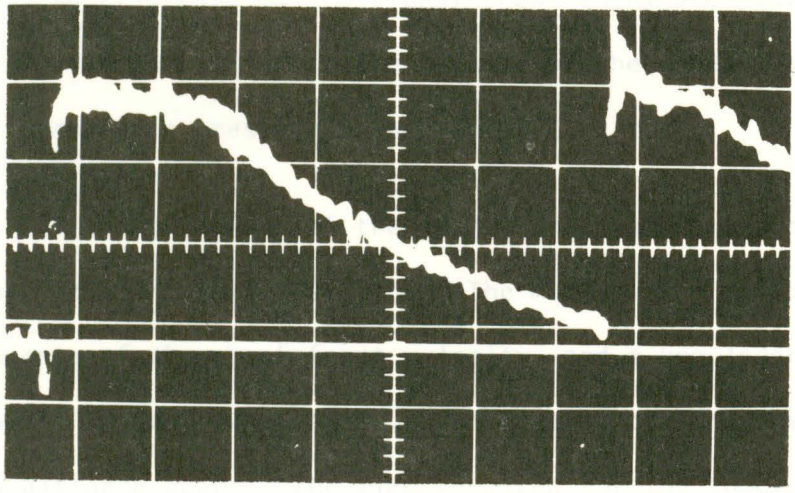

Fig. 5.5.1 Pressure-time record from the 3" x 10" metal shock tube section with gauge located 5.35 meters from the diaphragm.

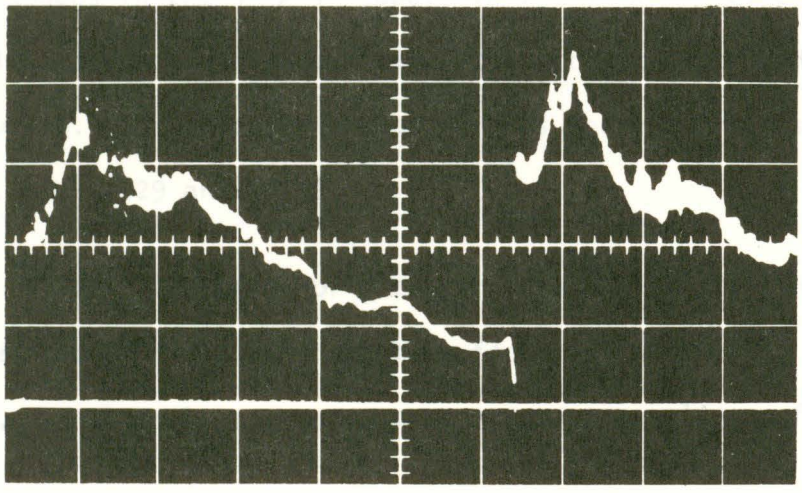

Fig. 5.5.2 Pressure-time record from the 3" x 10" wooden shock tube section with gauge located 5.75 meters from the diaphragm.

A pressure profile obtained from the wooden shock tube section is shown in Figure 5.5.2. There appeared to be an oscillatory wave-form superimposed on the signal shown in Figure 5.5.1. This phenomenon was attributed to the flexing of the wooden walls which created transverse pressure pulses across the tube.

The mach number of the shock front was required for determining the "theoretical" gas temperature. The mach number was determined from measurements of the shock front velocity, and a knowledge of the speed of sound at ambient temperature. Two piezoelectric gauges were placed a known distance apart. The time required for the shock wave to traverse the distance between the two gauges was recorded on a Racal* interval timer. Thus the average velocity of the shock wave was calculated. The velocity of sound was taken from gas tables provided in the shock tube laboratory. Figure 4.1.1 illustrates the position of the gauges in the 4" x 4" tube. In the 3" x 10" tube (Figure 4.1.2) piezoelectric gauges were substituted for the trigger and temperature transducers. The respective mach numbers for experiments A, B and C were 1.189, 1.329 and 1.178.

The calculation of a temperature profile from a pressure profile assumed that the shock tube flow was isentropic, i.e. P/ρ^{γ} = const., and that the pressure gauge output was a linear function of

---

* Racal Timer Model SA535, Racal Instruments Ltd., Berkshire, England

the gas pressure. Thus, for an isentropic gas flow

$$\frac{T}{T_2} = \left(\frac{P}{T_2}\right)^{\frac{\gamma-1}{\gamma}} \qquad (5.5.1)$$

T_2 and P_2 were calculated using the Rankine Hugoniot relationships (Appendix C).

The temperature behind the reflected shock front was calculated in a similar manner. Since there was an entropy change across the reflected shock, the temperature directly behind the front was required and the procedure is given in Appendix D. Since the experiments involved weak shock waves, $m < 2$, the entropy change across each shock front was small. Thus the theoretical gas temperature profiles were deduced using equation 5.5.1 for the entire flow. Table 5.5.1 illustrates the temperatures calculated using equations 5.5.1 and D.6 for experiment A.

Attenuation of the shock wave in the 3" x 10" wooden shock tube section was apparent from velocity measurements. In the metal section the mach number was 1.348, while in the wooden section it was 1.329. This represented a temperature difference of approximately 3^{o} C across the incident shock front.

Table 5.5.1

Gas temperatures T_a derived from equation 5.5.1, and T_b derived from equation D.6 for experiment A.

Flow Time (msec.)	T_a (^oC)	T_b (^oC)
0	58.79	
1.0	60.20	
2.0	62.95	
3.0	61.78	
3.2	58.79	
4.0	93.33	93.60
5.0	93.33	93.60
6.0	90.01	89.12
7.0	85.46	85.69
8.0	80.76	80.99
9.0	75.90	76.12
10.0	72.13	72.35
11.0	68.27	68.48
12.0	64.29	64.50
13.0	61.57	61.78
14.0	58.79	59.00
15.0	55.96	56.10

Note: Time of arrival of the reflected shock was 3.2 msec.

5.6 Experimental temperature measurements

Three regions in the shock tube flow can be defined as shown in Figures 5.6.1 and 5.6.2. Region 1 denotes a theoretically constant temperature directly behind the incident shock front. Region 2 has a similar temperature profile located directly behind the reflected shock front and Region 3 contains a section of gas providing a monotonic decrease in temperature. Figures 5.6.1 and 5.6.2 illustrate the sequence and comparative magnitudes of the temperature regions with respect to fixed gauge positions for experiments A and B respectively. The magnitudes of the profiles were calculated from pressure-time measurements. The three gas regions imposed different thermodynamic conditions on the temperature transducer, depending on their sequence of arrival at the gauge location. This provided a method of assessing the dynamic gauge response.

Since a single temperature transducer was used to gather the temperature-time profiles, several shock tube trials, each trial having a different initial transducer starting temperature, but the same initial tube conditions, were required to determine the gas temperature profiles. The duplication of initial tube conditions was essential to ensure that the gas temperature at a particular time in the gas flow was identical for each trial. In the 4" x 4" tube eight trials were performed, while in experiments B and C, conducted in the 3" x 10" shock tube, eighteen and ten trials were executed respectively. A larger number of trials was required in experiment B to substantiate the existence of an anomaly in Region 1.

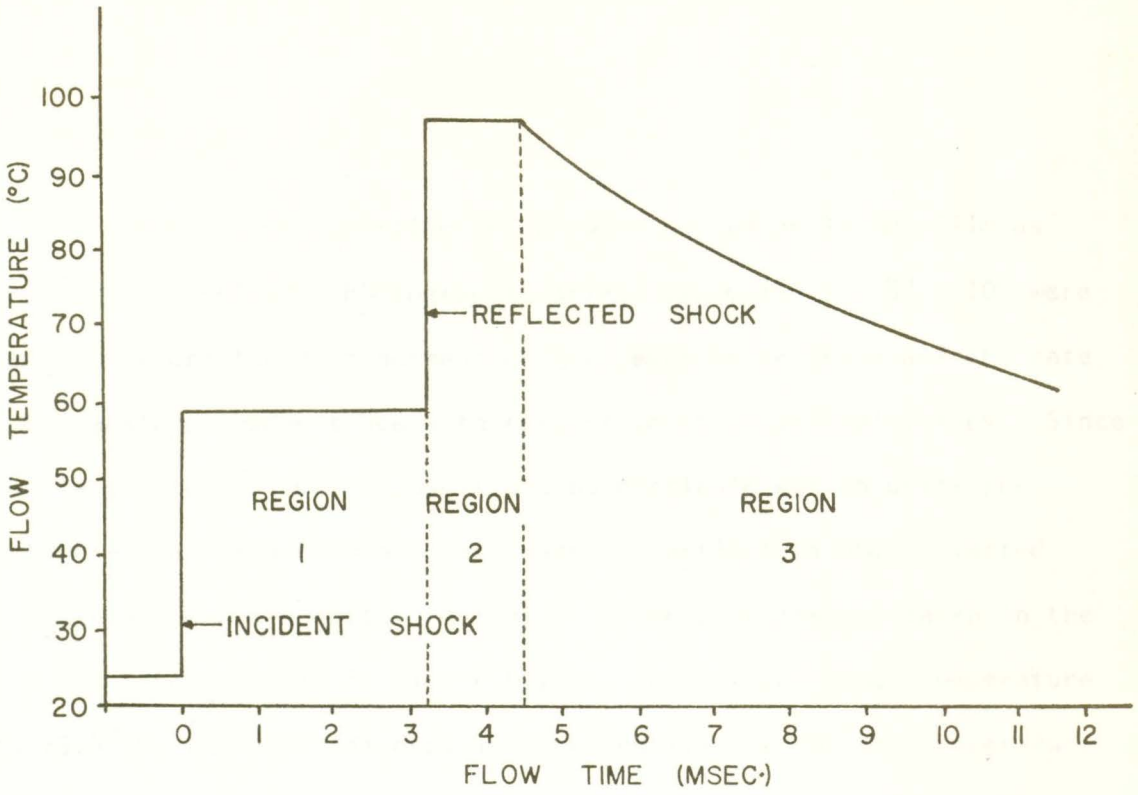

Fig. 5.6.1 Temperature regions of experiment A

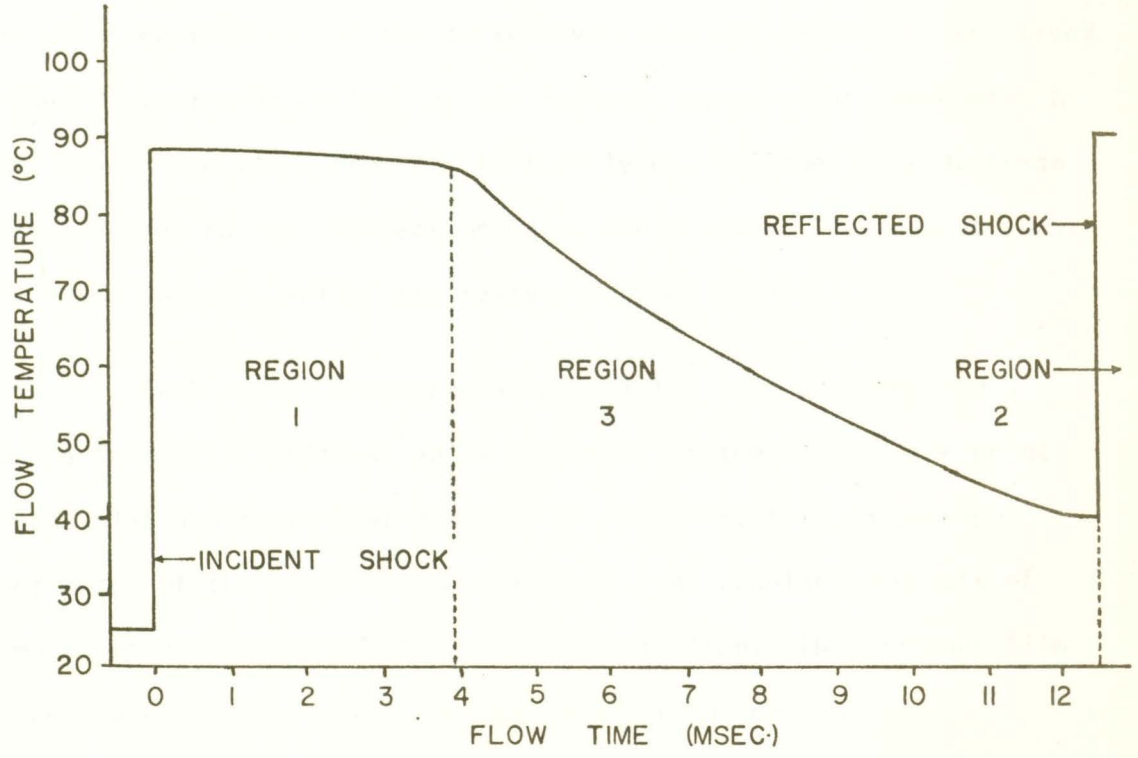

Fig. 5.6.2 Temperature regions of experiment B

5.7 Data analysis

The temperature-time traces were stored on 35 mm. film as previously described. Photographic prints approximately 8" x 10" were used to measure the displacement of the temperature trace and the rate of temperature change trace with respect to their initial values. Since each large division on the oscilloscope graticule was in units per centimeter, all measurements were made in centimeters and converted to their appropriate units. A typical temperature record taken in the 3" x 10" tube is shown in Figure 5.7.1. The initial gauge temperature was 25.4° C, the vertical oscilloscope sensitivity for the temperature trace was .1 V/cm, while the horizontal setting was 2 msec/cm. The latter setting was standard for all temperature records taken. The vertical sensitivity for the derivative trace was .5 V/cm. The record clearly reveals the arrival of the incident shock front, indicated by the rise in the trace from its initial level, followed by a decrease with time due to the rarefaction wave, and a sudden increase at about 12.0 msec upon arrival of the reflected shock front.

Each set of photographic prints for an experiment had a "scale factor"; a unitless value dependent on the size of the print which related a centimeter measured on the print to a photographic centimeter of the oscilloscope graticule. At regular intervals of 1 msec. after arrival of the incident shock front, the platinum film temperature and its rate of change were determined.

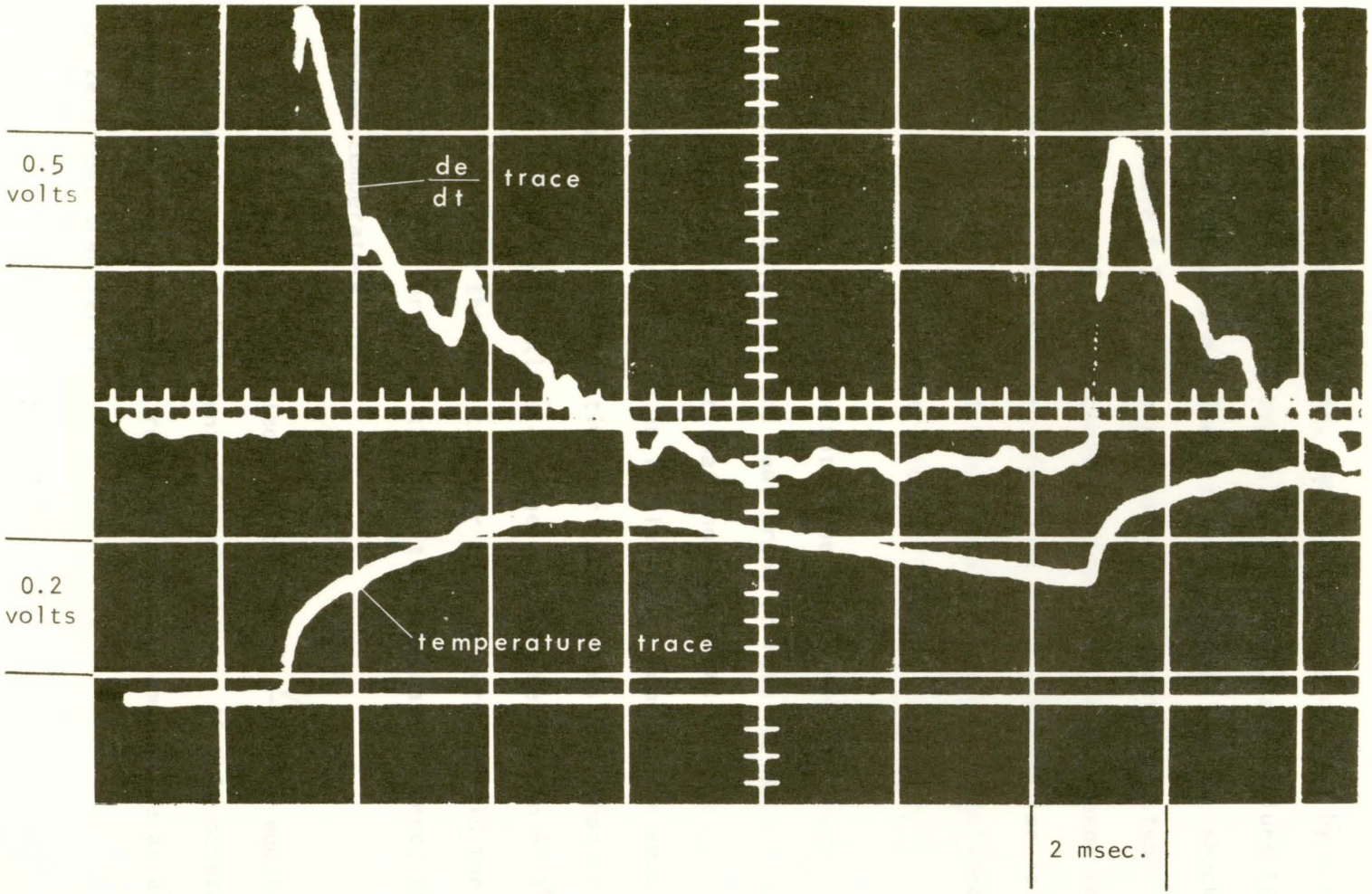

Fig. 5.7.1 A typical temperature record from experiment B. Initial Gauge Temperature = 25.4 C.

As previously mentioned, several shock tube trials were required for each experiment, each trial being defined by a new initial gauge temperature, T_o. A typical set of calculated values from data of experiment A, taken 2 milliseconds after arrival of the shock front is given in Table 5.7.1. This procedure was repeated in steps of 1 millisecond from 1 - 15 milliseconds of flow-time for each experiment. Using equation 3.3.1, the heat transfer rate was calculated for each trial at a specified time in the gas flow history. The steps outlined above were incorporated into a computer program listed in Appendix E.

Table 5.7.2 illustrates the use of the data acquired from Table 5.7.1 to calculate the heat transfer rate for each initial gauge temperature. It is evident that the heat transfer rate is positive for all shock tube trials with an initial gauge temperature equal to or less than 60.3° C and negative for temperatures less than or equal to 68.6° C. Thus there exists a gauge temperature between 60.3° C and 68.6° C for which the heat transfer rate is zero. It is the gauge temperature, T_g, for which the heat transfer rate is zero, that yields the gas temperature, θ.

It will be recalled that the factor $\frac{\sqrt{\rho C K \pi}}{2}$ in equation 3.3.1 was assumed to be independent of temperature. If this constant is denoted by A, the equation relating the gas temperature as a function of zero heat transfer is

$$\dot{q}(t) = A(\theta - T_g) \qquad (5.7.2)$$

Table 5.7.1

Calculated values of the gauge temperature as a function of time in the first 2 msec. of flow for experiment A.

Flow Time (msec.)	Initial Gauge Temperature (T_o)	Gauge Temperature Change (ΔT)	Film Temperature (T_g)
1	32.9	.44	33.3
	41.1	.35	41.5
	55.4	.23	55.6
	60.3	.09	60.3
	68.6	-.05	68.6
	76.8	-.16	76.6
	88.0	-.37	87.6
	99.0	-.51	98.5
2	32.9	.68	33.6
	41.1	.51	41.6
	55.4	.31	55.7
	60.4	.10	60.4
	68.6	-.10	68.5
	76.8	-.29	76.5
	88.0	-.63	87.4
	99.0	-.88	98.1

Table 5.7.2

Evaluation of the terms in equation 3.3.1 using the experimental data from Table 5.7.1, at a time of 2 milliseconds, in experiment A.

T_o	λ	ΔT	$T(t)-T(\lambda)$	$(t-\lambda)^{3/2}$	$\Sigma\frac{T(t)-T(\lambda)}{(t-\lambda)^{3/2}}$	$q(t)$
32.9	0	0.0	.68	2.83	.24	
	1	.44	.24	1.00	.48	
	2	.68	0.0	0.00		+1.43
41.1	0	0.0	.51	2.83	.18	
	1	.35	.16	1.00	.34	
	2	.51	0.0	0.00		+1.06
55.4	0	0.0	.31	2.83	.11	
	1	.23	.08	1.00	.19	
	2	.31	0.0	0.00		+.644
60.4	0	0.0	.10	2.83	.035	
	1	.09	.01	1.00	.045	
	2	.10	0.0	0.00		+.183
68.6	0	0.0	-.10	2.83	-.035	
	1	-.05	-.05	1.00	-.085	
	2	-.10	0.0	0.00		-.223
76.8	0	0.0	-.29	2.83	-.10	
	1	-.16	-.13	1.00	-.23	
	2	-.29	0.0	0.00		-.658
88.0	0	0.0	-.63	2.83	-.22	
	1	-.37	-.26	1.00	-.48	
	2	-.63	0.0	0.00		-1.364
99.0	0	0.0	-.88	2.83	-.31	
	1	-.51	-.37	1.00	-.68	
	2	-.88	0.0	0.00		-1.935

CHAPTER 6

RESULTS AND DISCUSSION

The results of the temperature measurements in the 4" x 4" and 3" x 10" shock tubes are discussed in two sections. The first compares the "theoretical" temperature-time curves with the "gauge temperature change profiles". The second section presents the results obtained using equation 5.6.3 to evaluate the gas temperature at any time in the flow.

6.1 Temperature change profiles

The transducer temperature change profiles were developed as a means by which the platinum-film gauge response, with respect to time and initial gauge temperature, could be assessed. The temperature change was the difference between the gauge starting temperature and the gauge temperature at any time during the gas flow. The profiles for several gauge starting temperatures were superimposed on the "theoretical" gas temperature curve for the particular experiment. The vertical axis of the latter was defined on the left while the former was defined on the right of each figure. The horizontal time axis was common to both curves. The method of superposition provided a visual comparison of the gauge response versus the flow temperature at any time.

Typical temperature oscillograms taken in the 4" x 4" shock tube are shown in Figures 6.1.1 to 6.1.4, for initial gauge temperatures of 32.9° C, 60.3° C, 76.8°C and 99.0° C. In Figure 6.1.5 the temperature change profiles are plotted for the above trials together with the "theoretical" temperature curve.

Important features of the gauge temperature profiles, when compared to the "theoretical" flow temperatures of the three regions are:

1) The transducer temperature change in Region 1 appeared to be closely related to the difference between the initial gauge temperature T_o and the "theoretical" gas temperature. For example, a positive temperature change was recorded for an initial gauge temperature T_o, lower than the gas temperature, while a negative temperature change was recorded for an initial gauge temperature T_o, higher than the "theoretical" gas temperature. In section 3.2 it was shown that, for an instantaneous increase in the gas temperature, the gauge surface temperature change varied linearly with the initial gauge temperatures. This characteristic of the gauge response was found to hold for about 3 milliseconds of flow time. Upon arrival of the reflected shock, the linear relationship no longer existed. These characteristics are shown graphically in Figure 6.1.6.

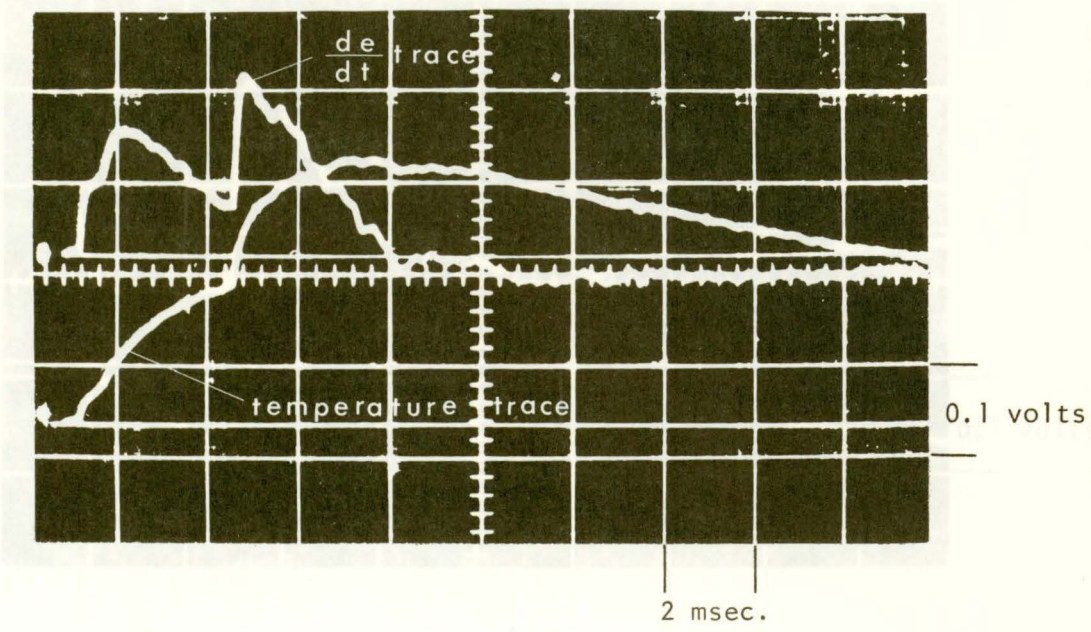

Fig. 6.1.1 Initial Gauge Temperature = 32.9 C.

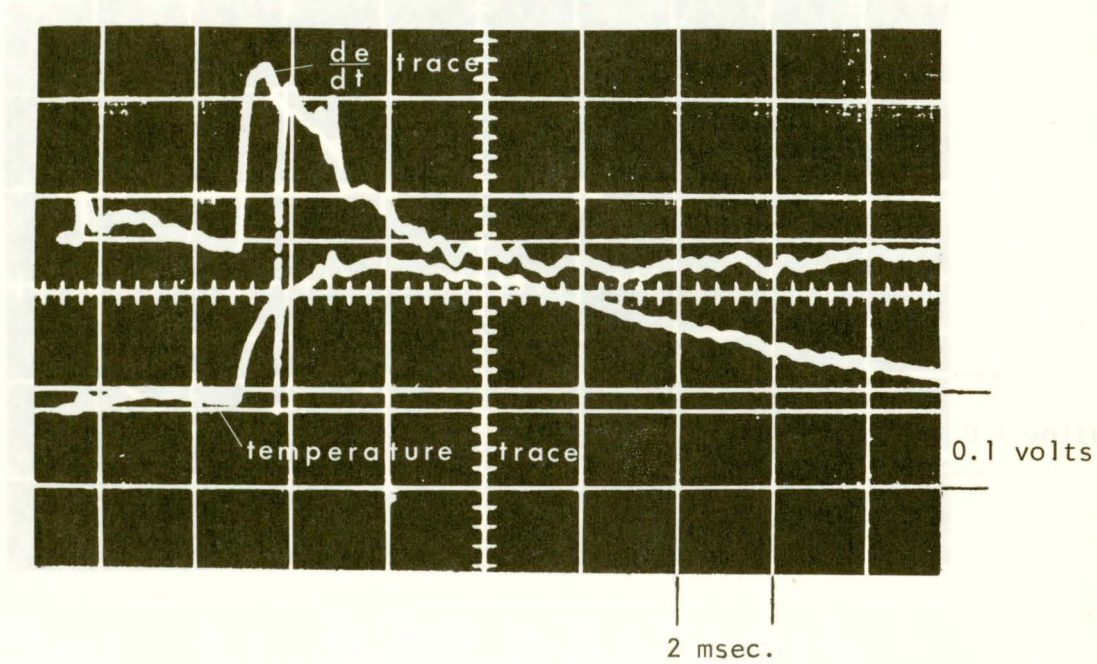

Fig. 6.1.2 Initial Gauge Temperature = 60.3 C.

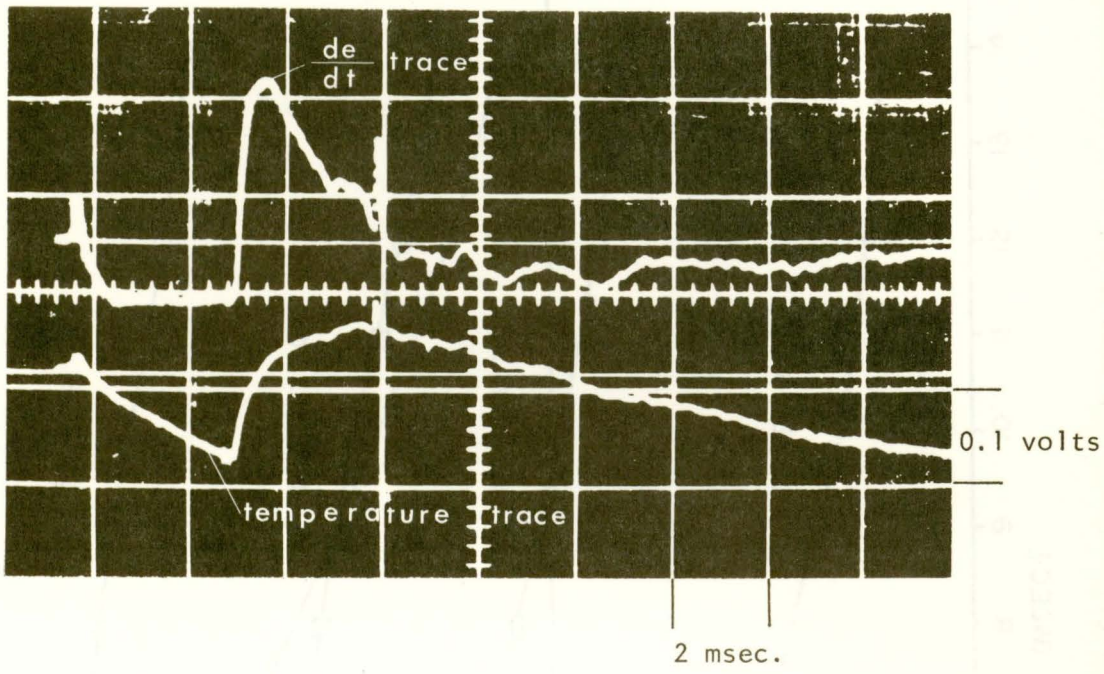

Fig. 6.1.3 Initial Gauge Temperature = 76.8 C.

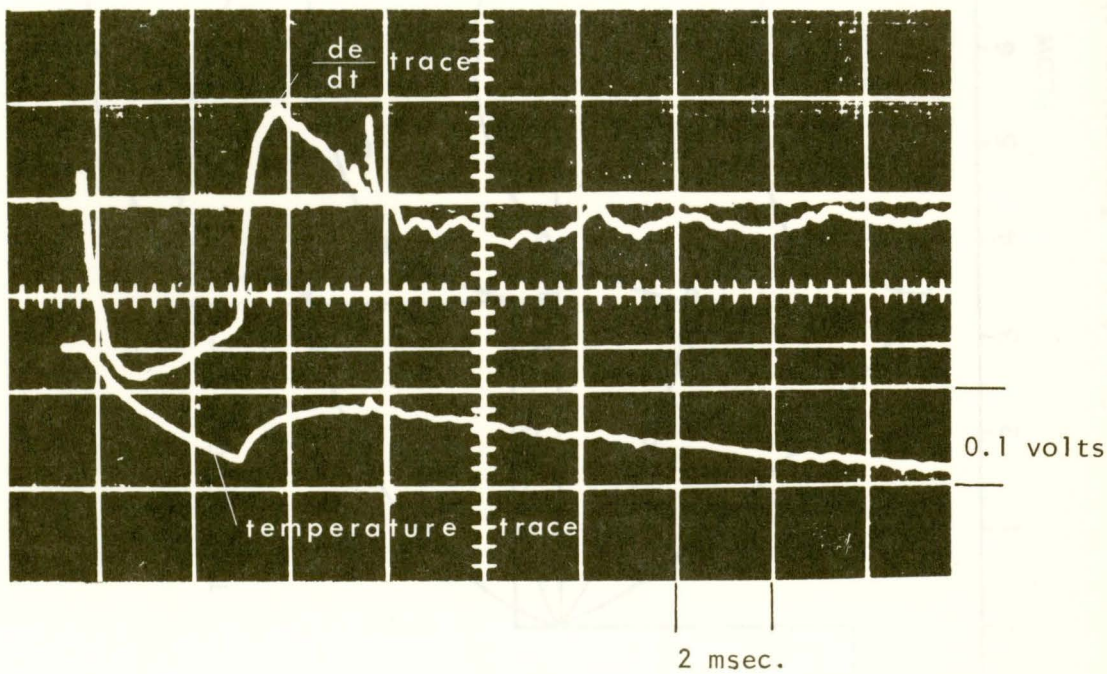

Fig. 6.1.4 Initial Gauge Temperature = 99.0 C.

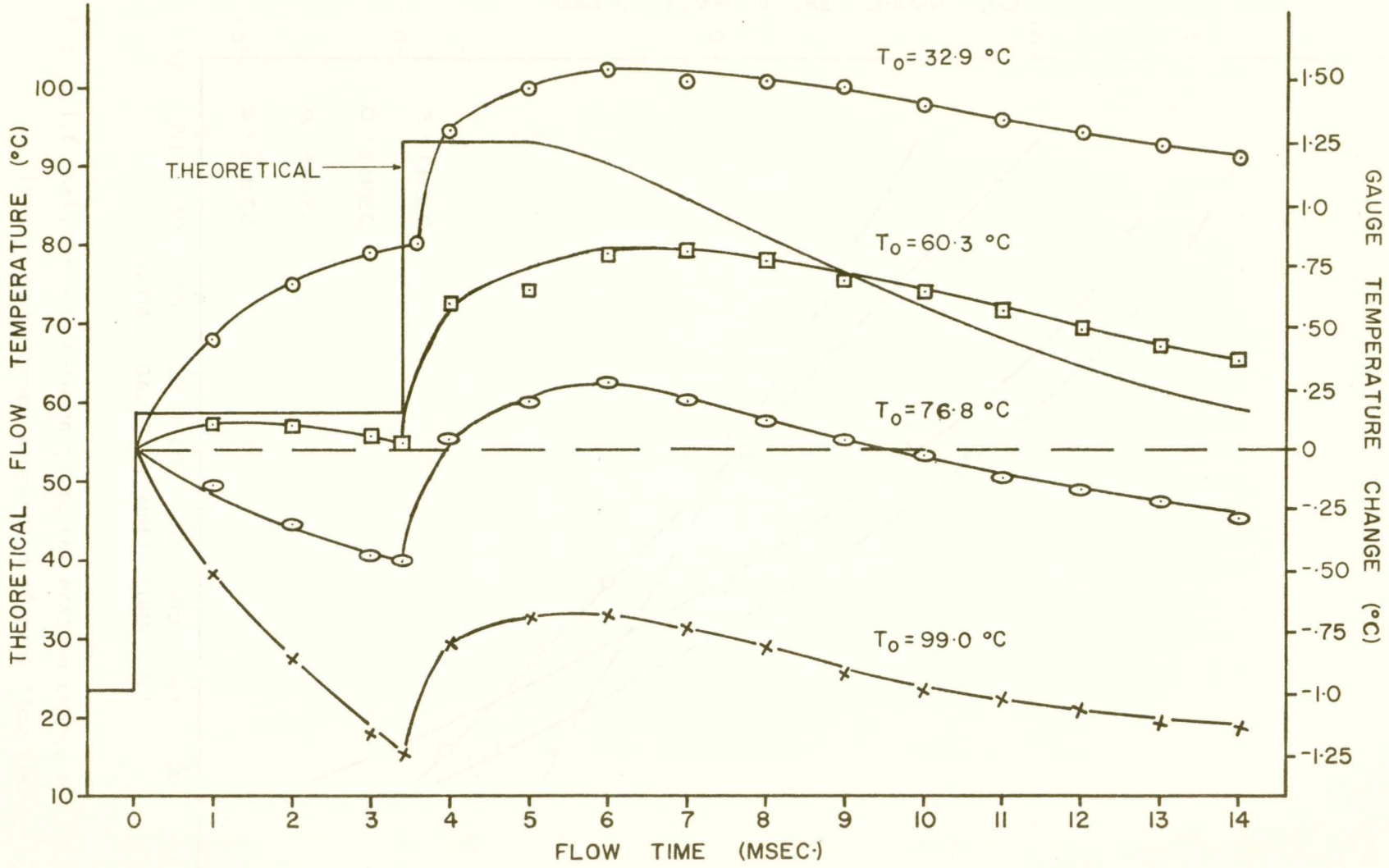

Fig. 6.1.5 Temperature change profiles for experiment A.

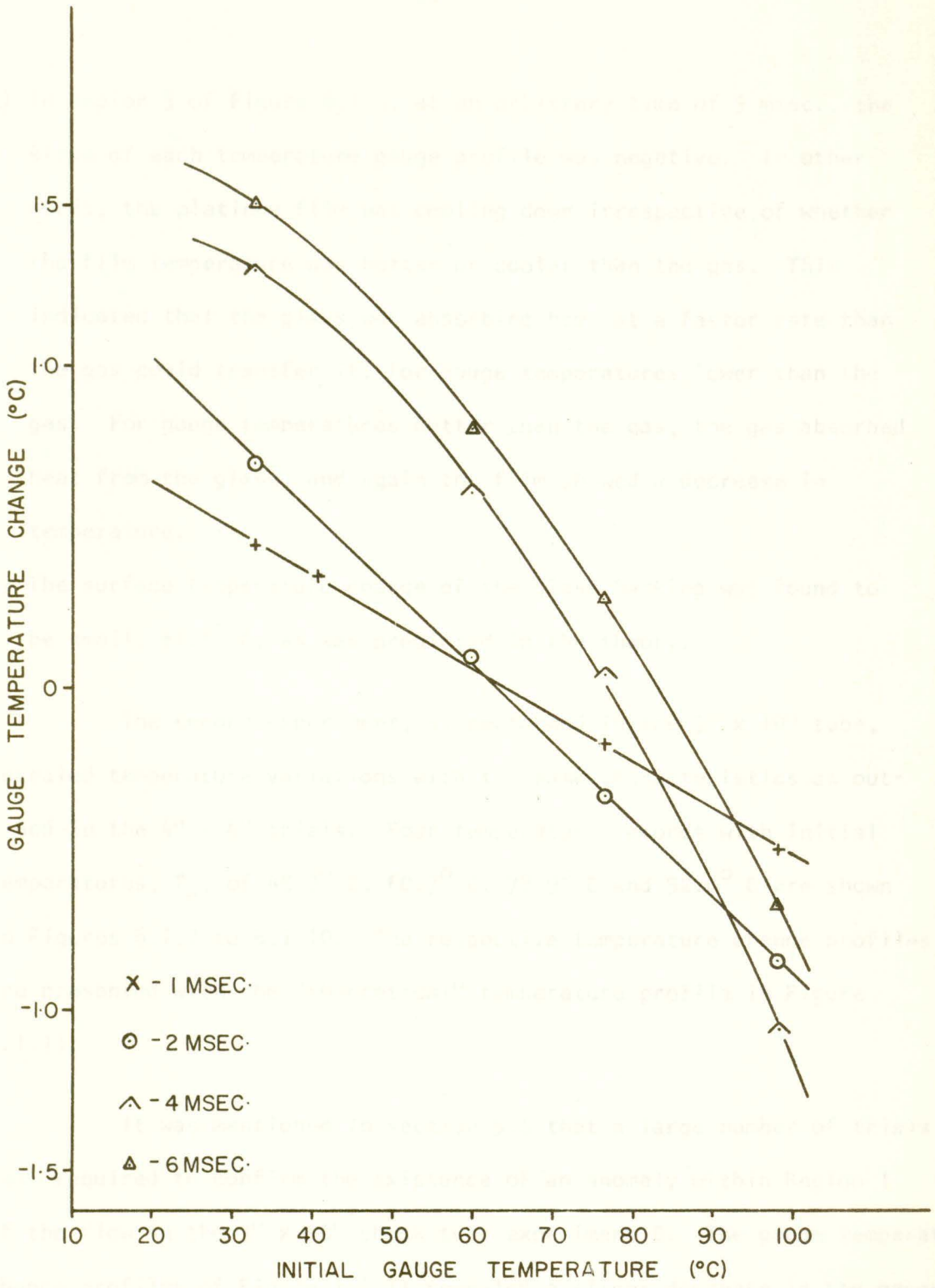

Fig. 6.1.6 Relationship between gauge temperature change and initial gauge temperature at different flow times

2) In Region 3 of Figure 6.1.5, at an arbitrary time of 9 msec., the slope of each temperature gauge profile was negative. In other words, the platinum film was cooling down irrespective of whether the film temperature was hotter or cooler than the gas. This indicated that the glass was absorbing heat at a faster rate than the gas could transfer it, for gauge temperatures lower than the gas. For gauge temperatures hotter than the gas, the gas absorbed heat from the glass, and again the film showed a decrease in temperature.
3) The surface temperature change of the glass backing was found to be small, $\pm 1.5^{o}$ C, as was predicted in the theory.

The second experiment, B, performed in the 3" x 10" tube, revealed temperature variations with the same characteristics as outlined in the 4" x 4" trials. Four temperature records with initial temperatures, T_o, of 45.2^{o} C, 60.7^{o} C, 78.9^{o} C and 92.8^{o} C are shown in Figures 6.1.7 to 6.1.10. The respective temperature change profiles are presented with the "theoretical" temperature profile in Figure 6.1.11.

It was mentioned in section 5.6 that a large number of trials was required to confirm the existence of an anomaly within Region 1 of the flow in the 3" x 10" shock tube experiment B. The gauge temperature change profiles of Figure 1.1.11 revealed a slight decrease in the gauge temperature change about two milliseconds after arrival of the shock front. The effect was not apparent in the 4" x 4" profiles and was attributed to vibrations within the wooden shock tube section.

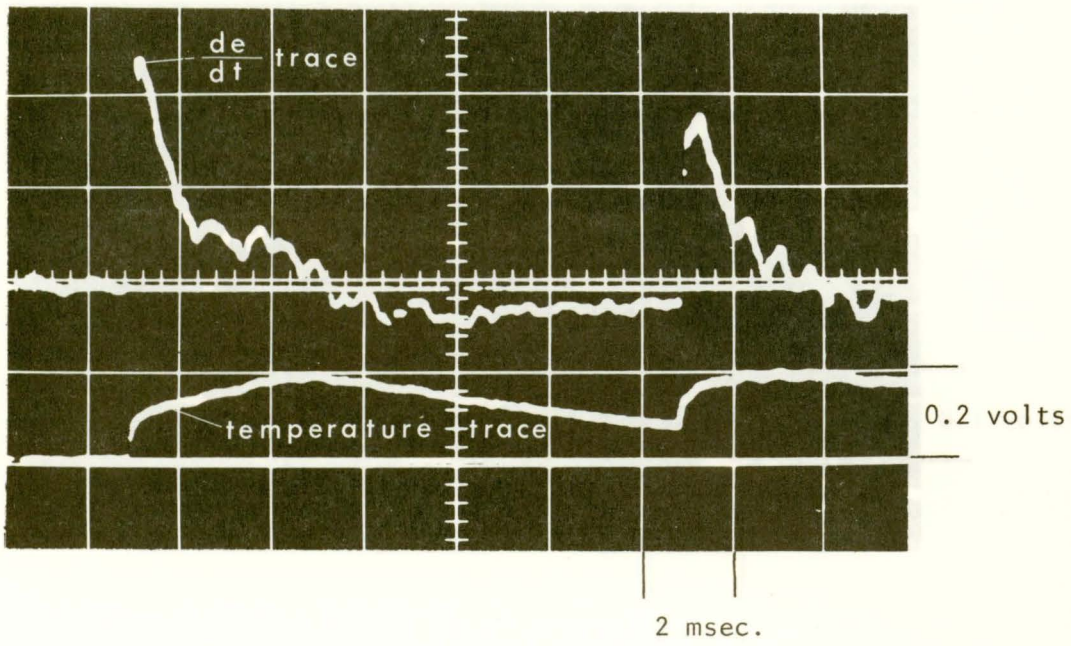

Fig. 6.1.7 Initial Gauge Temperature = 45.2 C.

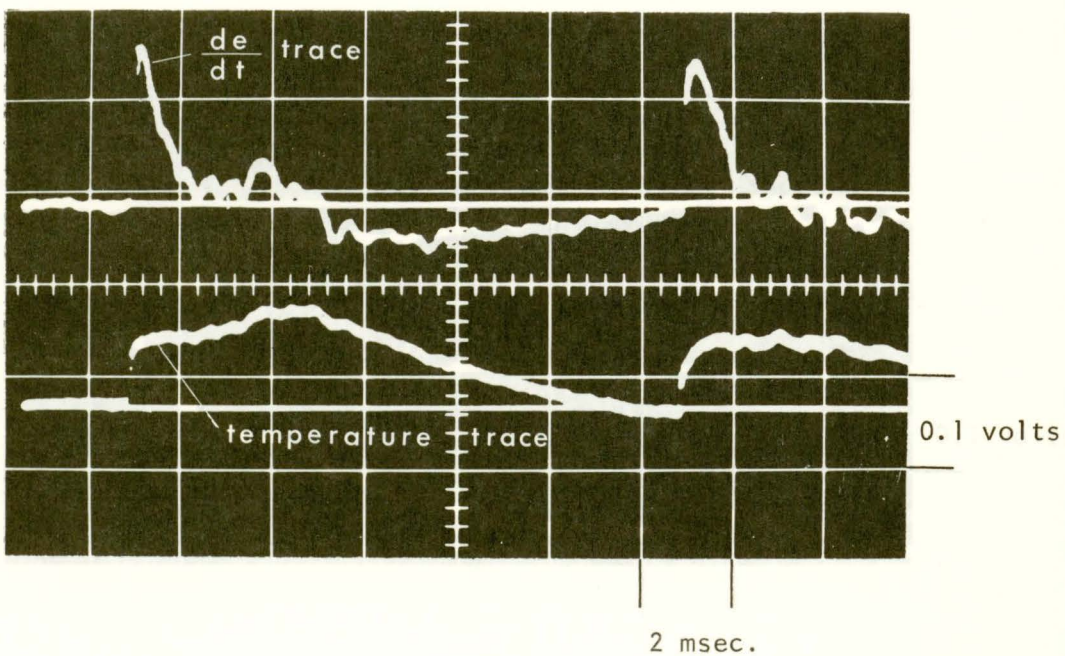

Fig. 6.1.8 Initial Gauge Temperature = 60.7 C.

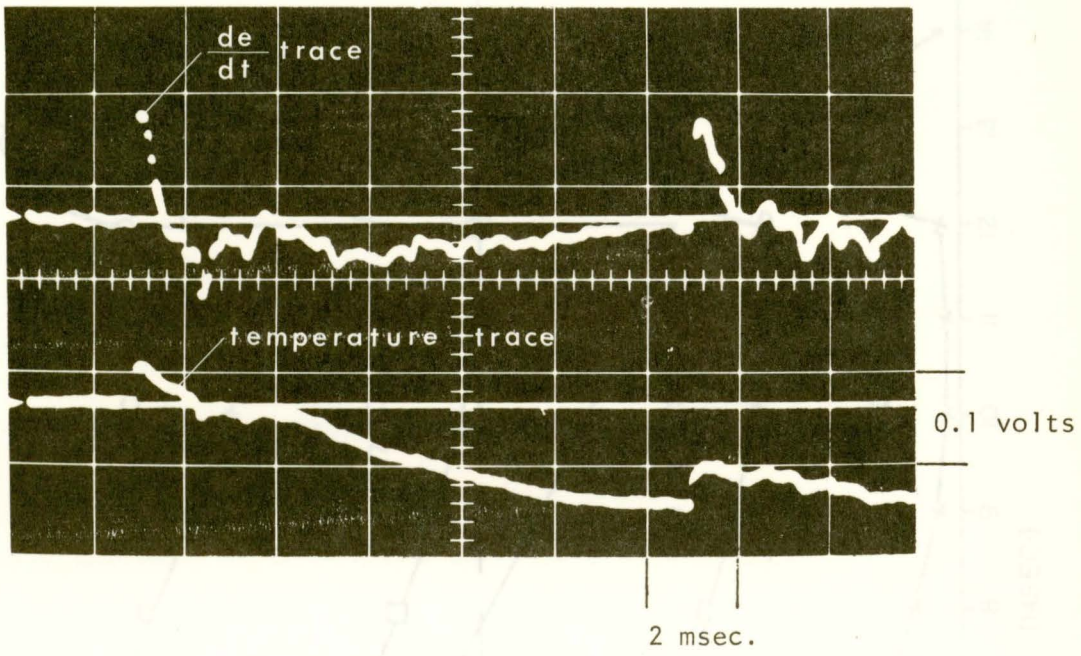

Fig. 6.1.9 Initial Gauge Temperature = 78.9 C.

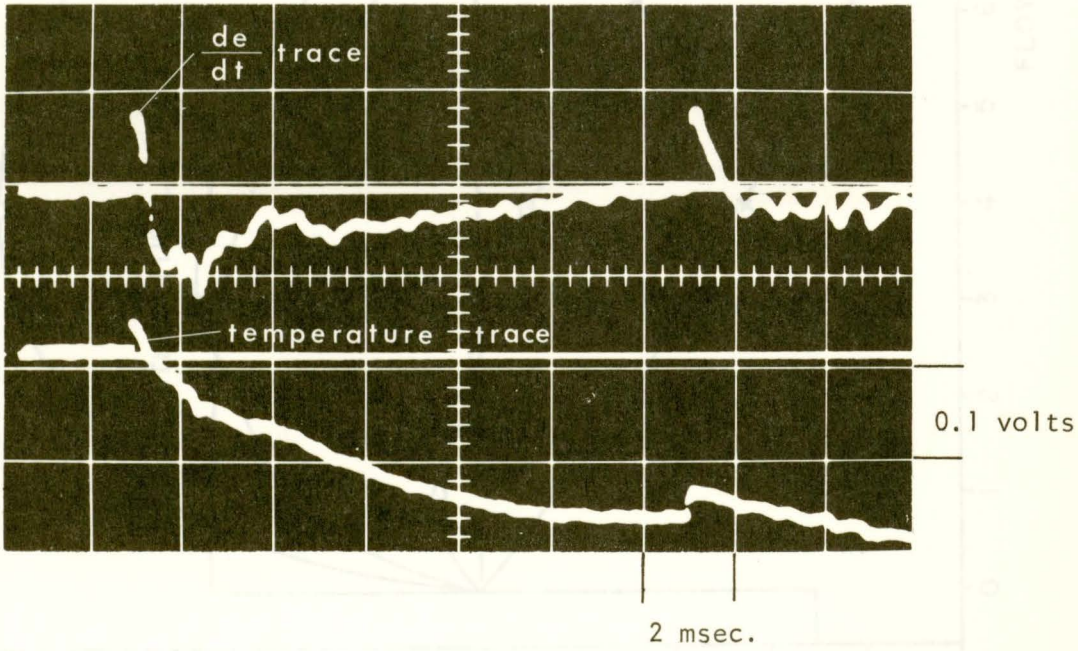

Fig. 6.1.10 Initial Gauge Temperature = 92.8 C.

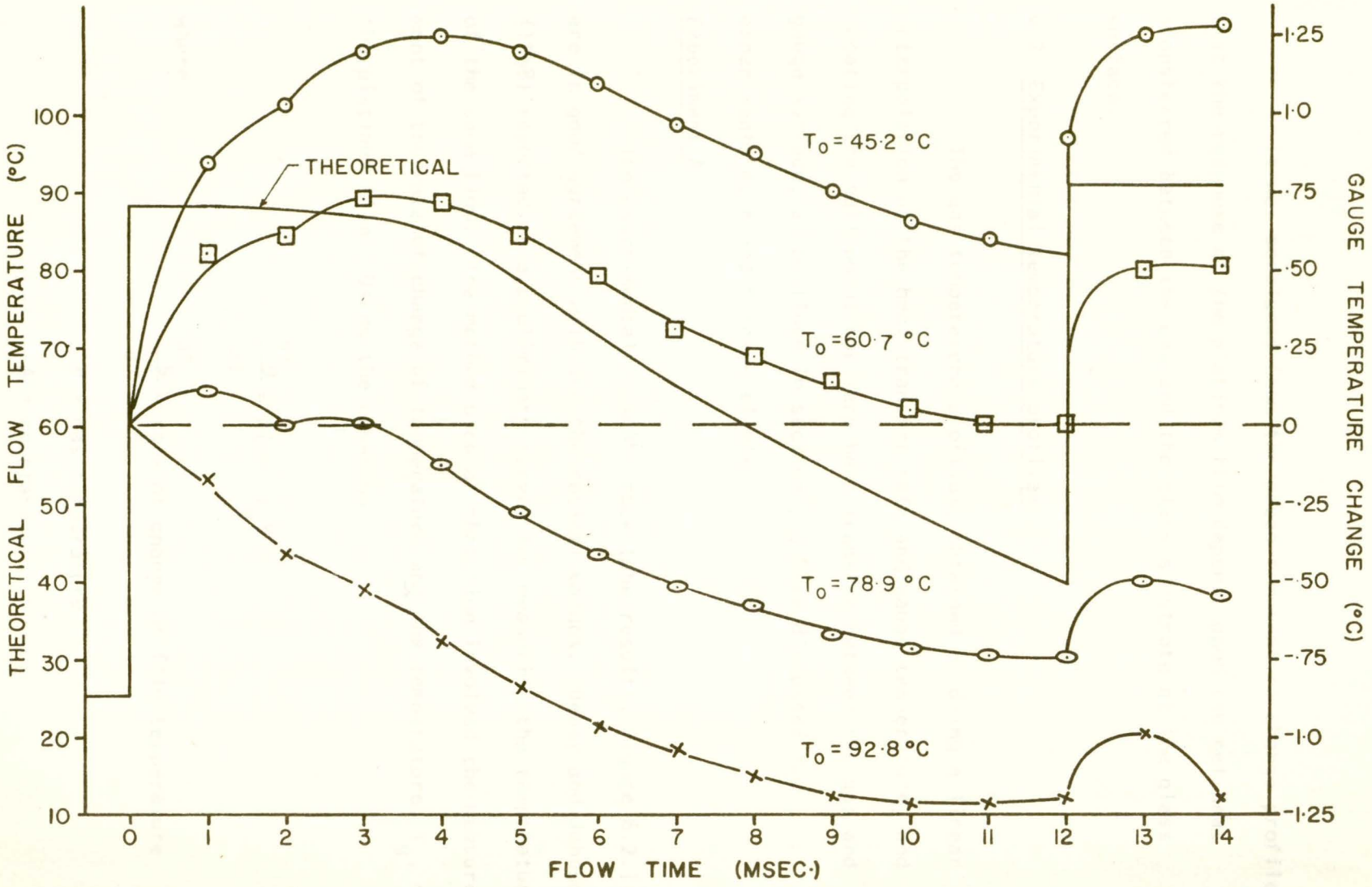

Fig. 6.1.11 Temperature change profiles for experiment B

It was concluded from the gauge temperature change profiles that the response of the platinum film depends upon the net heat transferred between the gas and the glass substrate at the glass surface.

6.2 Experimental temperature profiles

The gas temperature profiles, obtained by doing a linear interpolation of the heat transfer rate and gauge temperature, and locating the null point for zero heat transfer between the gas and gauge surface, as outlined in section 5.3, are discussed for experiments A, B and C respectively.

Experiment A

The experimental 4" x 4" shock tube results, Figure 6.2.1, are in good agreement with the theoretical values. Dewey and Johnson (1968) reported on a preliminary survey for measuring the temperature of the same flow. The method used at that time involved the measurement of the rate of change of temperature and the temperature, T_g, of the platinum film. Using the equation

$$\frac{dT_g}{dT} = A(\theta - T_g)$$

where

$\frac{dT_g}{dT}$ = rate of change of film temperature

θ = gas temperature

A = constant

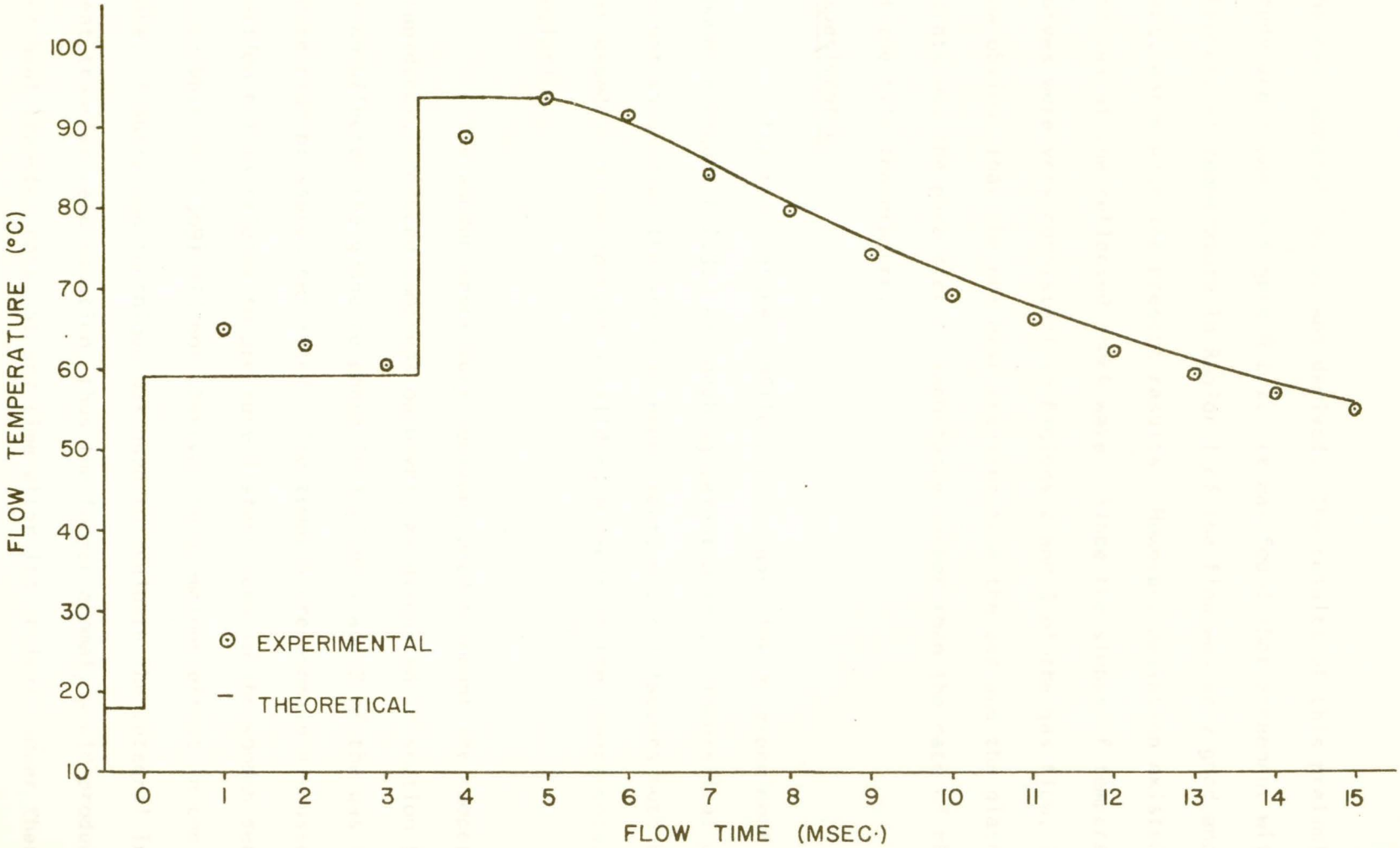

Fig. 6.2.1 Temperature results for experiment A

the gas temperature, θ, was derived. The results of this preliminary study are shown in Figure 6.2.2. It was found that agreement with the theoretical temperature in Region 1 of the flow was very good and, in fact, agree with the present results. However, deviation existed after arrival of the reflected shock wave. Since the slopes of temperature curves were very consistent in Regions 2 and 3 of the gas flow, it is now obvious that the net heat transfer from the gas and the glass substrate was the parameter of importance rather than the rate of change of the film temperature.

Experiment B

The temperature profile for the gas flow of experiment B is shown in Figure 6.2.3. Although agreement with the theoretical values is not as good as the previous experiment, several factors must be discussed in order to make a valid assessment of the experimental deviations.

The wooden shock tube section, used to mount the temperature transducer, produced compression waves, as discussed in section 5.4, which affected the gauge response in Regions 1 and 2 of the gas flow where high pressures persisted. The temperature anomaly discussed in section 6.1 is related to pressure disturbances in the wooden section, since Whitten (1969) did not observe the anomalous effect in the metal tube. A summation technique was used to evaluate the integral in the heat transfer rate equation, thus the former anomaly would produce a net heat transfer rate, at any time after its arrival, lower than an

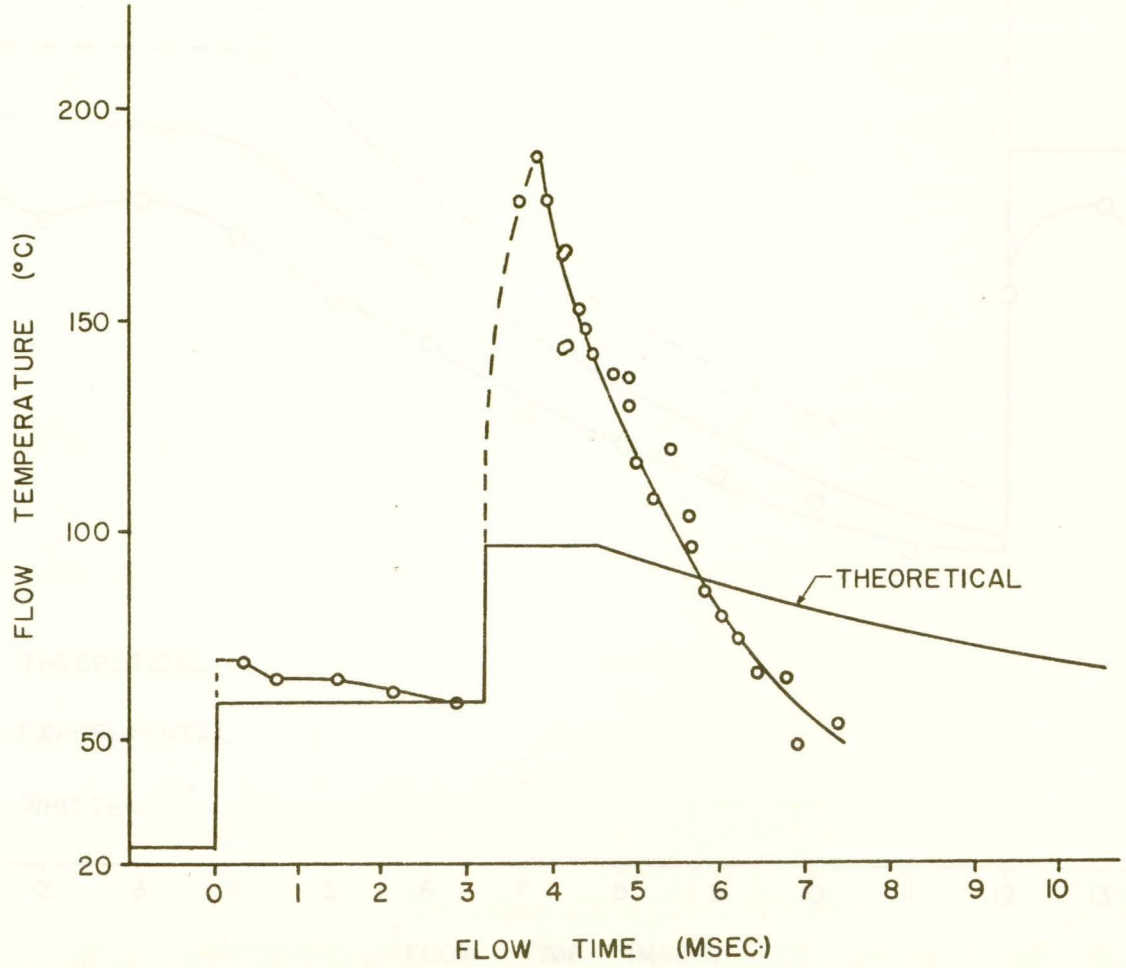

Fig. 6.2.2 Preliminary temperature results for experiment A, based on the principle that the gas temperature equals the gauge temperature when the rate of change of the gauge temperature is zero

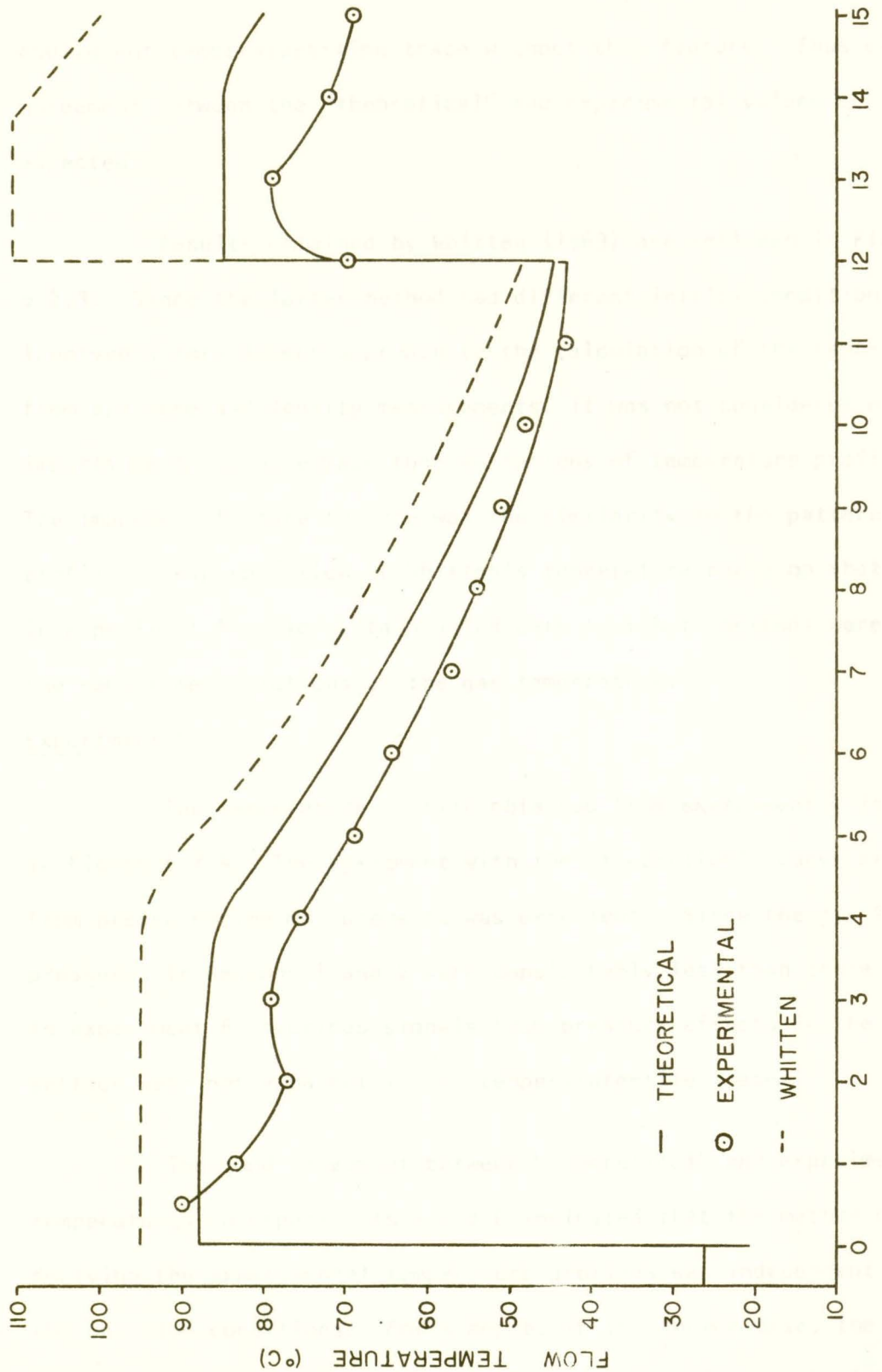

Fig. 6.2.3 Temperature results for experiment B

equivalent temperature-time trace without this feature. Thus closer agreement between the "theoretical" and experimental values could be expected.

Results obtained by Whitten (1969) are included in Figure 6.2.3. Since the latter method had different initial conditions, and involved a less direct approach to the calculation of the temperature from pressure and density measurements, it was not considered of great importance to compare magnitude variations of temperature profiles. The important feature to note was the similarity in the pattern of the profiles. Superposition of Whitten's temperature curve on that obtained in experiment B would certainly indicate that both methods were following the same time variations of the gas temperature.

Experiment C

The temperature profile obtained from experiment C is shown in Figure 6.2.4. The agreement with the "theoretical" curve derived from pressure-time measurements was excellent. Since the gas flow pressures in Regions 1 and 2 were considerably less than those incurred in experiment B, spurious signals from pressure effects in the wooden section were not apparent in the temperature-time traces.

The good agreement between "theoretical" and experimental temperatures in experiments A and C indicated that the method of deriving the experimental temperature profiles was independent of the gas flow conditions. For example, in the former case, the flow sequence was Region 1, Region 2, and Region 3, while in the latter

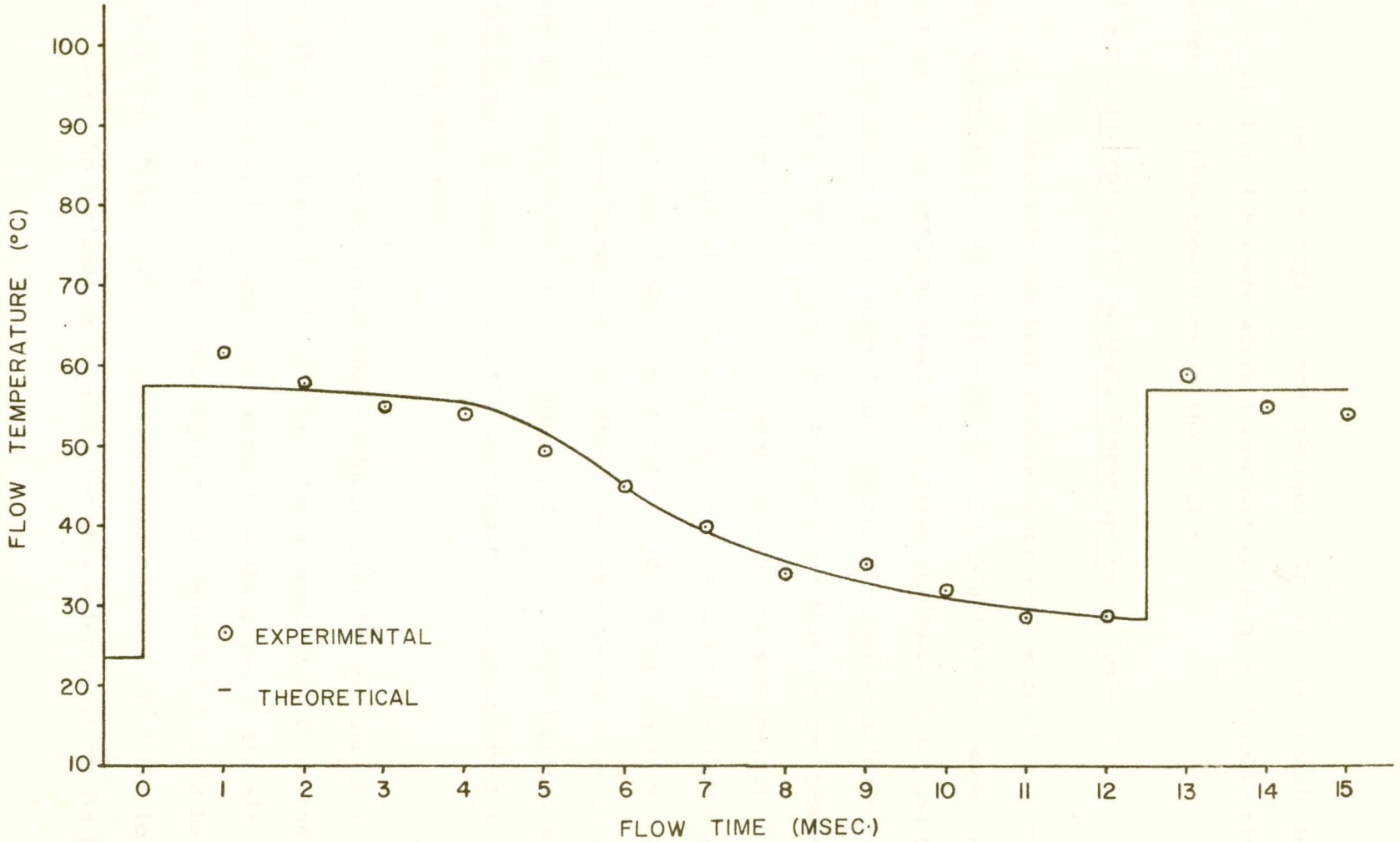

Fig. 6.2.4 Temperature results for experiment C

case the last two regions were reversed. It seems reasonable to conclude that the temperature transducer would give reliable results under most flow conditions in the shock tube.

6.3 Justification for using a linear approximation

Values of the heat transfer rate and the gauge temperature for experiments A and C at times of 1, 3, 5 and 9 milliseconds after arrival of the incident shock are plotted in Figures 6.3.1 and 6.3.2. It is evident that a linear least squares fit approximation could be used to determine the abscissa intercept and thus the gas temperature at any of the above times. In experiment B, the same method of analysis was used, but it is apparent from Figure 6.3.3 that there exist two straight lines, one on either side of the abscissa intercept. This figure indicates, on the other hand, that the error in calculating the gas temperature was less than $\pm$ 2.0^{o} C. In experiments A and C the difference of slope for positive and negative values of heat transfer rate was not apparent.

Substitution of heat conductivities for air and glass in equation 3.1.1 would indicate that, for a negative value of the heat transfer rate, i.e. heat transferred from the glass to the air, the slopes of the lines below the abscissa in Figure 6.3.3 would be less steep than those above the abscissa. The opposite was found to be the case. No explanation is given for this effect. It should be

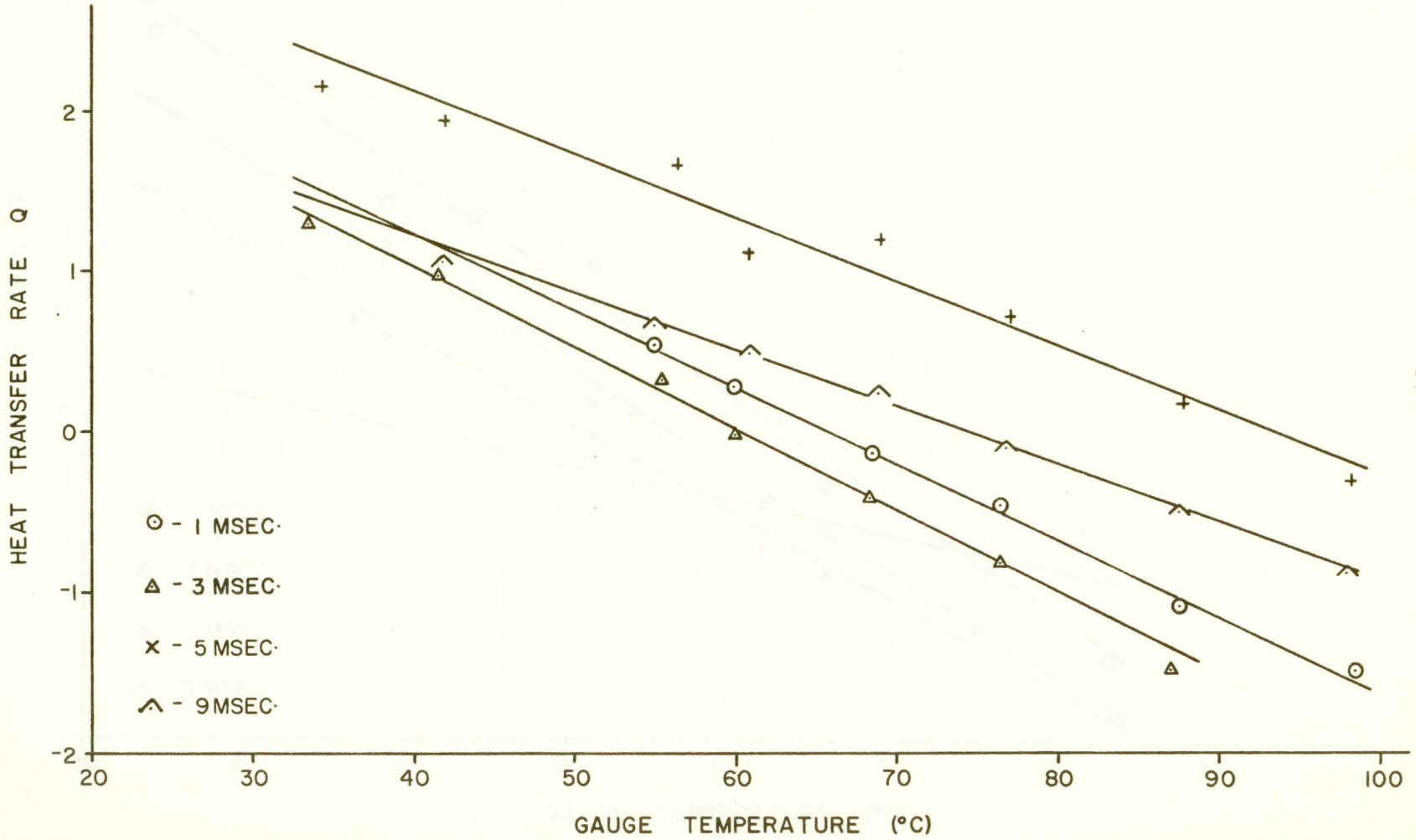

Fig. 6.3.1 Heat transfer rate as a function of the gauge temperature for experiment A

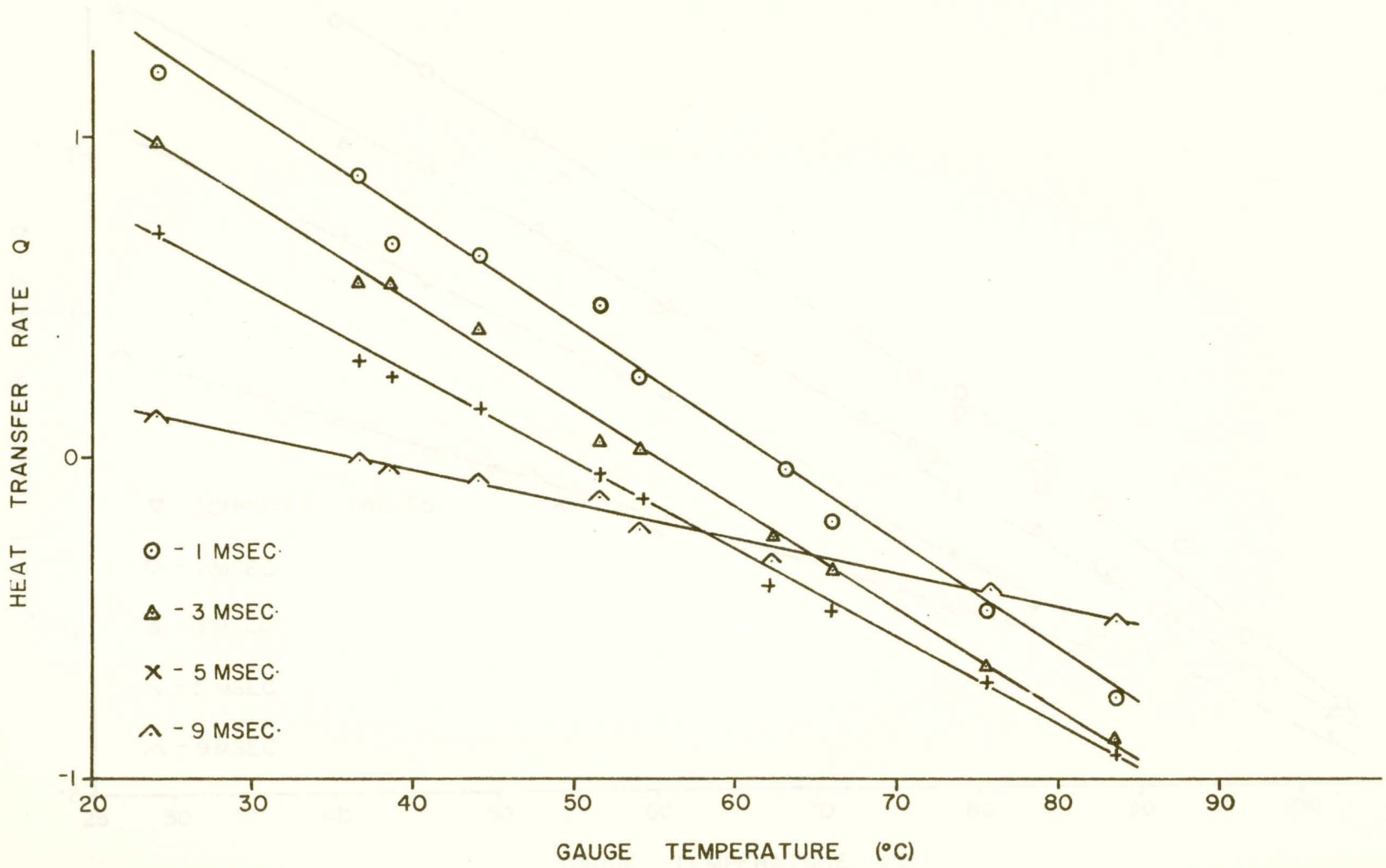

Fig. 6.3.2 Heat transfer rate as a function of the gauge temperature for experiment C

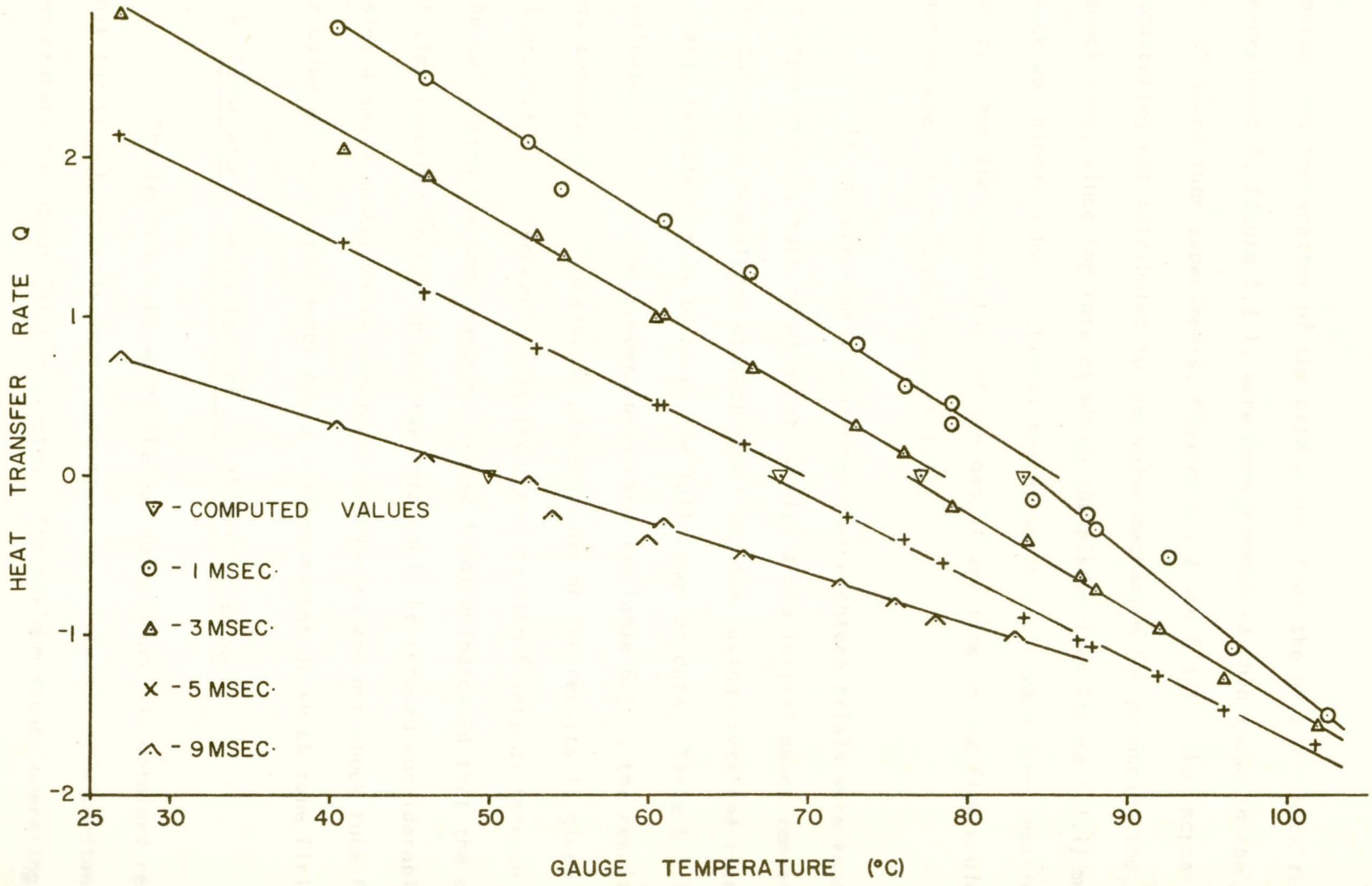

Fig. 6.3.3 Heat transfer rate as a function of the gauge temperature for experiment B

noted that the scatter of the data points from the 4" x 4" shock tube, experiment A, Figure 6.3.1, were more pronounced than those in the 3" x 10" shock tube experiments, Figures 6.3.2 and 6.3.3. The increased scattering was attributed to the valve mechanism for producing the shock wave, since the rate at which the piston (see Figure 4.1.1) moved back was hindered by frictional forces which could vary from shot to shot. Thus the temperature of the gas at any time in the flow would not be exactly the same for each trial.

It was previously mentioned that eighteen trials were recorded in experiment B, each trial starting with a new initial gauge temperature. The data were reanalyzed at each specified time using seven and then four trials, selected so as to cover the full range of data. Table 6.3.1 indicated the starting temperatures used and Table 6.3.2, the resulting gas temperatures. A graphical presentation of the results is given in Figure 6.3.4. It appeared that there was no significant difference in the calculated gas temperatures. These findings indicated that the amount of time required to gather the raw data could be reduced considerably by using a small number of temperature transducers and one shock tube firing, or using a single transducer and a limited number of shock tube firings.

6.4 Temperature limitations of the thin film gauge

The technique by which the gas temperature was obtained required that the thin film resistance thermometer be maintained at a constant temperature for about fifteen minutes. The maximum steady operating temperature of the present system was about 110° C. This temperature

TABLE 6,3.1

Initial gauge temperatures used for three linear least squares fits, to determine the gas temperature in experiment B.

INITIAL GAUGE TEMPERATURE (^{o} C)		
18 Trials	7 Trials	4 Trials
25.42	25.42	25.42
39.59		
45.15		
52.00	52.00	
53.94		
59.96		
60.70	60.70	60.70
66.04		
72.64		
76.16	76.16	
78.85		
78.94		
84.03	84.03	84.03
87.74		
88.48		
92.83	92.83	
97.18		
103.02	103.02	103.02

TABLE 6.3.2

Variation of the gas temperature determined using a linear least squares fit and the initial temperatures given in Table 6.3.1.

Flow Time (msec.)	Gas Temperature (° C)		
	18 Trials	7 Trials	4 Trials
1	83.6	83.1	81.9
2	76.2	76.0	75.6
3	76.9	77.1	76.7
4	74.0	73.9	74.2
5	68.3	68.5	68.7
6	63.4	64.0	63.9
7	57.6	57.3	57.0
8	53.9	54.1	54.3
9	50.0	51.3	51.7
10	46.5	48.0	48.0
11	43.4	42.6	43.0
12	64.7	65.0	68.9
13	79.1	78.8	79.3
14	73.0	72.9	73.0
15	70.2	69.2	69.0

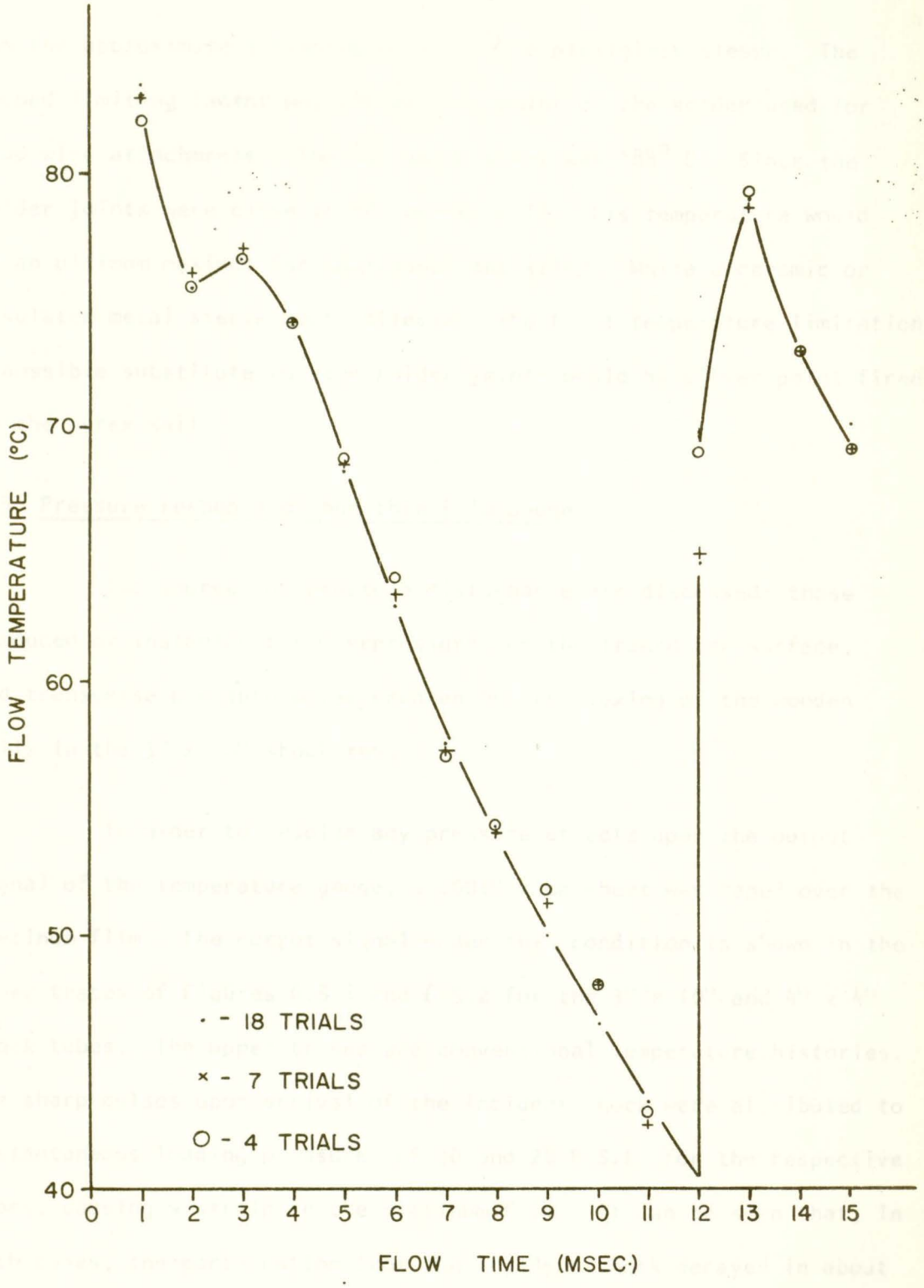

Fig. 6.3.4 Temperature results using 18, 7, and 4 shock tube trials in experiment B

was the approximate softening point of the plexiglass sleeve. The second limiting factor was the melting point of the solder used for lead wire attachments. The softening point was 188° C. Since the solder joints were close to the heater coil, this temperature would be an ultimum maximum for continuous operation. While a ceramic or insulated metal sleeve would alleviate the first temperature limitation, a possible substitute for the solder joints would be silver paint fired to the pyrex wall.

6.5 Pressure response of the thin film gauge

Two sources of pressure disturbance are discussed: those produced by instantaneous overpressures on the transducer surface, and transverse pressure waves created by the flexing of the wooden walls in the 3" x 10" shock tube.

In order to resolve any pressure effects upon the output signal of the temperature gauge, a .001" mica sheet was taped over the platinum film. The output signal under this condition is shown in the lower traces of Figures 6.5.1 and 6.5.2 for the 3" x 10" and 4" x 4" shock tubes. The upper traces are conventional temperature histories. The sharp pulses upon arrival of the incident shock were attributed to instantaneous loading pressures of 30 and 20 P.S.I. for the respective tubes, causing a strain in the platinum film. It can be seen that, in both cases, the perturbation from the incident shock decayed in about 3 msec. and its contribution to the measured film temperature was negligible.

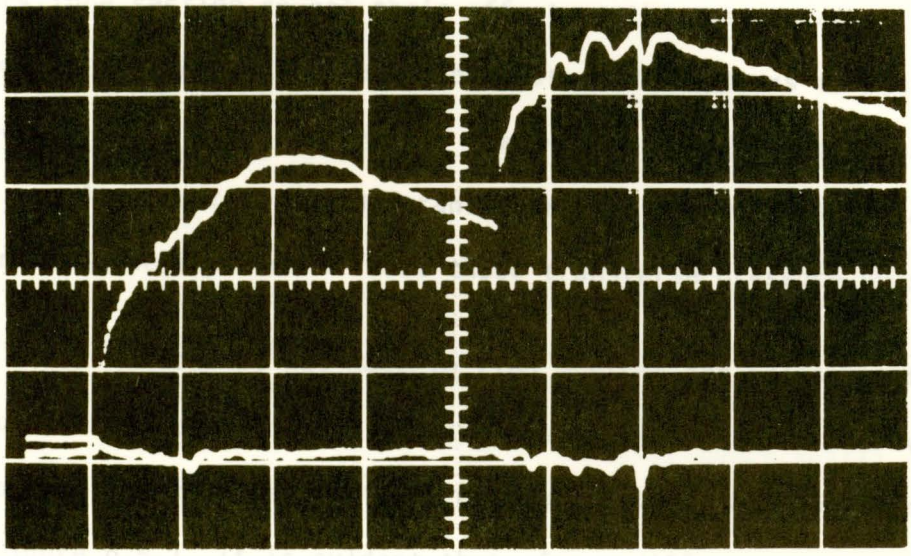

Fig. 6.5.1 Sensitivity of the temperature transducer to pressure in the 3" x 10" shock tube

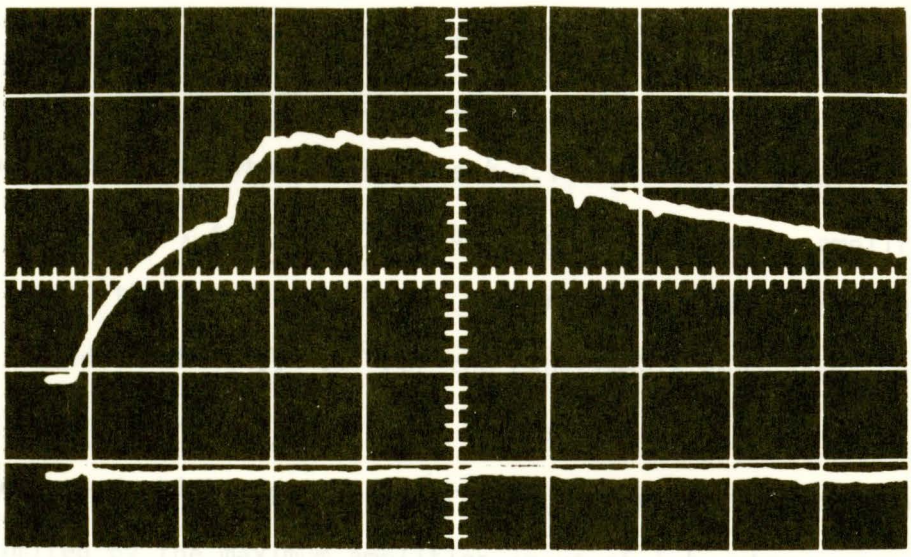

Fig. 6.5.2 Sensitivity of the temperature transducer to pressure in the 4" x 4" shock tube

The transverse pressure waves created in the 3" x 10" wooden shock tube section reveal their effect on the transducer output signal shown in Figure 6.5.1. The major disturbance appears to occur approximately 2 msec. after arrival of the incident and reflected shock waves. The resultant output of the transducer is a signal of lower amplitude than would be expected without these transverse pressure pulses.

No attempt was made to find whether the pressure effects had a functional dependence on the transducer temperature. However, upon comparing the temperature trace of Figure 6.1.10 and the lower trace of Figure 6.5.1, it is evident that, for a difference of about 73° C in the initial gauge temperature, the strain effect is still apparent.

6.6 Electronic limitations

It is shown in Appendix B that the maximum voltage output of the TAA243 amplifier is ± 5 volts. The calibrations of the temperature transducer illustrated in Figures 4.7.1 and 4.7.2 indicate a sensitivity of 7.04° C/volt, so that, for a balanced bridge and an amplifier gain of 500 times the input signal, the temperature change across the thin film is limited to about 35° C. For the experiments conducted, this is about 20 times the maximum temperature change recorded. If the amplifier gain is decreased, higher gauge temperature changes can be tolerated but will be limited by the maximum amplifier input of 1.4 volts.

6.7 Boundary layer considerations

Due to the viscous nature of the gas flow, a velocity gradient will exist normal to the flow, close to the walls of the shock tube, and will give rise to a layer of gas across which the flow will be retarded. For weak shocks, Mirrels (1956) has shown that the boundary layer was a region of laminar flow. Mirrels also showed that, in theory, the pressure gradient across the layer is zero.

However, within the boundary layer, there exists shearing stresses caused by the velocity gradient. This shearing work tends to alter the temperature of the fluid particles. Shapiro (1954) illustrated the effect of cooling and heating the walls of the shock tube on the temperature distribution within the boundary layer, Figure 6.7.1. Since the latter figure was for a steady gas flow, it may be anticipated that directly behind the shock front the gas temperature at the wall will be less than the free gas temperature but owing to the short intervals of steady flow (1 - 4 msec.) it is reasonable to assume that the difference between the gas temperature at the gauge surface and the free gas temperature will be small.

6.8 Discussion of errors

Since the temperature changes of the platinum film were small, approximately $\pm$ 1.5^{o} C, errors in the calculation of $\Delta T/\Delta V$ had little effect on the determined temperature. This was confirmed

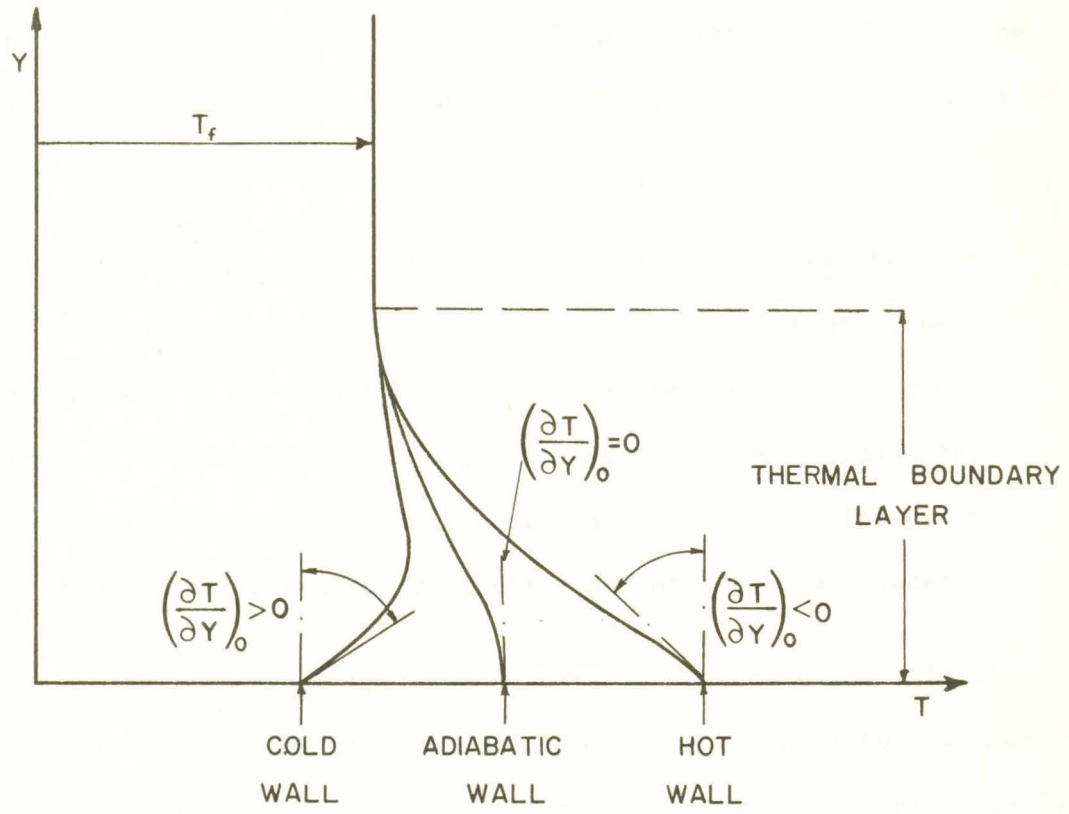

Fig. 6.7.1 The effect of heating and cooling on the temperature distribution near the wall of a shock tube

by arbitrarily changing $\Delta T/\Delta V^{o}$ C/volt by ± 1.0 and comparing the resultant temperatures with those obtained using the calibrated value. The changes were about ± .04%. The important calibration was thus the determination of $\Delta T/\Delta P$ (Figure 4.7.2) from which the initial gauge temperature was obtained. An error of approximately ± $.5^{o}$ C in the initial gauge temperature would occur for an error of ± .005 turns of the potentiometer dial for a balanced bridge.

In Figures 6.2.1, 6.2.3 and 6.2.4, it is seen that the experimental temperature at 1 msec. of flow time is higher, by approximately 5^{o} C, than the "theoretical" temperature for each experiment. This deviation is attributed to the numerical method of evaluating the integral in equation 3.3.1. If time intervals less than 1 msec. are used, this error can probably be reduced.

On accounting for inaccuracies in measuring the initial gauge temperature, and the approximation of an integral by a summation routine, an error of ± 6^{o} C has been estimated for the experimentally determined temperatures.

CHAPTER 7

CONCLUSIONS

The method developed for measuring the temperature of an unsteady gas flow, by calculating the heat transfer rate from the measured surface temperature of a thin film resistance thermometer, has proved to be quite successful. With modifications outlined in section 6.4, it would seem that temperatures up to 400° K could be measured. This would extend the usefulness of the gauge to shock tube flows with incident shock front mach numbers of about 1.6.

It has been shown that the method of Thureau and De Casteljau (1962) and A.T. Frobel (1963) was valid for temperature measurements directly behind the shock front and possibly up to about 3 msec. of flow thereafter. For longer periods of time, and for unsteady flow situations, heat diffusion within the glass backing of the temperature transducer would produce erroneous results.

During the initial work on this project, the rate of change of the film temperature was monitored. Consequently its trace has been shown in conjunction with each temperature record. In using the heat transfer technique, there is no need to use the rate of change of the temperature. The only measurement required is the temperature-time history of the platinum film.

In future experiments, it will be possible to use a set of at least five temperature transducers, the number being limited by the tape recorder facility, at a common tube position and one shock tube firing. This should provide quite an efficient method for determining the gas temperature.

As gas flows with stronger incident shock strengths are investigated, the existence of laminar and turbulent boundary layers should be verified. This may be done with schlieren photography or smoke traces techniques. It is the existence of these layers which will limit the use of the technique described in this thesis to determine the free-gas temperature of a shock tube flow.

REFERENCES

Benderskey, D. 1953. A Special Thermocouple for Measuring Transient Temperatures. Mechanical Engineering, 75, 117-121.

Carslaw, H.S. and J.C. Jaeger. 1947. Conduction of Heat in Solids. (Oxford University Press).

Clouston, J.G., A.G. Gaydon and I.R. Hurle. 1959. Temperature Measurements of Shock Waves by Spectrum-line Reversal. Proc. Roy. Soc. (London) A252, P. 143.

Dewey, J.M. and R.M. Johnson. 1968. A Technique for the Measurement of Temperatures of Unsteady Gas Flows. Paper presented at the Annual Meeting of the Division of Fluid Dynamics, Seattle, Washington, November 25-27, 1968.

Froebel, A.T. 1963. On the Measurement of Temperature in Shock Waves, Suffield Experimental Station, Ralston, Alberta, PMMP No. 200.

Gaydon, A.G. and I.R. Hurle. 1963. The Shock Tube in High-Temperature Chemical Physics. (Chapman and Hall, London).

Glass, I.I. and G.N. Patterson. 1955. A Theoretical and Experimental Study of Shock-Tube Flows. Journal of Aeronautical Sciences, 22, 73-100.

Ingersoll, L.R. and O.J. Zobel. 1913. Mathematical Theory of Heat Conduction. (Ginn and Co., Boston).

Johnson, R.M. 1968. Type 549 Tektronic Oscilloscope 35 mm Camera Adaptor. University of Victoria Shock Tube Laboratory Note 69/1.

Kovasznay, L.S.G. 1964. The Hot-Wire Anemometer. Johns Hopkins University.

Lowell, H.H. 1950. Design and Application of Hot-Wire Anemometers for Steady State Measurements at Transonic and Supersonic Air Speeds. NACA TN 2117.

Marlow, D.G., C.R. Nisewanger and W.M. Cady. 1949. A Method for the Instantaneous Measurement of Velocity and Temperature in High Speed Air Flows. J. Appl. Phys., 20, p. 771.

Mirrels, H. 1956. Boundary Layer Behind Shock or Thin Expansion Wave Moving into Stationary Fluid. NACA TN 3712, Washington.

Rabinowicz, J. 1957. Aerodynamic Studies in the Shock Tube. Guggenheim Aeronautical Laboratory Hypersonic Research Project, Memorandum Mp. 38.

Shand, E.B. 1958. Glass Engineering Handbook. (McGraw-Hill Book Co. Inc.).

Shapiro, A.H. 1954. The Dynamics and Thermodynamics of Compressible Fluid Flow. (The Ronald Press Co., New York).

Soloukhin, R.I. 1966. Shock Waves and Detonations in Gases. (Mono Book Corp., Baltimore).

Taylor, B.W. 1959. Development of a Thin Film Heat-Transfer Gauge for Shock-Tube Flows. UTIA Technical Note No. 27.

Thureau, P. and M. De Casteljau. 1962. Determination de la Temperature en Paroi d'une Onde de Choc par l'Utilisation de Couches Minces Metalliques Thermoresistances. Laboratoire de Physique Experimentale, Faculté des Sciences de Caen.

Vidal, R.J. 1956. Model Instrumentation Techniques for Heat Transfer and Force Measurements in a Hypersonic Shock Tunnel. C.A.L. Report No. AD-917-A-1.

Vidal, R.J. 1956. A Resistance Thermometer for Transient Surface Temperature Measurements. Presented at the American Rocket Society Meeting, Buffalo, N.Y.

Vidal, R.J. and J.H. Hilton. 1956. The Construction and Application of a Rapid Response Resistance Thermometer Probe. Cornel Aeronautical Laboratory, Report No. IM-1062-A-1.

Whitten, B.T. 1969. Calibration of a Shock Tube by Analysis of the Particle Trajectories. M.Sc. Thesis, University of Victoria.

APPENDIX A

HEAT CONDUCTION THEORY

If the temperature-time history of the thin film can be obtained, the heat transfer rate is found by solving the classical heat conduction equation. For a thin narrow film, the longitudinal and tangential heat flows will be much less than the normal heat flow so to a good approximation the problem is one dimensional.

Since the film is very thin, and the platinum has a high thermal conductivity, the effect of the film on the temperature of the glass will be small. Thus the surface temperature of the glass can be obtained by solving the heat transfer equation for a semi-infinite homogeneous glass body. The system to be solved is:

$$k \frac{\partial^2 q}{\partial y^2} = \frac{\partial q}{\partial t} \qquad (A.1)$$

$q = q(t)$ $\quad y = 0,\ t \geq 0$ $\quad T = 0,\ t < 0$

$q = 0$ $\quad y = 0,\ t < 0$

where q is the heat transfer rate, T is the change from the initial temperature, and k is the thermal diffusivity.

A solution to this equation is given by Carslaw and Jaeger (1947):

$$T(y,t) = \frac{k^{\frac{1}{2}}}{K\pi^{\frac{1}{2}}} \int_0^t \frac{q(t)\, e^{-\frac{y^2}{4k(t-\lambda)}}}{(t-\lambda)^{\frac{1}{2}}}\, d\lambda \qquad (A.2)$$

and for y = 0,

$$T(t) = \frac{k^{\frac{1}{2}}}{K\pi^{\frac{1}{2}}} \int_0^t \frac{q(t)}{(t-\lambda)^{\frac{1}{2}}}\, d\lambda \qquad (A.3)$$

If the film thickness is to be accounted for in the heat conduction equation, the model to be considered is:

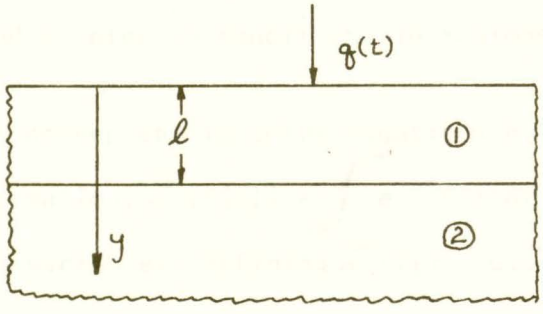

Fig. A.1 Model for heat conduction theory

The heat conduction equations for Regions 1 and 2 in Figure A.1 are:

<u>For Region 1</u>: $0 \le y \le \ell$ $\qquad \frac{\partial T_1}{\partial t} = k_1 \frac{\partial^2 T_1}{\partial y^2}$ $\qquad (A.4)$

with boundary conditions:

$t \le 0$; $T_1(y) = 0$

$t > 0$, $y = 0$: $\qquad \left(\frac{\partial T_1}{\partial y}\right)_{y=0} = -\frac{1}{K_1} q(t)$

For Region 2: $\ell \leq y \leq \infty$ $$\frac{\partial T_2}{\partial t} = k_2 \frac{\partial^2 T_2}{\partial y^2} \tag{A.5}$$

with the boundary conditions:

$$t \leq 0 : T_2(y) = 0$$

$$t > 0 , y = \ell : T_1(\ell) = T_2(\ell) \qquad K_1\left(\frac{\partial T_1}{\partial y}\right)_{y=\ell} = K_2\left(\frac{\partial T_2}{\partial y}\right)_{y=\ell}$$

$$\lim_{y \to \infty} T_2 = 0$$

where T is the increment of temperature above the initial temperature prevailing for $t \leq 0$, t is time, K is thermal conductivity, ρ is the density, C_p is the specific heat, $k = K/\rho C_p$ is thermal diffusivity, $q(t)$ is an arbitrary rate of heat transfer to the surface, and the subscripts 1 and 2 refer to conditions in Regions 1 and 2.

It is convenient to solve equations A.4 and A.5 using the Laplace transformation, $\mathcal{L}\{F(t)\} = \int_0^\infty e^{-st} F(t)dt = f(s)$, where s is the transformed variable. Defining $\mathcal{L}\{T_1\} = u$, $\mathcal{L}\{T_2\} = v$, $\mathcal{L}\{q(t)\} = q(s)$, the transformations of equations A.4 and A.5 are

For Region 1: $0 \leq y \leq \ell$ $$su = k_1 \frac{d^2 u}{dy^2} \tag{A.6}$$

with boundary conditions:

$$y = 0 : \left(\frac{du}{dy}\right)_{y=0} = -\frac{1}{K_1} q(s)$$

For Region 2: $\ell \leq y \leq \infty$ $\qquad sv = k_2 \frac{d^2v}{dy^2}$ (A.7)

with boundary conditions:

$$y = \ell : u = v \ , \ \left(\frac{du}{dy}\right)_{y=\ell} = \frac{K_2}{K_1}\left(\frac{dv}{dy}\right)_{y=\ell}$$

$$\lim_{y \to \infty} \quad v = 0$$

The solutions of equations A.6 and A.7 are:

$$u = C_1 e^{y\sqrt{\frac{s}{k_1}}} + C_2 e^{-y\sqrt{\frac{s}{k_1}}} \tag{A.8}$$

$$v = C_3 e^{y\sqrt{\frac{s}{k_2}}} + C_4 e^{-y\sqrt{\frac{s}{k_2}}} \tag{A.9}$$

and after applying the boundary conditions to evaluate the arbitrary constants, the solutions of the transformed temperatures are

$$u = \frac{\sqrt{k_1}}{K_1}\frac{q(s)}{\sqrt{s}} e^{-y\sqrt{\frac{s}{k_1}}} \left[\frac{1 + \sigma e^{-2(\ell-y)\sqrt{\frac{s}{k_1}}}}{1 - \sigma e^{-2\ell\sqrt{\frac{s}{k_1}}}}\right] \tag{A.10}$$

$$v = 1 + \sigma \frac{\sqrt{k_1}}{K_1}\frac{q(s)}{\sqrt{s}} e^{-\ell\sqrt{\frac{s}{k_1}}} \left[\frac{e^{-(y-\ell)\sqrt{\frac{s}{k_2}}}}{1 - \sigma e^{-2\ell\sqrt{\frac{s}{k_1}}}}\right] \tag{A.11}$$

$$\sigma = \frac{\sqrt{\frac{K_1\rho_1 C_{p1}}{K_2\rho_2 C_{p2}}} - 1}{\sqrt{\frac{K_1\rho_1 C_{p1}}{K_2\rho_2 C_{p2}}} + 1}$$

In this form these solutions for the transformed temperatures are not readily inverted; however, the denominator of each solution may be expanded in series form for $\sigma < 1$ to yield:

$$u = \frac{\sqrt{k_1}}{K_1}\frac{q(s)}{\sqrt{s}}\left(e^{-y\sqrt{\frac{s}{k_1}}} + \sum_{n=1}^{\infty}\sigma^n\left[e^{-(2n\ell+y)\sqrt{\frac{s}{k_1}}} + e^{-(2n\ell-y)\sqrt{\frac{s}{k_1}}}\right]\right) \quad (A.12)$$

$$v = (1+\sigma)\frac{\sqrt{k_1}}{K_1}\frac{q(s)}{\sqrt{s}}e^{-(y-\ell)\sqrt{\frac{s}{k_2}}}\sum_{n=0}^{\infty}\sigma^n e^{-(2n+1)\ell\sqrt{\frac{s}{k_1}}} \quad (A.13)$$

These expressions for u and v can now be inverted to obtain the solutions for the temperature T_1 and T_2 by using the inverse transform

$$\mathcal{L}^{-1}\left(\frac{1}{\sqrt{s}}e^{-\gamma\sqrt{s}}\right) = \frac{1}{\sqrt{\pi t}}e^{-\frac{\gamma^2}{4t}} \quad (\gamma \geq 0)$$

and the convolution integral

$$\mathcal{L}^{-1}\left(f(s)g(s)\right) = \int_0^t F(t-\lambda)G(\lambda)d\lambda \ *$$

$$T_1 = \frac{1}{K_1}\sqrt{\frac{k_1}{\pi}}\int_0^t \frac{q(\lambda)}{\sqrt{t-\lambda}}e^{-\frac{y^2}{4k_1(t-\lambda)}}d\lambda$$

$$+ \frac{1}{K_1}\sqrt{\frac{k_1}{\pi}}\sum_{n=1}^{\infty}\sigma^n\int_0^t \frac{q(\lambda)}{\sqrt{t-\lambda}}\left[e^{-\frac{(2n\ell+y)^2}{4k_1(t-\lambda)}} + e^{-\frac{(2n\ell-y)^2}{4k_1(t-\lambda)}}\right]d\lambda \quad (A.14)$$

---

* The symbol $\mathcal{L}^{-1}\{f(s)\}$ denotes a function F(t) whose Laplace transform is f(s).

$$T_2 = \left(\frac{1+\sigma}{K_1}\right)\sqrt{\frac{k_1}{\pi}}\sum_{n=0}^{\infty}\sigma^n\int_0^t \frac{q(\lambda)}{\sqrt{t-\lambda}}\, e^{-\frac{[(2n+1)\frac{\ell}{\sqrt{k_1}} + \frac{y-\ell}{\sqrt{k_2}}]}{4(t-\lambda)}}\, d\lambda \qquad (A.15)$$

where γ is the integration variable.

Within the limits of the initial assumptions equation A.14 is an exact expression for T_1. It should be noted that equation A.14 gives the film temperature as a function of distance from the surface, whereas the thin film thermometer measures only the average temperature of the film. Equation A.14 would have to be integrated over the interval $0 \leq y \leq \ell$ to obtain the average temperature before it can be used to find a value for the heat transfer rate.

Two important features of the model should be noted:

1. The thickness of the film is very small, thus the characteristic time ℓ^2/k_1 of the film is short compared with the testing time.
2. The heat conductivity of the platinum is much greater than that of the glass.

On the basis of these features, it can be assumed that the measured temperature is the surface temperature of the glass. Therefore equation A.14 simplifies to:

$$T(t) = \frac{1}{K_1}\sqrt{\frac{k_1}{\pi}}\int_0^t \frac{q(\lambda)}{\sqrt{t-\lambda}}\, d\lambda + \frac{1}{K_1}\sqrt{\frac{k_1}{\pi}}\sum_{n=1}^{\infty} 2\sigma^n\int_0^t \frac{q(\lambda)}{\sqrt{t-\lambda}}\, e^{-\frac{n^2\ell^2}{k_1(t-\lambda)}}\, d\lambda \qquad (A.16)$$

Vidal (1956) has shown that the solution is predominantly that for a homogeneous glass body. To obtain equation A.16 in a form showing this explicitly, Vidal has added and subtracted:

$$\frac{1}{K_1}\sqrt{\frac{k_1}{\pi}}\sum_{n=1}^{\infty} 2\sigma^n \int_0^t \frac{q(\lambda)}{\sqrt{t-\lambda}}\,d\lambda$$

to equation A.16. The result is

$$T(t) = \frac{1}{\sqrt{\pi\rho_2 C_{p2} K_2}}\int_0^t \frac{q(\lambda)}{\sqrt{t-\lambda}}\,d\lambda - \frac{2}{\sqrt{\pi\rho_1 C_{p1} K_1}}\sum_{n=1}^{\infty}\sigma^n \int_0^t \frac{q(\lambda)}{\sqrt{t-\lambda}} \left[1 - e^{-\frac{n^2\ell^2}{k_1(t-\lambda)}}\right] d\lambda \qquad (A.17)$$

Finally, integrating the second term by parts, expanding it and neglecting terms of order ℓ^2

$$T(t) = \frac{1}{\sqrt{\pi\rho_2 C_{p2} K_2}}\int_0^t \frac{q(\lambda)}{\sqrt{t-\lambda}}\,d\lambda - q(t)\,\frac{\ell}{K_1}\left(\frac{K_1\rho_1 C_{p1}}{K_2\rho_2 C_{p2}} - 1\right) \qquad (A.18)$$

If the second term in equation A.18 is omitted, the result is that of equation A.3. Thus the second term is a correction term to account for the thickness of Region 1. Vidal has shown that, for a .1 micron thick film, the error introduced by neglecting the correction term in equation A.18 is about 3%. Therefore the homogeneous glass solution (equation A.3)

$$T(t) = \frac{1}{\sqrt{\pi \rho_2 C_{p_2} K_2}} \int_0^t \frac{q(\lambda)}{\sqrt{t-\lambda}} \, d\lambda$$

is satisfactory for reducing experimental data.

It has been shown by Carslaw and Jaeger (1947) that, for an unsteady heat transfer rate, equation A.3 can be inverted and integrated by parts to give:

$$q(t) = \sqrt{\pi} \frac{\sqrt{\rho_2 C_{p_2} K_2}}{2} \left(2 \frac{T(t)}{\sqrt{t}} + \int_0^t \frac{T(t)-T(\lambda)}{(t-\lambda)^{3/2}} \, d\lambda \right) \qquad (A.19)$$

For a constant heat transfer rate, equation A.3 may be integrated to give:

$$q(t) = \sqrt{\pi} \frac{\sqrt{\rho_2 C_{p_2} K_2}}{2} \frac{T(t)}{\sqrt{t}} \qquad (A.20)$$

APPENDIX B

DATA CONCERNING THE TAA243 OPERATIONAL AMPLIFIER

ABSOLUTE MAXIMUM RATINGS

Supply voltage between pin 8 and 4	21	V
Common mode input voltage	-6.0 to +1.5	V
Differential input voltage	±5	V
Load current	50	mA
Power dissipation (T_{amb} = 25° C)	200	mW
Storage temperature range	-65 to 150	°C
Operating ambient temperature range	-25 to 100	°C

CHARACTERISTICS (T_{amb} = 25° C)

Supply voltages	V^+		+12	V
	V^-		- 6	V
	Min.	Typical	Max.	
Differential open loop voltage gain	900	2300	—	
Differential open loop voltage gain at f = 550 KHz	630	1600	—	
Input common mode range	-4	—	+0.5	V
Input impedance	6	20	—	KΩ
Input common mode rejection ratio	65	80	—	dB
Output impedance	—	200	600	Ω
Input offset voltage between 0 and 70°C $R_s \leq 2$ KΩ	—	7	15	mV
Input offset current	—	3	5	µA
Input bias current	—	5	15	µA
Output voltage swing ($R_L \geq 100$ KΩ)	±5	±5.3	—	V
D.C. supply power	—	80	125	mW

APPENDIX C

CALCULATION OF TEMPERATURE BEHIND A SHOCK WAVE IN TERMS OF THE MACH NUMBER

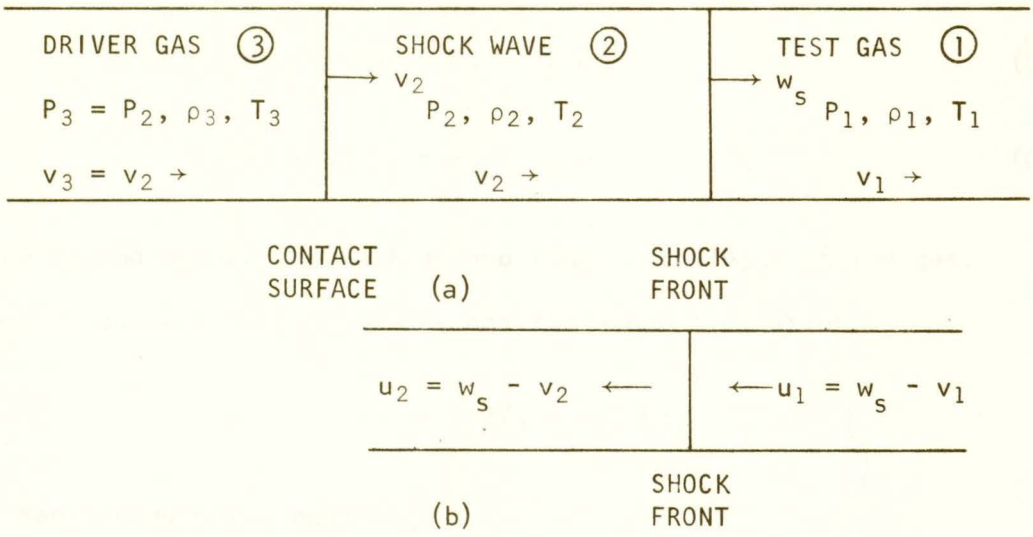

(a) Laboratory-fixed co-ordinates, i.e. shock tube at rest

(b) Shock-fixed co-ordinates, i.e. shock front at rest

Fig. C.1 Gas parameters associated with a shock wave in the two basic co-ordinate systems

Considering the passage of the gas through a unit area of shock front which is considered to be at rest, one may write from the conservation of mass, momentum and energy, respectively

$$\rho_1 u_1 = \rho_2 u_2 \tag{C.1}$$

$$P_1 + \rho_1 u_1^2 = P_2 + \rho_2 u_2^2 \tag{C.2}$$

$$H_1 + \tfrac{1}{2} u_1^2 = H_2 + \tfrac{1}{2} u_2^2 \tag{C.3}$$

where H_1 and H_2 are the initial and final enthalpies of the gas. From the conservation equations and the general equation

$$H = (\gamma/(\gamma - 1))\ P/\rho$$

the Rankine-Hugoniot equations

$$\frac{P_2}{P_1} = \frac{1 - \left(\frac{\gamma-1}{\gamma+1}\right)\frac{\rho_1}{\rho_2}}{\frac{\rho_1}{\rho_2} - \frac{\gamma-1}{\gamma+1}} \tag{C.4}$$

$$\frac{\rho_2}{\rho_1} = \frac{\frac{\gamma-1}{\gamma+1} + \frac{P_2}{P_1}}{\left(\frac{\gamma-1}{\gamma+1}\right)\frac{P_2}{P_1} + 1} = \frac{u_1}{u_2} \tag{C.5}$$

may be derived. From the first two conservation equations

$$\frac{P_2}{P_1} = 1 + \frac{\rho_1 u_1^2}{P_1}\left(1 - \frac{\rho_1}{\rho_2}\right) \tag{C.6}$$

Now introducing the concept of the mach number

$$M_1 = \frac{u_1}{a_1} = \frac{w_s}{a_1} \tag{C.7}$$

where a_1 is the velocity of sound in air ahead of the shock front.

Since

$$a_1 = \left(\frac{\gamma P_1}{\rho_1}\right)^{\frac{1}{2}} \tag{C.8}$$

$$M_1 = u_1\left(\frac{\rho_1}{\gamma P_1}\right)^{\frac{1}{2}} \tag{C.9}$$

use of the latter relation in equation C.6 leads to

$$\frac{P_2}{P_1} = 1 + \gamma M_1^2 \left(1 - \frac{\rho_1}{\rho_2}\right) \tag{C.10}$$

Combining equations C.5 and C.10 gives

$$\frac{P_2}{P_1} = \frac{2\gamma M_1^2 - (\gamma - 1)}{\gamma + 1} \tag{C.11}$$

The latter two equations give

$$\frac{\rho_2}{\rho_1} = \frac{(\gamma + 1)\ M_1^2}{(\gamma-1)M_1^2 + 2} \tag{C.12}$$

and using equations C.11 and C.12 with the ideal gas relations

gives the temperature ratio

$$\frac{T_2}{T_1} = \frac{(\gamma M_1^2 - \frac{\gamma-1}{2})(\frac{\gamma-1}{2} M_1^2 + 1)}{(\frac{\gamma+1}{2})^2 M_1^2} \qquad (C.13)$$

From relations C.11, C.12 and C.13, the pressure density and temperature in a shock wave through an ideal gas may be obtained if the initial conditions and shock speed W are known.

APPENDIX D

DERIVATION OF THE GAS TEMPERATURE BEHIND A REFLECTED SHOCK IN AN ISENTROPIC FLOW

The equation relating the gas pressure P at any time t in the gas flow, to the measured displacement from a pressure time record, is

$$\frac{P}{P_1} = \left(P(t) \frac{(P_2/P_1 - 1)}{\Delta PM} + 1\right) \tag{D.1}$$

If the pressure directly behind the reflected shock is denoted by P_5, then multiplying equation D.1 by P/P_5 yields

$$\frac{P}{P_5} = \left(P(t) \frac{(P_2/P_1 - 1)}{\Delta PM} + 1\right) \frac{P_1}{P_5} \tag{D.2}$$

Since equation D.2 is dependent on the ambient pressure P_1, and an entropy change exists across the reflected shock front, the Rankine-Hugoniot equations must be used to determine the conditions across the discontinuity. Multiplying equation D.2 by P_2/P_1 gives

$$\frac{P}{P_5} = \left(P(t) \frac{(P_2/P_1 - 1)}{\Delta PM}\right) \frac{P_2}{P_5} \frac{P_1}{P_2} \tag{D.3}$$

P_1/P_2 is obtained from the inverse of equation C.11.

The values of P_2 and P_5 can be found using equation D.1.

$$P_2 = \left(P_2(t)\ \frac{(P_2/P_1 - 1)}{\Delta PM} + 1\right) P_1 \qquad (D.4)$$

$$P_5 = \left(P_5(t)\ \frac{(P_2/P_1 - 1)}{\Delta PM} + 1\right) P_1 \qquad (D.5)$$

where $P_2(t)$ = pressure directly before the reflected shock,

$P_5(t)$ = pressure directly after the reflected shock,

ΔPM = pressure-time displacement directly behind the incident shock.

Note that an explicit value of P_1 is not required since the ratio P_2/P_5 is required.

The equation relating the temperature T in the region directly behind the reflected shock front, assuming an isentropic flow, is

$$\frac{T}{T_5} = \left(\frac{P}{P_5}\right)^{\frac{\gamma-1}{\gamma}} \qquad (D.6)$$

T_2, the temperature of the flow directly before the reflected shock is known, and T_2 and T_5 may be directly related using the equation of state for a perfect gas. Therefore T_5 is given by

$$\frac{P_5}{P_2} = \frac{\rho_5}{\rho_2}\frac{T_5}{T_2} \qquad (D.7)$$

The Rankine-Hugoniot equation D.12 is used to determine the density ratio ρ_5/ρ_2 across the reflected shock. Thus

$$T_5 = \frac{P_5}{P_2} T_2 \left(\frac{\beta P_5/P_2 + 1}{\beta + P_5/P_2} \right) \qquad (D.8)$$

where $\beta = (\gamma-1)/(\gamma+1)$. Thus explicit solutions for the ratio P/P_5, equation D.3, and T_5, equation D.8, yields the temperature T from equation D.6 at any time in the gas flow behind the reflected shock front.

APPENDIX E

COMPUTER PROGRAM FOR DATA ANALYSIS

A computer program for data analysis was written in Fortran IV language for the University of Victoria IBM 360 Model 44 computer. A flow diagram has been constructed to show the sequence of operations in the program. The flow diagram has been supplemented with comment cards in the program listing to define the input variables.

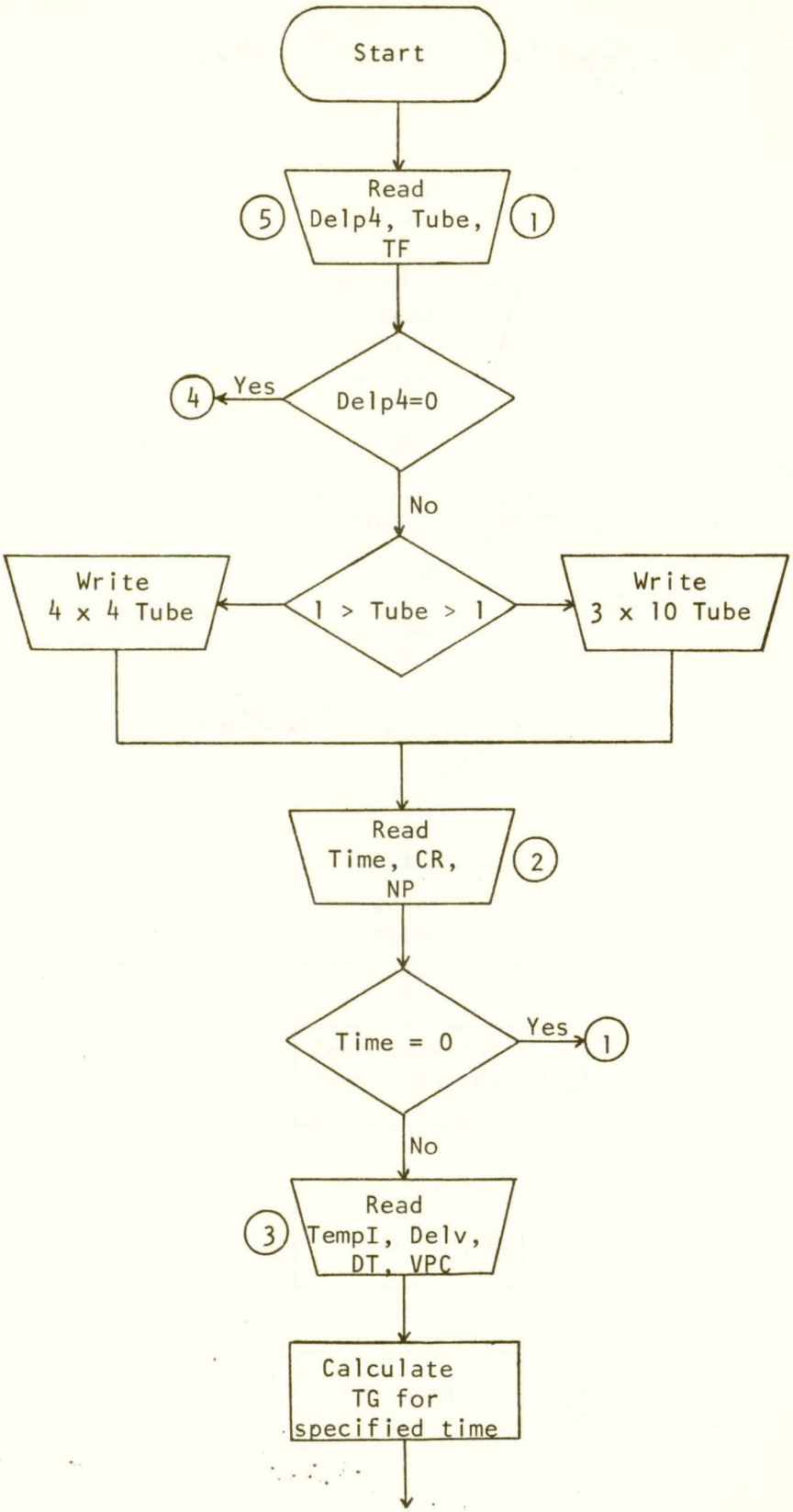
Start
Read
Delp4, Tube,
TF
5
1
Yes
4
Delp4=0
No
Write
4 x 4 Tube
1 > Tube > 1
Write
3 x 10 Tube
Read
Time, CR,
NP
2
Time = 0
Yes
1
No
Read
TempI, Delv,
DT, VPC
3
Calculate
TG for
specified time

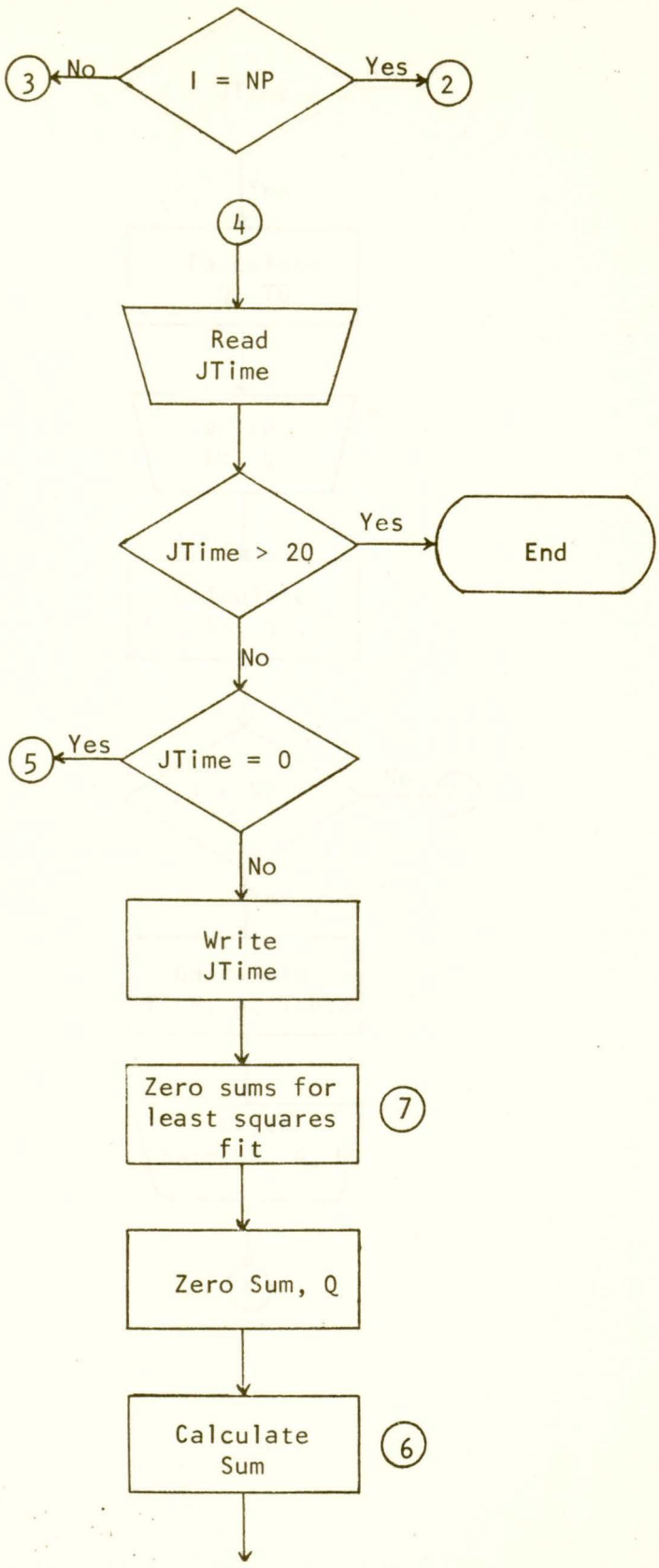
I = NP
No
Yes
3
2
4
Read
JTime
JTime > 20
Yes
End
No
JTime = 0
Yes
5
No
Write
JTime
Zero sums for
least squares
fit
7
Zero Sum, Q
Calculate
Sum
6

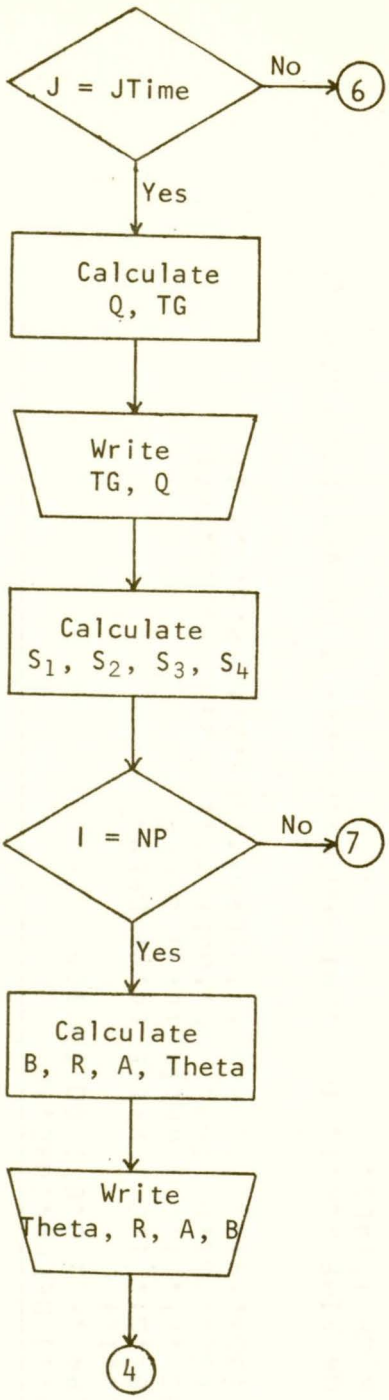
J = JTime
No
6
Yes
Calculate
Q, TG
Write
TG, Q
Calculate
S_1, S_2, S_3, S_4
I = NP
No
7
Yes
Calculate
B, R, A, Theta
Write
Theta, R, A, B
4

```
      DIMENSION DELT(300),TG(300)
    6 FORMAT(3X,'THETA=',1F10.5,4X,'R=',1E12.5,4X,'A=',1E12.5,4X,'B=',1E
     112.5/)
   16 FORMAT(30X,'FIT  OF  ORDER  2'/)
    5 FORMAT (4E12.5)
    4 FORMAT (2F7.3,I2)
    1 FORMAT (3F7.3)
   12 FORMAT ('1')
C
C     DELP4=COMPRESSION CHAMBER PRESSURE,TUBE=1 IMPLIES 3*10 ,TUBE=0  IM
C     PLIES 4*4, TF=DEGREES/VOLT ( GAUGE CALIBRATION).
C     ------------------------------------------------------------------
  108 READ (5,1) DELP4,TUBE,TF
      IF (DELP4 .EQ. 0.0 ) GO TO 105
      WRITE (6,12)
      IF (TUBE .GT. 1.0 ) WRITE (6,2) DELP4
      IF (TUBE .LT. 1.0 ) WRITE (6,3) DELP4
    2 FORMAT (30X,'3X10  TUBE   ','DELP4=',1F6.2,'  P.S.I.'//)
    3 FORMAT (30X,'4X4   TUBE   ','DELP4=',1F6.2,'  P.S.I.'//)
      KK=0
C
C     TIME=FLOW TIME W.R.T. INCIDENT SHOCK, CR=PRINT CONVERSION FACTOR,N
C     P=NUMBER OF TRIALS.
C     ------------------------------------------------------------------
  104 READ (5,4) TIME,CR,NP
      IF ( TIME .EQ. 0.00 ) GO TO 108
      DO 100 I=1,NP
      KK=KK+1
C
C     TEMPI=INITIAL GAUGE TEMP., DELV=TEMP. TRACE DISPLACEMENT (CM.), DT
C     =0.0, VPC=SCOPE SENSITIVITY .
C     ------------------------------------------------------------------
      READ(5,5) TEMPI,DELV,DT,VPC
      DELV=VPC*DELV/CR
      DELT(KK)=DELV*TF
```

```
      TG(KK)=DELT(KK)+TEMPI
      NPP=NP
  100 CONTINUE
      GO TO 104
C
C     JTIME=TIME AT WHICH Q  IS CALCULATED
C     ------------------------------------------------------------------
  105 READ(5,8)JTIME
      IF (JTIME .GT. 20 ) GO TO 110
      IF ( JTIME .EQ. 0 ) GO TO 108
      WRITE(6,9) JTIME
    8 FORMAT(I12)
    9 FORMAT (2X,'FLOW TIME=',I12,2X,'MSEC.'/)
      S1=0.0
      S2=0.0
      S3=0.0
      S4=0.0
      K=NPP
      DO 106 I=1,K
      SUM=0.0
      Q=0.0
      DO 107 J=1,JTIME
      LL= (JTIME-1 )*K+I
      IF ( J .GT. 1 ) L=(J-2)*K+I
      IF ( J .GT. 1 ) C=DELT(LL)-DELT(L)
      IF ( J .EQ. 1 ) C=DELT(LL)
      IF ( J .EQ. 1 ) H=DELT(LL)
      DD=JTIME-J+1
      D=DD**1.5
      IF ( D .GT. 0.0 ) Y=C/D
      IF ( D .EQ. 0.0 ) Y=0.0
      IF ( D .LT. 0.0 ) Y=C/D
      SUM=SUM+Y
      DD=JTIME
      IF ( J .EQ. JTIME ) Q=2*H/SQRT(DD)+SUM
```

```
      IF (J .EQ. 1 ) HH=TG(LL)
      IF (J .EQ. JTIME ) WRITE(6,123) HH,Q
  123 FORMAT(2X,'GAUGE TEMP =',1E12.5,2X,'Q=',1E12.5/)
  107 CONTINUE
C
C     LINEAR LEAST SQARES FIT BEGINS.
C     ------------------------------------------------------------------
      M=(JTIME-1)*K+I
      S1=S1+TG(M)
      S2=S2+TG(M)*TG(M)
      S3=S3+Q
      S4=S4+TG(M)*Q
  106 CONTINUE
      B=K*S2-S1*S1
      R=(S2*S3-S1*S4)/B
      A=(K*S4-S3*S1)/B
      THETA=-R/A
      WRITE (6,16)
      WRITE (6,6) THETA,R,A,B
      GO TO 105
  110 CONTINUE
      CALL EXIT
      END
```

Surname: JOHNSON Given Names: Robert Matthew Waller

Place of Birth: Berwyn, Alberta Date of Birth: November 11, 1938

Educational Institutions Attended, with Dates of Entering and Leaving:

University of British Columbia	1957	to	1961
University of Victoria	1961	to	1963
University of Victoria	1966	to	1969

Degrees, Diplomas, Etc., Awarded, with Dates and Names of Institutions:

B.Sc.	1963	University of British Columbia (Victoria College)
M.Sc.	1969	University of Victoria

Publications:

Type 549 Tektronic Oscilloscope 35 mm Camera Adapter (1968)

A Technique for the Measurement of Temperatures of Unsteady Gas Flows (with J.M. Dewey) (1968)

THE UNIVERSITY OF VICTORIA LIBRARY MANUSCRIPT THESIS

AUTHORITY TO DISTRIBUTE

AUTHOR: This thesis may be lent or microfilm copies made available:

(a) Without restriction [redacted]

(b) With the restriction that, for a period of five years (until November, 1974) the written approval of the following is required:

(1) The Dean, Faculty of Graduate Studies _____

(2) The Author _____

(3) both the Dean, Faculty of Graduate Studies, and the Author _____

BORROWERS: The borrower undertakes, by signing below, to give proper credit for any use made of the thesis, and to obtain the consent of the author if it is proposed to make extensive quotations, or to reproduce the thesis in whole or in part.

Signature of Borrower	Address	Date